



Universität für Bodenkultur Wien

## DISSERTATION

# **Strontium isotopic and elemental fingerprints as tools for source determination in aquatic ecosystems**

Submitted by

**Dipl.-Ing. Anastassiya Tchaikovsky**

Supervised by

**Univ.Prof.Dipl.-Ing.Dr.techn. Thomas Prohaska**

and

**Dipl.-Ing.Dr.nat.techn. Andreas Zitek, MSc.**

University of Natural Resources and Life Sciences, Vienna

Department of Chemistry,

Division of Analytical Chemistry

VIRIS Group for Analytical Ecogeochemistry

Vienna, April 2019



## Acknowledgements

This PhD work would not have been possible without the significant help from a number of people and institutions to which I express my deep gratitude.

First of all, I thank my supervisor Prof. Thomas Prohaska for his valuable support and supervision; the possibility to conduct my PhD thesis in the VIRIS laboratory and to attend numerous scientific conferences; as well as the wisdom he shared with me.

I thank my co-supervisor Dr. Andreas Zitek for his tireless scientific and personal mentoring, the fruitful discussions and sharing his extensive knowledge.

I thank Dr. Johanna Irrgeher for her priceless support in helping me learn new scientific methods, writing manuscripts and being a role model.

I thank Prof. Hermann Häusler and Dr. Martin Kralik from the University of Vienna who enabled me to gain fascinating insights on hydrology and geology during our collaboration.

I thank my colleagues Melanie Diesner, Christoph Höfer, Christine Opper, Jennifer Sarne, Rudolf Scheiber and Sabrina van der Oeven for the great teamwork on the CSI: Trace Your Food and origin determination of sturgeon caviar projects.

I thank all my colleagues from the University of Natural Resources and Life Sciences, Vienna for their valuable cooperativeness, support and company during the past years.

I want to thank my partner, family and friends for their love, support and company during this intense period of life.

This work was partly funded by the Federal Ministry of Science, Research and Economy within the Sparkling Science program (Project „CSI:Trace your Food“, SPA 05\_052) and the COMET-K1 competence centre FFoQSI. The COMET-K1 competence centre FFoQSI is funded by the Austrian ministries BMVIT, BMDW and the Austrian provinces Niederoesterreich, Upper Austria and Vienna within the scope of COMET - Competence Centers for Excellent Technologies. The programme COMET is handled by the Austrian Research Promotion Agency FFG.

## Abstract

Chemical fingerprints are characteristic chemical pattern, which can be used to investigate sources, pathways and sinks of matter in the environment. Strontium isotopic and elemental fingerprints are of particular interest in the investigation of aquatic ecosystems, as water and living organisms absorb them from the environment without alteration. Thus, these natural markers can be used to link water and fish to their environment of origin. Mixing of several natural components can significantly hinder source determination using strontium isotopic and elemental pattern. Therefore, identification of environmental markers requires statistical and mathematical methods.

The origin of water and fish products was investigated using wet precipitation, surface water, groundwater, fish, sturgeon caviar, fish feed and salt samples. The strontium isotopic and elemental composition of the samples was analysed by (multi-collector) inductively coupled plasma mass spectrometry ((MC) ICP-MS). Mixing processes were investigated using multiple linear regression, linear algebra, mixing model calculations and variance analysis. Strontium isotopic and elemental fingerprints were determined by cluster analysis. Attribution of fish to their environment of origin was performed by discriminant analysis.

Surface water from the Leitha and Rosalia mountains in East Austria, a pre-alpine catchment in Germany, the Danube River, as well as fish farms in Europe and Iran reflected the strontium isotopic and elemental composition of local lithology. The chemical composition of water showed significant regional variation, which represents an important prerequisite for origin determination of water and fish.

The  $n(^{87}\text{Sr})/n(^{86}\text{Sr})$ ,  $\delta(^{88/86}\text{Sr})_{\text{SRM987}}$  and elemental pattern of groundwater in a clastic aquifer in East Austria were determined by dissolution of surrounding bedrock material as well as the mean groundwater residence time. They indicated a continuous groundwater flow from shallow to deep aquifers. In contrast to previous theories, these results showed neither the existence of marine connate water nor the upwelling of thermal groundwater to the surface. Furthermore, the  $\delta(^{88/86}\text{Sr})_{\text{SRM987}}$  values of groundwater revealed additional insights on geochemical processes such as rock weathering and mineral precipitation.

Otoliths of fish from rivers, lakes and fish farms of the Lake Chiemsee area reflected the  $n(^{87}\text{Sr})/n(^{86}\text{Sr})$  isotopic and Sr/Ca elemental pattern of water. This allowed attribution of fish to their water body of origin. Sturgeon caviar from aquaculture production showed six site-specific chemical markers ( $n(^{87}\text{Sr})/n(^{86}\text{Sr})$ , Na, Mn, Cu, Mo, Fe/Ca). Salting of sturgeon caviar altered the composition of four of the six chemical markers ( $n(^{87}\text{Sr})/n(^{86}\text{Sr})$ , Na, Mn, Fe/Ca).

Isotope pattern deconvolution (IPD) proved to be the most suitable mathematical method for the determination of the contribution of individual natural sources to the  $n(^{87}\text{Sr})/n(^{86}\text{Sr})$  isotopic composition of mixed samples. IPD showed that recent rainfall accounted for 60 % and bedrock dissolution for 40 % of the strontium isotope amount ratio of shallow groundwater of the clastic aquifer in East Austria. The  $n(^{87}\text{Sr})/n(^{86}\text{Sr})$  isotopic composition of otoliths and raw sturgeon caviar was made up of 80 % water and 20 % fish feed. Salt contributed up to 78 % to the strontium isotopic composition of salted sturgeon caviar. IPD provided the basis for the development of a novel mathematical method for the determination of the  $n(^{87}\text{Sr})/n(^{86}\text{Sr})$  isotopic composition of an unknown component in a known mixture.

This work showed that the combination of analytical and chemometric methods facilitate the investigation of complex research questions in the fields of hydrology, ecology and origin determination of food using strontium isotopic and elemental fingerprints.

## Kurzfassung

Chemische Fingerabdrücke sind charakteristische chemische Muster, die für die Erforschung von Quellen, Kreisläufen und Senken von Materie in der Umwelt verwendet werden können. Strontiumisotopen- und Elementfingerprints sind für die Untersuchung aquatischer Ökosysteme von besonderer Bedeutung, da sie von Wasser und Lebewesen unverändert aus der Umwelt absorbiert werden. Dadurch kann diese natürliche Signatur für die Bestimmung der Herkunft von Wasser oder Fischen verwendet werden. Herkunftsbestimmung kann erheblich erschwert werden, wenn die Strontiumisotopen- und Elementmuster durch Mischung mehrerer natürlicher Komponenten entstanden sind. Die Identifizierung der Umweltmarker erfordert deshalb den Einsatz statistischer und mathematischer Methoden.

Für die Untersuchung der Herkunft von Wasser und Fischprodukten wurden Regen-, Oberflächen- und Grundwasser sowie Fisch-, Störkaviar-, Fischfutter- und Salzproben gesammelt. Die Strontiumisotopen- und Elementzusammensetzung der Proben wurde mittels (Multikollektor)- Induktiv gekoppelter Plasma- Massenspektrometrie ((MC) ICP-MS) analysiert. Die Untersuchung von Mischprozessen erfolgte mittels multipler linearer Regression, linearer Algebra, Mischmodellberechnungen und Varianzanalyse. Strontiumisotopen- und Elementfingerprints wurden durch Clusteranalyse bestimmt. Die Zuordnung von Fischen zu ihrem Herkunftsgewässer erfolgte mittels Diskriminanzanalyse.

Oberflächenwasser aus dem Leitha- und Rosalingebirge in Ostösterreich, dem deutschen Alpenvorland, der Donau, sowie von Fischzuchten in Europa und dem Iran spiegelten die Strontiumisotopen- und Elementzusammensetzung der lokalen Lithologie wieder. Die chemische Zusammensetzung der Wasserproben zeigte signifikante regionale Unterschiede, die eine wichtige Voraussetzung für die Herkunftsbestimmung von Wasser und Fisch sind.

Die  $n(^{87}\text{Sr})/n(^{86}\text{Sr})$ ,  $\delta(^{88/86}\text{Sr})_{\text{SRM987}}$  und Elementmuster von Grundwasser in einem klastischen Grundwasserspeicher in Ostösterreich wurden durch Auflösung des umliegenden Gesteins sowie der mittleren Verweildauer des Wassers beeinflusst. Sie deuteten auf einen kontinuierlichen Wasserfluss von seichten zu tiefen Aquiferen hin. Im Gegensatz zu bisherigen Theorien zeigten diese Ergebnisse, dass in tiefen klastischen Aquiferen weder eingeschlossenes marines Porenwasser existiert, noch dass Thermalwasser zur Oberfläche aufsteigt. Die  $\delta(^{88/86}\text{Sr})_{\text{SRM987}}$  Werte von Grundwasser brachten zusätzliche Erkenntnisse über geochemische Prozesse wie Gesteinsverwitterung und mineralische Präzipitation.

Gehörsteine von Fischen aus Flüssen, Seen und Fischzuchten der Chiemsee Region spiegelten die  $n(^{87}\text{Sr})/n(^{86}\text{Sr})$  Isotopen- und Sr/Ca Elementmuster von Wasser wieder und konnten so ihrem Herkunftsgewässer zugeordnet werden. Störkaviar aus Aquakultur wies sechs ortsspezifische chemische Marker auf ( $n(^{87}\text{Sr})/n(^{86}\text{Sr})$ , Na, Mn, Cu, Mo, Fe/Ca). Das Salzen von Störkaviar veränderte die Zusammensetzung von vier der sechs Marker ( $n(^{87}\text{Sr})/n(^{86}\text{Sr})$ , Na, Mn, Fe/Ca).

Isotopenmusterdekonvolution (IPD) erwies sich als die geeignetste mathematische Methode für die Berechnung des Beitrags einzelner natürlicher Komponenten zur  $n(^{87}\text{Sr})/n(^{86}\text{Sr})$  Isotopenzusammensetzung von Mischproben. IPD zeigte, dass das Strontiumisotopenverhältnis von seichtem Grundwasser des klastischen Aquifers in Ostösterreich zu 60 % von Regenwasser und zu 40 % von Auflösung des umliegenden Gesteins bestimmt war. Die  $n(^{87}\text{Sr})/n(^{86}\text{Sr})$  Isotopenzusammensetzung von Otolithen und ungesalzenem Störkaviar wurde zu 80 % von Wasser und zu 20 % von Fischfutter beeinflusst. Im Fall von gesalzenem Störkaviar machte Salz bis zu 78 % der Strontiumisotopenzusammensetzung aus. IPD bildet die Grundlage für die Entwicklung eines neuen mathematischen Verfahrens, das die Berechnung der  $n(^{87}\text{Sr})/n(^{86}\text{Sr})$  Isotopenzusammensetzung einer unbekannt Komponente in einer bekannten Mischung ermöglicht.

Diese Arbeit zeigte, dass die Kombination von analytischen und chemometrischen Methoden die Untersuchung komplexer Fragestellungen in Hydrologie, Ökologie und Lebensmittelherkunftsbestimmung mittels Strontiumisotopen- und Elementfingerprints ermöglicht.

# TABLE OF CONTENT

<b>INTRODUCTION .....</b>	<b>1</b>
Aim of the study .....	1
The importance of aquatic ecosystems .....	2
Investigation of isotopes and chemical elements in aquatic ecosystems .....	4
Analysis of strontium isotope amount ratios and elemental pattern .....	10
Chemometrics .....	18
<b>PUBLICATIONS.....</b>	<b>29</b>
<b>I. Isotope pattern deconvolution of different sources of stable strontium isotopes in natural systems .....</b>	<b>30</b>
<b>II. Chemometric tools for determining site-specific elemental and strontium isotopic fingerprints in sturgeon caviar .....</b>	<b>42</b>
<b>III. Analysis of <math>n(^{87}\text{Sr})/n(^{86}\text{Sr})</math>, <math>\delta^{88}\text{Sr}/^{86}\text{Sr}_{\text{SRM987}}</math> and elemental pattern to characterise groundwater and recharge of saline ponds in a clastic aquifer in East Austria .....</b>	<b>74</b>
<b>IV. The <math>^{87}\text{Sr}/^{86}\text{Sr}</math> river water isoscape of the Danube catchment.....</b>	<b>96</b>
<b>V. The potential of <math>^{87}\text{Sr}/^{86}\text{Sr}</math> and Sr elemental mass fractions in fish otoliths as a fisheries management tool in a European pre-alpine river catchment.....</b>	<b>103</b>
<b>SUMMARY AND CONCLUSION .....</b>	<b>106</b>
<b>APPENDICES .....</b>	<b>109</b>
List of Abbreviations.....	109
Curriculum Vitae .....	110
Eidesstattliche Erklärung.....	113

# **Introduction**

## **Aim of the study**

This PhD project focuses on the development and application of analytical and chemometric methods for source determination of abiotic and biotic samples using strontium isotopic and elemental fingerprints. It seeks to provide new insights on the spatial variation of the strontium isotopic and elemental composition of water and to use this information to explore hydrologic and ecologic research questions. Furthermore, this study examines statistical and mathematical methods focusing on the investigation of natural water fluxes, the uptake of strontium isotopes and elements into fish tissues and origin determination of fish and fish products.

## The importance of aquatic ecosystems

An *ecosystem* consists of living organisms and the physical environment with which they interact [1, 2]. The abiotic physical environment such as water, soil, rocks and the atmosphere represents the basis for life of the biotic organisms such as plants, animals and humans. Ecosystem research deals with the interactions between organisms and their environment, thus providing the basis for sustainable management and use of resources in a time influenced by growing human population, increased consumption and rapid transformation of global environment [1].

In *aquatic ecosystems*, water represents the fundamental abiotic physical environment of aquatic organisms such as plankton, algae and fish. Table 1 summarises the basic properties of water and air that determine the structural differences between aquatic and terrestrial ecosystems [3]. For example, the oxygen concentration in surface ocean water is 30-fold lower than in air. This circumstance renders oxygen the limiting resource for aquatic organisms, whereas the ability and success to acquire water determine life on land. Furthermore, in oceans and lakes, the physical environment is structured by a decrease of light, oxygen, temperature and salinity along the vertical profile. This causes most aquatic organisms to live near the water surface, where light and oxygen availability is highest [1, 4].

Property	Water	Air	Ratio (water:air)
Oxygen concentration mL L <sup>-1</sup> at 25 °C	7.0	209.0	1:30
Density kg L <sup>-1</sup>	1.000	0.0013	800:1
Viscosity cP	1.0	0.02	50:1
Heat capacity cal L <sup>-1</sup> °C <sup>-1</sup>	1000.0	0.31	3000:1
Diffusion coefficient mm s <sup>-1</sup>			
Oxygen	0.00025	1.98	1:8000
Carbon dioxide	0.00018	1.55	1:9000

Table1. Basic properties of water and air at 20°C at sea level that influence ecosystem processes; data from Moss [3]

Water not only represents the habitat of aquatic organisms but also a solvent and transportation media for *nutrients* such as oxygen, carbon, phosphorus and other elements, which are essential for life. Water is a molecule consisting of two hydrogen atoms and one oxygen atom yielding the chemical formula H<sub>2</sub>O. While hydrogen atoms carry a positive charge, oxygen atoms are negatively charged forming an electrical dipole (similar to a magnet with a positive and negative pole [5]). This property creates a weak electrostatic attraction between water molecules rendering it liquid at normal atmospheric pressure and temperatures between 0 and 100°C. Furthermore, it allows water to dissolve charged substances such as cations (e.g. sodium Na<sup>+</sup> or calcium Ca<sup>2+</sup>) and anions (e.g. nitrate NO<sub>3</sub><sup>-</sup> or phosphate PO<sub>4</sub><sup>3-</sup>).



These materials are present in abiotic pools (sources), mainly rocks and soil, wherefrom they are released into water due to chemical weathering as well as biotic pools such as plants, animals and microorganisms [1].

Aquatic organisms, especially fish, take up dissolved nutrients and other elements from water and feed. These elements are then transferred to fish compartments such as soft tissues (flesh, fish eggs) and hardparts (bones and otoliths, *i.e.* the earstone used for hearing and orientation). The incorporation of elements from ambient water is a multi-stage physiological process, which differs between marine and freshwater fish. While marine fish absorb elements mainly through the intestinal walls, freshwater fish accumulate dissolved elements via gills [6]. Elements are then stored in fish compartments, representing biotic pools or sinks, until they are transferred to another pool by consumption by predators or released into the environment in the form of excrements or decomposed matter. In this way elements become available to other organisms again. Thus, fluxes (pathways) of elements from one pool to another are a fundamental part of *ecosystem processes* [1].

## Investigation of isotopes and chemical elements in aquatic ecosystems

### *Chemical elements in aquatic ecosystems*

Investigation of the *elemental composition* of water and aquatic organisms is a key tool for the understanding of sources, pathways and sinks of elements within an ecosystem [7]. For example, the analysis of the elemental content of nitrogen in streams before and after sewage outfalls allows to identify sources of nitrogen pollution, which can lead to eutrophication and fish-kill in lakes and coastal areas [4]. Studies of mercury content in fish from the Western Mediterranean Sea revealed that first trophic level fish showed harmless mercury content. In contrast, a considerable number of second and third trophic level fish accumulated mercury in concentrations exceeding the maximum level proposed by the European legislation for human consumption [8]. Investigations of Danube River water showed that after the construction of the Iron Gate hydroelectric power plant in the 1970s the dissolved silicon concentration of water decreased by two-thirds. This silicon loss was linked to diatom bloom; an algae consuming silicon to build its shell. As a consequence, the lack of silicon downstream the dam lead to a nutrient shortage in the Northern Black Sea, which affected the entire food web [9].

### *Isotopic systems in aquatic ecosystems*

The *isotopic composition of elements* provides additional information about ecosystem processes [7, 10, 11, 12]. *Isotopes* are atoms of the same element with the same number of protons but different number of neutrons in the nucleus. For example, the composition of hydrogen in ocean water accounts to about 99.985 % of the hydrogen isotope  ${}^1_1\text{H}$  displaying one proton and one neutron and about 0.015 % of the hydrogen isotope  ${}^2_1\text{H}$  with one proton and two neutrons in the nucleus. The proportion of two isotopes to each other is expressed as the *isotope amount ratio* of the heavier (higher atomic mass) to the lighter (lower atomic mass) isotope, e.g.  $n({}^2\text{H})/n({}^1\text{H})$ . In nature, only 27 out of 118 elements have just one stable (*i.e.* not radioactive) isotope, while the majority of elements display two or more stable isotopes [13, 14].

The isotopic composition of certain elements varies in nature [12]. Figure 1 shows the stable isotopic systems of dissolved elements investigated in natural water up to now. Table 2 gives an overview of stable isotope amount ratios most commonly uses for studying ecological processes in aquatic ecosystems. Remarkably, environmental research focuses on the investigation of light stable isotopes of the elements hydrogen, carbon, nitrogen, oxygen and sulphur. These elements constitute the bulk composition of water and living organisms and display the highest degree of isotopic *variation* in nature [11].

H																	He
Li	Be										B	C	N	O	F		Ne
Na	Mg										Al	Si	P	S	Cl		Ar
K	Ca	Sc	Ti	V	Cr	Mn	Fe	Co	Ni	Cu	Zn	Ga	Ge	As	Se	Br	Kr
Rb	Sr	Y	Zr	Nb	Mo	Tc	Ru	Rh	Pd	Ag	Cd	In	Sn	Sb	Te	I	Xe
Cs	Ba		Hf	Ta	W	Re	Os	Ir	Pt	Au	Hg	Tl	Pb	Bi	Po	At	Rn
Fr	Ra		Rf	Db	Sg	Bh	Hs	Mt	Ds	Rg	Cn	Uut	Ff	Uup	Lv	Uus	Uuo
			La	Ce	Pr	Nd	Pm	Sm	Eu	Gd	Tb	Dy	Ho	Er	Tm	Yb	Lu
			Ac	Th	Pa	U	Np	Pu	Am	Cm	Bk	Cf	Es	Fm	Md	No	Lr

Figure 1. The periodic table of the elements with stable isotopic systems of dissolved elements investigated in natural water marked in blue; data on H, C, N, O and S from Micherer and Lajtha [7]; Li, B, Mg, Si, Cl, Ca, Cr and Fe from Coplen *et al.* [15]; Br from Wieser *et al.* [16]; Sr, Nd, Pb from Nakano [17]; Ni from Elliott [18]; Zn and Cu from Moynier [19]; Ge from Rouxel [20]; Se from Stüeken [21]; Mo from Kendall [22]; Hg from Blum and Johnson [23]; Tl from Nielsen [24], Cd from Hoefs [25], K from Li *et al.* [26]; Sb from Rouxel *et al.* [27]; Ba from Horner *et al.* [28]; Hf from Rickli *et al.* [29], Os from Williams and Turekian [30] and Ce from Shimizu *et al.* [31]

Element	Isotope	Isotopic abundance	International standard	Isotope ratio	Natural variation* ‰
Hydrogen	<sup>1</sup> H	0.99985(70)	Vienna Standard Mean Ocean Water (VSMOW)	$\delta(^{2/1}\text{H})_{\text{VSMOW}}$	-700 to + 180
	<sup>2</sup> H (also D)	0.00015(70)			
Carbon	<sup>12</sup> C	0.9893(8)	Vienna Pee Dee Belemnite (VPDB)	$\delta(^{13/12}\text{C})_{\text{VPDB}}$	-130 to + 38
	<sup>13</sup> C	0.0107(28)			
Nitrogen	<sup>14</sup> N	0.99636(20)	Atmospheric nitrogen (air)	$\delta(^{15/14}\text{N})_{\text{Air}}$	-50 to + 150
	<sup>15</sup> N	0.00364(20)			
Oxygen	<sup>16</sup> O	0.99757(16)	VSMOS or VPDB	$\delta(^{18/16}\text{O})_{\text{VSMOW}}$	-63 to + 109
	<sup>17</sup> O	0.00038(1)			
	<sup>18</sup> O	0.00205(14)			
Sulphur	<sup>32</sup> S	0.9499(26)	Vienna Canon Diablo meteorite triolite (VCDT)	$\delta(^{34/32}\text{S})_{\text{VCDT}}$	-55 to + 135
	<sup>33</sup> S	0.0075(2)			
	<sup>34</sup> S	0.0425(24)			
	<sup>36</sup> S	0.0001(1)			
Strontium	<sup>84</sup> Sr	0.0056(1)	NIST SRM 987	$n(^{87}\text{Sr})/n(^{86}\text{Sr})$	0.70 to 0.78
	<sup>86</sup> Sr	0.0986(1)			
	<sup>87</sup> Sr	0.0700(1)		$\delta(^{87/86}\text{Sr})_{\text{SRM987}}$	-15 to + 98
	<sup>88</sup> Sr	0.8258(1)			

Table 2. Overview of stable isotope amount ratios most commonly used for the investigations of aquatic ecosystems; the isotopic composition of a sample is expressed relative to an internationally accepted standard using the "delta" ( $\delta$ ) notation; \* reported values in biotic and abiotic samples of the aquatic ecosystem; data from Micherer and Lajtha [7], Coplen *et al.* [15] and Wieser *et al.* [16]

The differences in the composition of light stable isotopes in natural samples are mainly a result of *isotopic fractionation* and *mixing* of sources with different isotopic compositions [7, 11, 12]. Isotopic fractionation occurs due to physical or chemical reactions, which preferably transfer a particular isotope of an element from one ecosystem pool to another. For example, during evaporation, water molecules containing  $^1\text{H}$  and  $^{16}\text{O}$  will preferentially form vapour, while the heavier isotopes  $^2\text{H}$  and  $^{18}\text{O}$  will preferably stay in the liquid phase [32]. The differences between the isotopic composition of vapour and residual water reflect evaporation rates of open water systems. Furthermore, tissues of aquatic organisms show a higher  $^{13}\text{C}$  content than those of their feeding source. Therefore, stable isotope amount ratios of carbon provide information on the position of an aquatic organism in the food chain [7].

Mixing of components with different isotopic composition is a natural process. Knowing the isotopic composition of the assumed sources and the mixed sample, it is possible to deduce the relative influence of each individual component to the mixture. For example, investigations of the nitrogen isotopic composition of nitrate in river water draining farmland in the US showed that soil and fertilisers represented the main contributors to the nitrate composition of river water [33]. Fertilisers are a non-point source pollution of water. Their contribution to river water would not be possible to determine by analysis of the nitrogen elemental content of water, soil and fertilisers alone.

#### *The strontium isotopic system*

The isotopic composition of strontium has become one of the most important *tracers* for the investigation of processes and sources in aquatic ecosystems (Table 2, [6, 34, 35]). Strontium is a natural, non-toxic element, which occurs in the Earth's crust at levels of about 0.03 – 0.04 % [35, 36]. In contrast to light stable isotopes, the natural variation of the strontium isotope amount ratio, expressed as  $n(^{87}\text{Sr})/n(^{86}\text{Sr})$ , is mainly influenced by *radioactive decay* of  $^{87}\text{Rb}$  to  $^{87}\text{Sr}$  with a half-life of about 50 billion years [12, 37]. As a result, the  $n(^{87}\text{Sr})/n(^{86}\text{Sr})$  isotope amount ratio of rocks varies depending on the initial relative amount of rubidium and the geological age of the bedrock material. For example, granitic rocks in northern Scotland formed 400 million years ago showed a  $n(^{87}\text{Sr})/n(^{86}\text{Sr})$  isotopic composition of 0.78, while marine carbonates formed 40 million years ago displayed a  $n(^{87}\text{Sr})/n(^{86}\text{Sr})$  isotope amount ratio of 0.71 (whole rock composition, [12]). Figure 2 illustrates the large diversity of bedrock material in Europe causing variation of the strontium isotope amount ratio in nature [38].

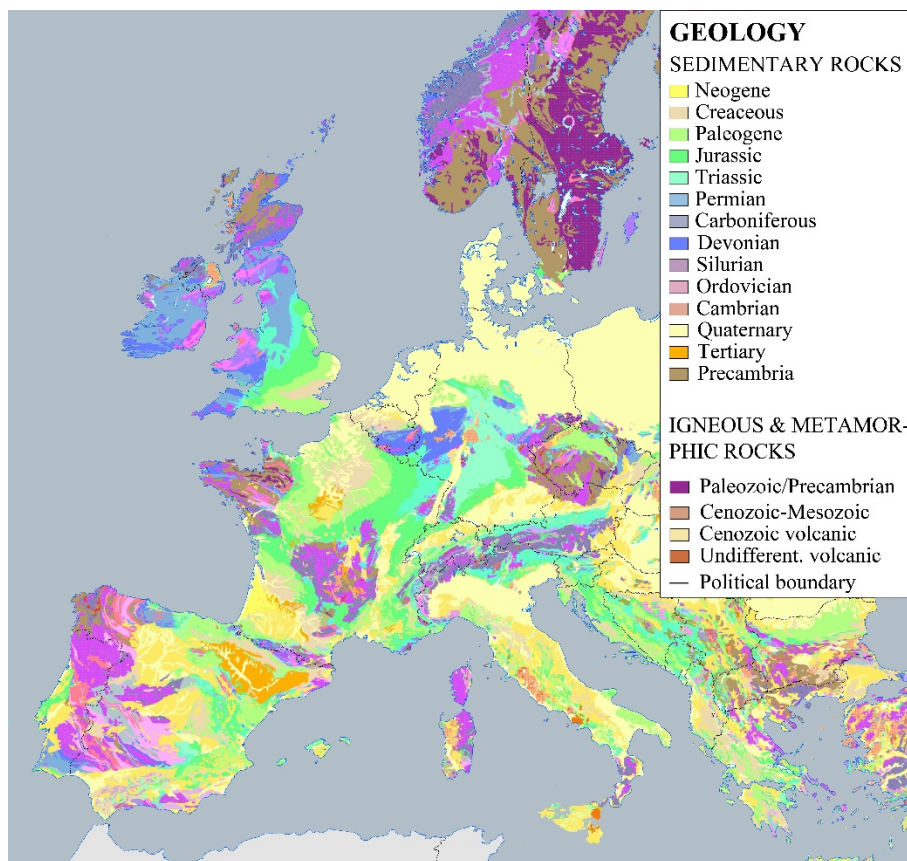


Figure 2. Geologic map of Europe; redrawn from Pawlewicz *et al.* [38]

Strontium is transferred from rocks to water by weathering of minerals [35]. Due to its chemical similarity to calcium, strontium is absorbed, metabolized and stored by organisms along with calcium [39]. These reactions occur without significant fractionation of the  $n(^{87}\text{Sr})/n(^{86}\text{Sr})$  isotope amount ratio [40]. As a consequence, the strontium isotopic composition of water and aquatic organisms reflect the  $n(^{87}\text{Sr})/n(^{86}\text{Sr})$  isotope amount ratio of their natural environment. Therefore, the strontium isotopic system acts as a natural marker that allows source identification of biotic (e.g. fish, mussels) and abiotic (e.g. water, sediments) aquatic samples and has numerous applications in geology [41], hydrology [34, 42], ecology [6, 43] and food origin determination [44, 45, 46].

In recent years, technical improvements of analytical instruments enabled the determination of the variation of the  $n(^{88}\text{Sr})/n(^{86}\text{Sr})$  isotope amount ratios, which had previously been considered constant in nature [47, 48]. This ratio is conventionally expressed in the  $\delta$ -notation relative to the certified reference material NIST SRM 987. The reported natural variation of  $\delta(^{88/86}\text{Sr})_{\text{SRM987}}$  ranges from about -1.1 to +1.4 ‰ as a result of mass-dependant isotopic fractionation [49]. Thus, the  $\delta(^{88/86}\text{Sr})_{\text{SRM987}}$  isotope amount ratio represents a novel isotopic system for the investigation of ecosystem processes that induce isotopic fractionation.

### *Strontium isotopic and elemental fingerprints for source determination in aquatic ecosystems*

The combination of the  $n(^{87}\text{Sr})/n(^{86}\text{Sr})$  isotopic and elemental pattern provides additional information on environmental sources determining the chemical composition of samples in aquatic ecosystems. For example, in hydrologic studies the strontium isotopic and elemental composition of rivers can be used to infer minerals forming the lithology of the drainage basin [12, 50]. Furthermore, studies showed that groundwater reflected the isotopic and elemental pattern of the aquifer host rock material [46]. Changes of the  $n(^{87}\text{Sr})/n(^{86}\text{Sr})$  isotope amount ratio and elemental content of groundwater along subsurface flow paths can be used for the determination of mixing of distinct water sources with different chemical composition [34]. Consequently, the  $n(^{87}\text{Sr})/n(^{86}\text{Sr})$  isotopic and elemental pattern have potential for the investigation of weathering processes and of water origin, quality and movement.

A valid interpretation of the strontium isotopic and elemental composition of water for solute source determination requires a sound knowledge of the potential hydrogeochemical processes along flow paths. These challenges can be addressed by the combination of  $n(^{87}\text{Sr})/n(^{86}\text{Sr})$ ,  $\delta(^{88/86}\text{Sr})_{\text{SRM987}}$  and elemental pattern as demonstrated in *PUBLICATION III*.

Provided that two water bodies show different natural geochemical signatures, tissues of aquatic organisms such as fish, which stayed a sufficient amount of time in those environments to absorb the local chemical tag, differ in their strontium isotopic and elemental pattern as well. This natural isotopic and elemental *fingerprint* in fish can be used to distinguish between fish stocks and fish products from different geologic areas [44, 45, 51]. Analysis of the otoliths (earstone) of fish provides additional information on habitat changes. Otoliths are calcified structures that grow in incremental layers, similar to tree rings (Figure 3, [6]). During growth, strontium isotopic and elemental pattern of the environment are incorporated and stored in the otolith [6]. Analysis of the chemical composition of otoliths along the growing line by techniques such as laser-ablation inductively coupled mass spectrometry (LA-ICP-MS) can reveal changes in the geochemical signatures incorporated from the environment over time. This has the potential to investigate fish migration between geologically distinct regions [6, 52].

Origin determination of fish and fish products is performed by comparing the  $n(^{87}\text{Sr})/n(^{86}\text{Sr})$  isotopic and elemental composition of the sample to the water of assumed origin. Source identification is successful if the chemical pattern of fish and water are in agreement within limits of measurement uncertainty. (This procedure is similar to forensic studies, where the fingerprint found at the crime scene is compared to the fingerprint of the suspect.)



Figure 3. Otolith cross-section of a brown trout *Salmo trutta f.f.*; figure from Irrgeher [53]

For example, Hegg *et al.* used geochemical signatures of otoliths and river water to identify birthplaces of salmon in the USA [54]. Zitek *et al.* analysed the  $n(^{87}\text{Sr})/n(^{86}\text{Sr})$  and elemental composition of water from fish farms and natural rivers in Austria. A subsequent comparison of the chemical signatures of otoliths and water allowed them to distinguish between fish of wild and of farmed origin [45].

Consequently, source determination of fish and fish products requires a database of the strontium isotopic and elemental composition of water to which an unknown test sample can be compared to. When dealing with isotopes, these comparative databases are called *isoscapes*, originating from the combination of the words 'isotopic' and 'landscape'. In the case of elements these databases are referred to as *elemental distribution maps* [55]. Aquatic isoscapes of the  $n(^{87}\text{Sr})/n(^{86}\text{Sr})$  isotopic composition of water were developed on different scales ranging from river systems [54, 56] to an UK-wide  $n(^{87}\text{Sr})/n(^{86}\text{Sr})$  isoscape for water samples [57] to a EU-wide strontium isoscape for groundwater [58].

The creation of a sound reference map is the fundamental basis for geographic origin determination and is demonstrated on the example of the Danube River in *PUBLICATION IV*. The application of an aquatic isoscape to determine the origin of fish from the Alpine foreland of Bavaria, Germany is the topic of *PUBLICATION V*.

The use of enriched stable isotopes to tag fish represents another application of strontium isotopic signatures for stock identification. For this, a spike, *i.e.* a solution containing strontium isotopes with a distinctly different isotopic composition than the natural environment, is administered to female spawners. The artificial isotopic tag is taken up by the fish, transferred into fish eggs by physiological processes, where it forms the inner core of the otolith of the offspring [43, 59]. This technique allows marking a large amount of fish larvae and represents an additional method for studying natural population processes, monitoring of restocking programs or identifying the origin of fish for food authentication [43].

## Analysis of strontium isotope amount ratios and elemental pattern

Sound data form the basis for valid interpretations of ecological processes. *Analytical ecogeochemistry* is an emerging discipline addressing this requirement [13]. It focuses on the development and application of modern analytical methods for the reliable measurement of isotope amount ratios and elemental pattern at trace levels in abiotic and biotic media [60].

### *Determination of elemental pattern for source identification*

Natural samples, such as water or aquatic organisms, absorb elements from their surrounding environment. The incorporated elemental pattern represents a natural tag which can be used for source determination of the investigated sample. Table 3 shows selected analytical methods for the determination and quantification of elements in liquid (water) or solid (animals, plants, sediments) samples of the aquatic environment. These instrumental techniques generate and measure *signals* that are specific for a given element such as the absorbed or emitted electromagnetic radiation or the relationship between the atomic mass and the number of its elementary charge [61]. A detailed description of the selected analytical methods can be found in literature such as Skoog and Leary [61], Lajunen and Perämäki [62], Hahn *et al.* [63] or Jakubowski *et al.* [64, 65].

Every analytical technique has its specific analytical characteristics, capabilities and costs. For example, X-ray fluorescence (XRF) instruments are robust, cost effective and portable, allowing for the analysis of major constituents of solid samples such as sediments [66] or filter deposits [67]. Laser induced breakdown spectroscopy (LIBS) can be operated in the laboratory or in the field allowing for the simultaneous detection of multiple elements down to  $\mu\text{g g}^{-1}$  levels in solid and liquid samples [63].

Analytical technique	Signal	Sample type	Working range	Coupling	Price
X-ray fluorescence (XRF)	Electromagnetic radiation	solid	$\text{mg g}^{-1}$ - $\text{g g}^{-1}$	no	€
Atomic absorption spectrometry (AAS)	Electromagnetic radiation	liquid	$\mu\text{g g}^{-1}$ - $\text{mg g}^{-1}$	yes	€
Optical emission spectrometry (OES)	Electromagnetic radiation	liquid/solid	$\text{ng g}^{-1}$ - $\text{mg g}^{-1}$	yes	€€
Laser induced breakdown spectroscopy (LIBS)	Electromagnetic radiation	liquid/solid	$\mu\text{g g}^{-1}$ - $\text{mg g}^{-1}$	yes	€€€
Inductively coupled plasma mass spectrometry (ICP-MS)	Mass to charge	liquid/solid	$\text{fg g}^{-1}$ - $\text{mg g}^{-1}$	yes	€€€

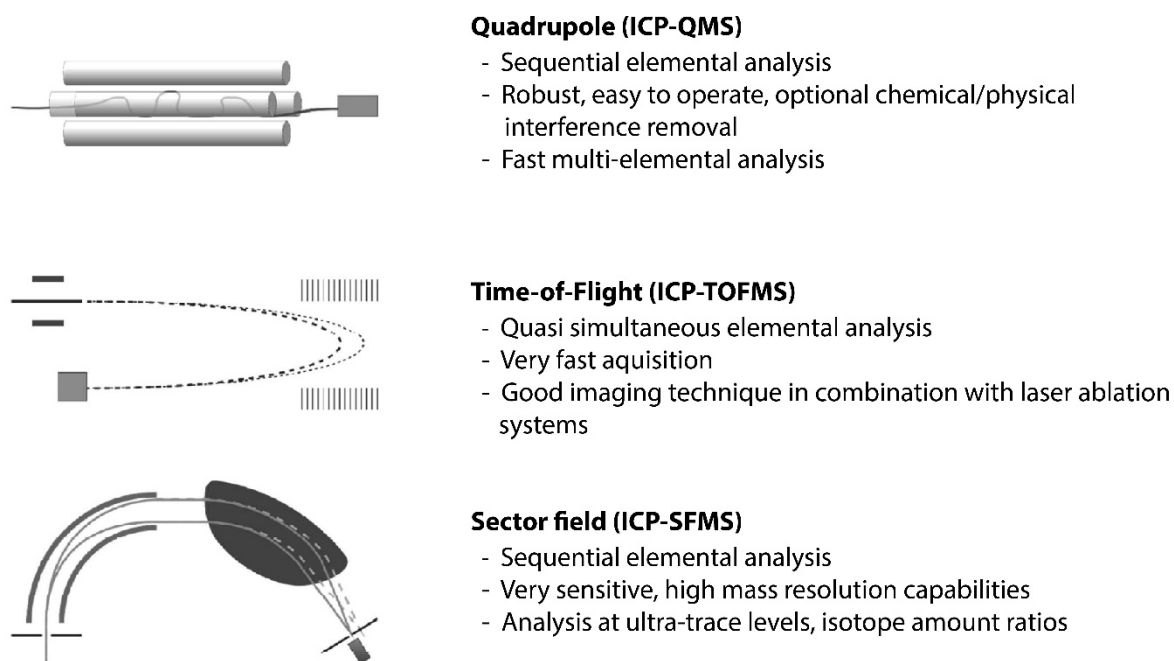
Table 3. Overview of analytical techniques for elemental analysis of environmental samples; data from Skoog and Leary [61], Friedbacher and Rosenberg [68], Hahn *et al.* [63], Limbeck [69] and Jakubowski *et al.* [65]



Sample preparation prior to the analysis, e.g. by digestion of solid samples using acids and heat, or hyphenation (coupling) of analytical instruments to additional analytical devices can further expand the spectrum of analytes and applications, as well as, costs. Consequently, analytical instruments and procedures have to be chosen thoughtfully based on the requirements needed.

Due to its outstanding analytical characteristics inductively coupled plasma mass spectrometry (ICP-MS) is one of the most powerful analytical techniques for multi-elemental analysis [65, 70, 71]. It facilitates the determination of nearly all elements of the periodic table with their isotopic composition, offers detection limits up to  $\text{fg g}^{-1}$  levels and a dynamic range of more than nine orders of magnitude [65]. Furthermore, an important feature of ICP-MS is its capability to be coupled to a variety of sample introduction systems.

For an ICP-MS analysis, the sample is introduced into an argon plasma. This charged gaseous matter contains charged particles, free ions and free electrons at temperatures of almost 10000 K. The plasma vaporises, atomises and ionises the introduced sample. The formed ions are then transferred from the plasma into the mass separator, where ions are separated according to their mass to charge ratio ( $m/z$ ). Figure 4 illustrates the three different types of mass separators applied in ICP-MS instruments, their particular features and fields of application. Finally, ions are detected using a secondary electron multiplier or in some set-ups (also) Faraday cups. The generated electronic signal is interpreted by computer software providing information on the amount of ions present in a sample [65].



**Quadrupole (ICP-QMS)**

- Sequential elemental analysis
- Robust, easy to operate, optional chemical/physical interference removal
- Fast multi-elemental analysis

**Time-of-Flight (ICP-TOFMS)**

- Quasi simultaneous elemental analysis
- Very fast acquisition
- Good imaging technique in combination with laser ablation systems

**Sector field (ICP-SFMS)**

- Sequential elemental analysis
- Very sensitive, high mass resolution capabilities
- Analysis at ultra-trace levels, isotope amount ratios

Figure 4. Schematic figure of quadrupole, time-of-flight and sector field based ICP-MS instruments; figures and description based on Frick [72]

The coupling of ICP-MS and laser ablation systems (LA-ICP-MS) facilitates the direct analysis of solid samples by focused laser irradiation [70]. Laser ablation spots can be as small as 1  $\mu\text{m}$  in diameter, allowing for the creation of microscale images of the chemical composition of solid samples [72]. Hyphenation of ICP-MS to high pressure liquid chromatographic (HPLC) systems offers the possibility to separate individual chemical components from a liquid sample mixture prior to analysis by the mass spectrometer [70]. These features made ICP-MS a versatile analytical technique with manifold applications in material research, nuclear science, life sciences, environmental science and food origin determination [70, 71, 73].

#### *Analytical challenges in element pattern determination of natural samples*

Accurate quantification of the elemental content in a sample by any analytical technique requires an appropriate calibration strategy. Ideally, quantification is performed by analysis of a measurement standard (*i.e.* a sample with known elemental content) to which a sample with unknown elemental content can be compared to. If possible, calibration should be performed using *reference materials* provided with a certificate stating the exact elemental content, the uncertainty of the given value and a statement on the metrological traceability. The latter confirms that the given elemental content (in *e.g.*  $\text{mg kg}^{-1}$ ) is traceable to the corresponding SI unit (*i.e.* the kilogram) according to the International System of Units [74].

In ICP-MS the ionisation of the analyte is influenced by the sample *matrix*, which is the physical and chemical composition of the sample [75]. Therefore, optimal quantification is achieved when samples and reference materials have identical matrices. Furthermore, the use of appropriate internal standards in order to monitor a) signal fluctuations and b) matrix-induced signal reduction or enhancement represents another prerequisite for accurate quantification of the elemental content of a sample.

Environmental samples of the aquatic ecosystem have very diverse matrixes, ranging from turbid water to fat rich tissues of aquatic animals. In contrast, the majority of commercially available measurement standards are aqueous solutions of 2 % nitric acid ( $\text{HNO}_3$ , *w/w*), which contain a specified amount of dissolved elements. (Note: Most elements are stable in a weak acidic solution.) Therefore, samples are subjected to *sample preparation* in order to remove the matrix prior to elemental measurements using the ICP-MS. This procedure highly depends on the type of sample and on the target analytes.

For example, sample preparation of river water for elemental analysis requires filtration, in order to remove sediments and microorganisms, followed by acidification to 2 %  $\text{HNO}_3$  (*w/w*). Conversely, determination of the bulk content of solid samples requires microwave assisted acid digestion using concentrated acids, heat and pressure in order to break chemical bonds. The product of the digestion procedure is a clear highly acidic solution, which has to be adjusted to 2 %  $\text{HNO}_3$  (*w/w*) before measurement. In case of very complex matrices,

measurement standards can be prepared in the same matrix as the sample (matrix-matching) in order to minimize possible matrix effects. This calibration method is frequently used for techniques such as LA-ICP-MS where solid samples are analysed or in cases where only a limited number of calibration standards is available.

Furthermore, natural samples contain elements in different concentrations. For example, calcium can occur in river water at elemental mass fractions of about 10000 ng g<sup>-1</sup>, while the elemental content of lead or cadmium of the same water can be below 0.1 ng g<sup>-1</sup> [76]. In addition, the amount of a certain element varies within the same sample type. *E.g.* the elemental content of strontium in river water can vary between 0.05-800 µg g<sup>-1</sup> [35, 76]. Consequently, it is necessary to prepare calibration standards with different concentrations in order to generate a calibration function that allows the quantification of low and high elemental content. Additional preparation steps such as dilution of highly concentrated samples or enrichment of elements which occur only at trace levels might be required.

When analysing samples with complex matrices, analytical chemists have to consider potential *spectroscopic interferences*. In that case, the analyte signal is disturbed by other components present in the sample [64, 75]. These components could be isobaric atomic ions (*i.e.* monoatomic single charged ions of a neighbouring element having similar masses, *e.g.* interference of <sup>87</sup>Rb<sup>+</sup> on <sup>87</sup>Sr<sup>+</sup>), monoatomic multiply charged ions (<sup>138</sup>Ba<sup>++</sup> can hamper the detection of <sup>69</sup>Ga<sup>+</sup>) and polyatomic ions (<sup>75</sup>As<sup>+</sup> suffers from interference of <sup>40</sup>Ar<sup>35</sup>Cl<sup>+</sup> in chlorine containing solutions). Several strategies are discussed in literature on how to overcome spectroscopic interferences [64, 77]. One of the most important approaches is the proper tuning of the analytical instrument, followed by the measurement of several isotopes of the element of interest in order to detect potential interferences. Subsequently, the isotope that is least interfered by ions of similar mass should be chosen for quantification, though in many cases this will not be the most abundant one. Other solutions include mathematical correction of spectral interferences, matrix separation prior to analysis as well as the use of mass spectrometers, which are capable of removing interfering ions. This can be achieved by the use of collision/reaction cells within the mass spectrometer (*e.g.* in ICP-QMS) or increased mass resolution (*e.g.* in ICP-SFMS) [77]. Consequently, elemental pattern analysis requires careful development of analytical procedures which are fit-for-the-intended-use.

In aquatic ecosystem research, (LA)-ICP-MS was successfully applied to the determination of elemental pattern in a variety of samples including surface water [78, 79, 80], groundwater [81, 82, 83], seawater [84, 85, 86], sediments [87, 88], soft tissues of aquatic animals [89, 90], fish eggs [44] and otoliths [45, 91, 92].

### *Analysis of strontium isotopic pattern for source determination*

Natural samples reflect the strontium isotopic pattern of their geochemical environment. This natural isotopic fingerprint can be used to establish a direct link between the sample and its environment of origin. The  $n(^{87}\text{Sr})/n(^{86}\text{Sr})$  isotope ratio varies in nature between 0.70 – 0.78 [58, 93] as a result of natural radiogenic processes and mass-dependant isotopic fractionation [94]. In areas with similar geology, differences between the strontium isotope ratios of natural samples are even less pronounced. Therefore, analytical techniques capable of *accurate* and *precise* determination of strontium isotope amount ratios down to the fourth and fifth decimal place are required for source determination.

Thermal ionisation mass spectrometry (TIMS) and multi-collector inductively coupled plasma mass spectrometry (MC ICP-MS) represent two state-of-the-art techniques that allow isotope determination with high-precision reaching 0.001% (*i.e.* precise determination up to the 6<sup>th</sup> decimal place). TIMS and MC ICP-MS are sector field based mass spectrometric techniques (compare Figure 5). Sample ions are separated according to their mass to charge ratio using a magnetic field, which once tuned for a specific range of isotopes is kept constant [14]. This creates multiple ion beams which are then detected simultaneously by an array of detectors (usually Faraday cups and/or multiple ion counters).

The main difference between TIMS and MC ICP-MS instruments is the type of ion source used for the ionisation of the sample. In TIMS ions are formed on a heated filament (*i.e.* a metal wire with a high melting point) in ultra-high vacuum. This technique allows for the determination of positive and negative sample ions, offering stable ion beams and comparably low *instrumental isotopic fractionation* (IIF) [95]. IIF is the sum of effects in mass spectrometry leading to a difference of the measured isotope amount ratio from the true isotope amount ratio in the sample [96]. Disadvantages of TIMS are the requirement for extensive sample preparation, long measurement time and the fact that TIMS instruments cannot be coupled to sample introduction sources such as laser ablation systems [14, 97].

In MC ICP-MS instruments ions form in an Ar plasma at temperatures of 10000 K under ambient pressure. The sampling interface extracts ions from the plasma and guides them into the mass analyser, which operates at ultra-high vacuum. This process requires the transmission of ions through a series of instrumental compartments with gradually reduced pressure. There, space-charge effects can lead to preferential transmission of heavy ions through the sampling interface region in comparison to light ions [97]. This results in a higher degree of instrumental isotopic fractionation compared to TIMS instruments [98], but can be corrected for using appropriate calibration strategies and mathematical instrumental isotopic fractionation correction [97].

Consequently, MC ICP-MS allows the determination of isotope ratios with high precision and accuracy, offering simple sample introduction, high sample throughput, high mass resolution

and the possibility to hyphenate the instrument to e.g. laser ablation systems [65, 97]. This made MC ICP-MS the method of choice for the determination of strontium isotope ratios in liquid and solid samples of the aquatic ecosystem [48, 58, 91, 99].

#### *Important considerations for accurate and precise strontium isotope ratio determination*

In order to achieve accurate and precise isotope ratio determination the procedure has to be under full analytical control. In the first step, the instrument parameters have to be fully optimized ensuring (1) stable signals and high sensitivity for the isotopes of interest; (2) low blanks; (3) flat-top peaks for all isotopes; (4) proper calibration of gain factors of the Faraday cups; (5) adequate measurement time for each run to achieve acceptable counting statistics; and (6) appropriate wash solutions and wash time in order to reduce possible contamination from preceding samples [97].

Furthermore, especially the presence of rubidium and calcium in the sample can lead to isobaric and polyatomic interferences (e.g.  $^{87}\text{Rb}^+$  on  $^{87}\text{Sr}^+$  or  $^{44}\text{Ca}^{40}\text{Ar}^+$ ,  $^{46}\text{Ca}^{40}\text{Ar}^+$ ,  $^{43}\text{Ca}^{44}\text{Ca}^+$  and  $^{44}\text{Ca}^{44}\text{Ca}^+$  on  $^{84}\text{Sr}^+$ ,  $^{86}\text{Sr}^+$ ,  $^{87}\text{Sr}^+$  and  $^{88}\text{Sr}^+$ ) [100]. Therefore, a pre-requisite for accurate determination of strontium isotope ratios is the separation of strontium from the sample matrix prior to mass spectrometric analysis. This procedure is usually accomplished by extraction chromatography using a strontium specific resin (e.g. Sr.Spec produced by TrisKem International [101]). More recently, Retzmann *et al.* developed a fully automated extraction method for strontium using DGA resin (TrisKem International) integrated in the prepFAST-MC™ system produced by Elemental Scientific [102]. The applied separation procedure has to ensure highest recovery rates (*i.e.* preferably no loss of strontium) and lowest residual Rb and Ca mass content in the separated strontium fraction. Furthermore, minor isobaric interferences of krypton (*i.e.*  $^{84}\text{Kr}^+$  and  $^{86}\text{Kr}^+$  on  $^{84}\text{Sr}^+$  and  $^{86}\text{Sr}^+$ ), which can be present at trace levels in argon gas used for plasma generation, can be corrected for by e.g. subtraction of the corresponding intensities measured in a blank solution [89].

Finally, accurate determination of strontium isotope ratios requires a sound calibration strategy. This procedure focuses on the correction of the instrumental isotopic fractionation (see previous chapter). This requires the analysis of the measurand (isotope ratio of interest in the sample) and the calibrant (reference isotope ratio in a standard or sample) by MC ICP-MS. This process can be performed simultaneously or sequentially, which is often referred to as internal or external calibration [74]. Traditionally, the variation of the radiogenic strontium isotope amount ratio is expressed in the absolute isotope ratio notation, *i.e.*  $n(^{87}\text{Sr})/n(^{86}\text{Sr})$ . Therefore, the measured signals of the isotopes of strontium have to be mathematically corrected for the influence of the blank, residual  $^{87}\text{Rb}$  and the IIF.

Several IIF correction strategies are available out of which the most important are 1) internal intra-elemental correction (via  $^{88}\text{Sr}/^{86}\text{Sr}$ ); 2) external intra-elemental correction (standard-

sample bracketing) using the isotope certified reference material NIST SRM 987; and 3) internal inter-elemental correction using a combination of the standard-sample bracketing technique with zirconium (Zr) used as internal standard [74]. Consequently, different data correction approaches are used within the analytical community. As a result, reported absolute strontium isotope amount ratios can be difficult to compare.

In recent years efforts were made to promote the reporting of isotope amount ratios relative to an internationally accepted isotopic certified reference material. This procedure facilitates transparency and comparability of measurement results on an international level [74]. Hence, strontium isotope ratios are increasingly expressed relative to the isotopic certified reference material NIST SRM 987, *i.e.* as  $\delta(^{87/86}\text{Sr})_{\text{SRM987}}$  and  $\delta(^{88/86}\text{Sr})_{\text{SRM987}}$  values. In this way, the ‘delta values’ account for all IIF effects as they affect the sample and reference material in the same way.

Successful applications of MC ICP-MS and LA-MC ICP-MS for source determination of samples of the aquatic ecosystem using strontium isotope amount ratios were reported for precipitation [103], river water [12, 50, 54, 104, 105, 106, 107], groundwater [34, 46], sediments [108], seawater [109], fossil shells [110], modern gastropod shells [111], deep sea corals [112], wild fish [51, 54], fish from aquaculture production [45], isotopically labeled fish [45, 59] and fish eggs [44].

#### *Uncertainty considerations*

The uncertainty indicates the quality of the reported analytical result. According to the EURACHEM/CITAC the *uncertainty* is “A parameter associated with the result of a measurement that characterises the dispersion of the values that could reasonably be attributed to the measurand.” [113]. This *parameter* can be a standard deviation or the width of a confidence interval. The *measurand* can be the elemental mass fraction of an element or the strontium isotope amount ratio of a natural sample. Consequently, the uncertainty is a value, which sets the limits within which an analytical result is regarded as accurate (*i.e.* precise and true) [71].

The measurement uncertainty is determined in a step-by-step mathematical procedure taking into account the uncertainties of all input variables used in the calculation of the final result. These could be the uncertainty of the used pipette, the blank, the measurement precision of the instrument, the reference values used for calibration or the applied correction strategy [114]. This procedure provides information about the contribution of each individual variable to the final measurement uncertainty. This is particularly useful in method development, as the analytical protocol can be adjusted in order to achieve an acceptable level of measurement uncertainty (*e.g.* by using a more precise balance or application of a procedure ensuring better

sample homogeneity) [113]. The final result of this procedure is the expanded combined uncertainty of an analytical result with a confidence level of 95 %.

Three major approaches are used in order to calculate the uncertainty of analytical results: 1) the 'GUM approach', performed by manual calculations or commercial software [115]; 2) the 'Kragten's method' based on simple spread sheet calculations [116]; and 3) the 'Monte Carlo approach', performed via open-source or commercially available software [117]. While the first two methods propagate uncertainties of individual sources by partial derivatives, the third method is based on the propagation of distributions [114].

Once the evaluation of the uncertainty of the results of a particular measurement procedure is accomplished, the uncertainty estimate obtained can be reliably applied to subsequent measurement results in the same laboratory, given the applied protocol is under full analytical control [113]. Consequently, the uncertainty of analytical results gives a clear indication of the quality of the data and enables the comparison of results independent of the used analytical method.

## Chemometrics

Mass spectrometric analysis allows accurate and precise determination of the strontium isotopic and elemental composition of natural samples. The thereby obtained dataset consists of *multivariate data* (*i.e.* has more than one variable), which can provide useful information about a property or the history of a sample. This information can be revealed by *chemometrics*, which is a chemical discipline that uses statistical and mathematical methods to extract relevant information from chemical data (Figure 5, [118]).

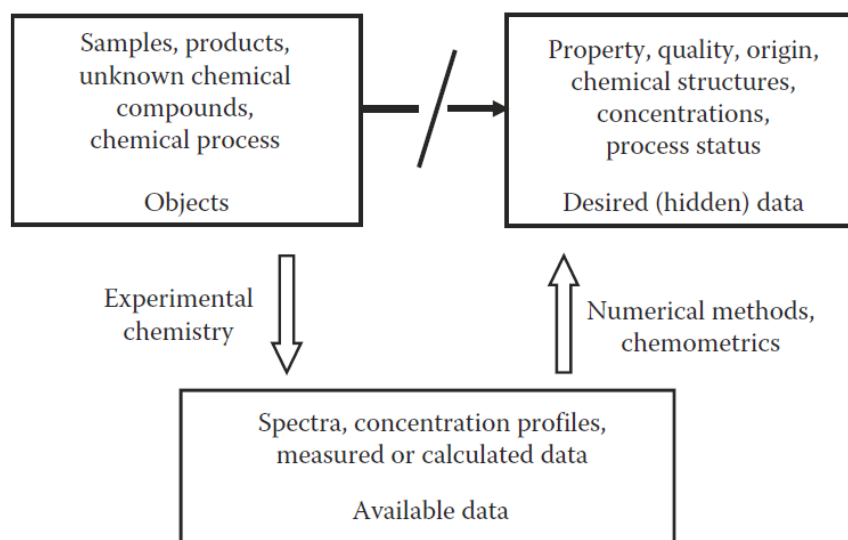


Figure 5. Desired information from natural samples (objects) can often not be assessed directly, but can be modelled or predicted using chemometric methods; figure from Varmuza and Filzmoser [118]

Chemometric tools are based on the combination of mathematical methods and statistical software to perform calculations on the often very large amount of data [119]. The most important mathematical procedures include a) statistical tests; b) data preprocessing; c) principal component analysis; d) calibration; e) classification; and f) cluster analysis [118, 120]. In order to perform these calculations, a multitude of software environments is available comprising of commercial software such as Microsoft Excel, SPSS and Matlab, and open source software such as R and OCTAVE [118, 119].

A prerequisite for any chemometric investigation is good quality data and a well-defined research question, which can then be investigated using a suitable mathematical method. In aquatic ecosystem studies focusing on the chemical composition of natural samples such a research question could be "What is the contribution of wet precipitation and bedrock dissolution to the  $n(^{87}\text{Sr})/n(^{86}\text{Sr})$  isotope amount ratio of groundwater?". The contribution of two components to a mixture can be calculated by mixing model calculations based on simple algebra, provided that the  $n(^{87}\text{Sr})/n(^{86}\text{Sr})$  isotopic and strontium elemental composition of both components (precipitation, bedrock) and the mixture (groundwater) is known [12]. Other



research questions can involve more variables. For example, “Can fish from different water bodies be distinguished based on their  $n(^{87}\text{Sr})/n(^{86}\text{Sr})$  and elemental composition?” This question can be addressed by classification methods such as linear discriminant analysis, aiming at generating a linear discriminant function that can be used for classification of samples based on their chemical composition [45]. Some tasks require a modelling approach. For example, in fish marking experiments the research question could be “How much strontium from a strontium double spike solution administered to a female spawner was transferred into fish eggs?” This research question cannot be solved using linear algebra, as the elemental mass fraction of strontium, which was actually absorbed by the fish from the administered double spike solution and transferred in the fish eggs, is unknown. This mathematical problem can be solved by multiple regression analysis using the strontium isotopic amount ratios of the spike and the sample as input variables [59]. This approach is known as isotope pattern deconvolution (IPD) and was successfully used in studies using isotopically enriched spikes of a variety of elements for the investigation of metabolic [121, 122, 123], technological [124] and environmental processes [125, 126, 127, 128, 129, 130].

#### *Chemometric challenges in source identification*

Chemometrics is a powerful tool that can be used to reveal ‘hidden’ information in chemical data [118]. However, some approaches have limitations when it comes to source determination of samples formed by mixing of several natural components. For example, traditional mixing model calculations use two variables, thus can only determine the contribution of two components to a mixture. Referring to the groundwater example in the previous paragraph, this would mean that contributions from e.g. irrigation or subsurface groundwater flow would not be accounted for. However, neglecting these additional sources to the chemical composition of groundwater could limit the validity of the results.

Furthermore, fish provenance studies are based on the assumption that fish absorb the geochemical signature of their habitat. This environmental tag can be used for classification of fish according to their water body of origin. However, in aquaculture production, fish are fed with commercial fish feed, which is usually of non-local origin. The feed represents an additional source of strontium isotopes and elements. Thus, the resulting isotopic and elemental pattern of fish is a mixture of the environmental tag and the fish feed. In addition, salt used for food processing represents a third source to the isotopic and elemental pattern of fish products. Consequently, in order to perform geographic origin determination of aquacultured fish and processed fish products the contribution of additional sources (fish feed, salt) to the chemical composition of the investigated sample has to be taken into account.

Finally, isotope pattern deconvolution is capable of determining the contribution of more than two components to the isotopic composition of a sample. A prerequisite for this is that the used

isotopic system has to display more than two isotopes and the isotopic variation between the components of interest has to be sufficiently high. These conditions are met for example by the strontium isotopic system consisting of four stable isotopes ( $^{84}\text{Sr}$ ,  $^{86}\text{Sr}$ ,  $^{87}\text{Sr}$ ,  $^{88}\text{Sr}$ ) and mixtures containing isotopically enriched spikes. However, in aquatic ecosystem research the isotopic variation of samples from different natural sources (e.g. water, fish feed, salt) is much lower compared to artificially prepared mixtures containing isotopically enriched material.

The potential and limitations of isotope pattern deconvolution to determine the contribution of individual natural sources to the  $n(^{87}\text{Sr})/n(^{86}\text{Sr})$  isotope amount ratio of fish samples were investigated in *PUBLICATION I*.

In order to facilitate traceability of processed fish products, a new mathematical method for the determination of strontium isotope amount ratios absorbed from ambient water into salted sturgeon caviar using reverse-mixing models was developed in *PUBLICATION II*.

## References

1. Chapin S, Matson P, Vitousek P. Principles of Terrestrial Ecosystem Ecology. New York Dordrecht Heidelberg London: Springer; 2011.
2. Tansley AG. The Use and Abuse of Vegetational Concepts and Terms. *Ecology*. 1935;16(3):284-307. doi: 10.2307/1930070.
3. Moss B. Ecology of Fresh Water: Man and Medium, Past to Future. 3rd ed. Oxford: Blackwell Scientific; 1998.
4. Doods W. Freshwater Ecology. San Diego: Academic Press; 2002.
5. Mortimer C, Müller U. Chemie. 8th ed. Stuttgart: Georg Thieme Verlag; 2003.
6. Campana SE. Chemistry and composition of fish otoliths: Pathways, mechanisms and applications. *Mar Ecol Prog Ser*. 1999;188:263-297. doi: 10.3354/meps188263.
7. Michener R, Lajtha K. Stable Isotopes in Ecology and Environmental Science. 2nd ed.: Blackwell Publishing; 2007.
8. Llull RM, Garí M, Canals M, et al. Mercury concentrations in lean fish from the Western Mediterranean Sea: Dietary exposure and risk assessment in the population of the Balearic Islands. *Environ Res*. 2017;158:16-23. doi: 10.1016/j.envres.2017.05.033.
9. Humborg C, Ittekkot V, Cociasu A, et al. Effect of Danube River dam on Black Sea biogeochemistry and ecosystem structure. *Natur*. 1997;386:385-388. doi: 10.1038/386385a0
10. Dawson T, Siegwolf R. Stable Isotopes as Indicators of Ecological Change. USA: Academic Press; 2007.
11. Sharp Z. Stable Isotope Geochemistry. USA: Pearson Education; 2007.
12. Faure G, Mensing T. Isotopes: principles and applications. 3rd ed. Hoboken, New Jersey: John Wiley & Sons; 2005.
13. Irrgeher J, Prohaska T. Application of non-traditional stable isotopes in analytical ecogeochemistry assessed by MC ICP-MS - A critical review. *Anal Bioanal Chem*. 2016;408(2):369-385. doi: 10.1007/s00216-015-9025-3.
14. Prohaska T. General Overview. In: Prohaska T, Irrgeher J, Zitek A, et al., editors. Sector Field Mass Spectrometry for Elemental and Isotopic Analysis. Cambridge 2015. p. 29-44.
15. Coplen TB, Böhlke JK, De Bièvre P, et al. Isotope-abundance variation of selected elements (IUPAC Technical Report). International Union of Pure and Applied Chemistry; 2002.
16. Wieser M, Holden N, Coplen T, et al. Atomic weights of the elements 2011 (IUPAC Technical Report). *Pure Appl Chem*. 2013;85(5):pp. 1047–1078. doi: 10.1351/PAC-REP-13-03-02.
17. Nakano T. Potential uses of stable isotope ratios of Sr, Nd, and Pb in geological materials for environmental studies. *Proceedings of the Japan Academy Series B, Physical and biological sciences*. 2016;92(6):167-184. doi: 10.2183/pjab.92.167.
18. Elliott T. The Isotope Geochemistry of Ni. In: Teng F-Z, Watkins J, Dauphas N, editors. Non-Traditional Stable Isotopes: De Gruyter; 2017.
19. Moynier F. The Isotope Geochemistry of Zinc and Copper. In: Teng F-Z, Watkins J, Dauphas N, editors. Non-Traditional Stable Isotopes: De Gruyter; 2017.
20. Rouxel O. Germanium Isotope Geochemistry. In: Teng F-Z, Watkins J, Dauphas N, editors. Non-Traditional Stable Isotopes: De Gruyter; 2017.
21. Stüeken E. Selenium Isotopes as a Biogeochemical Proxy in Deep Time. In: Teng F-Z, Watkins J, Dauphas N, editors. Non-Traditional Stable Isotopes: De Gruyter; 2017.
22. Kendall B. The Stable Isotope Geochemistry of Molybdenum. In: Teng F-Z, Watkins J, Dauphas N, editors. Non-Traditional Stable Isotopes: De Gruyter; 2017.

23. Blum J, Johnson M. Recent Developments in Mercury Stable Isotope Analysis. In: Teng F-Z, Watkins J, Dauphas N, editors. *Non-Traditional Stable Isotopes*: De Gruyter; 2017.
24. Nielsen S. Investigation and Application of Thallium Isotope Fractionation. In: Teng F-Z, Watkins J, Dauphas N, editors. *Non-Traditional Stable Isotopes*: De Gruyter; 2017.
25. Hoefs J. *Stable Isotope Geochemistry*. Springer; 2018. (8th, ed.).
26. Li W, Beard BL, Li S. Precise measurement of stable potassium isotope ratios using a single focusing collision cell multi-collector ICP-MS. *JAAS*. 2016;31(4):1023-1029. doi: 10.1039/c5ja00487j.
27. Rouxel O, Ludden J, Fouquet Y. Antimony isotope variations in natural systems and implications for their use as geochemical tracers. *ChGeo*. 2003;200(1):25-40. doi: 10.1016/S0009-2541(03)00121-9.
28. Horner TJ, Kinsley CW, Nielsen SG. Barium-isotopic fractionation in seawater mediated by barite cycling and oceanic circulation. *Earth Planet Sci Lett*. 2015;430:511-522. doi: 10.1016/j.epsl.2015.07.027.
29. Rickli J, Frank M, Halliday AN. The hafnium–neodymium isotopic composition of Atlantic seawater. *Earth Planet Sci Lett*. 2009;280(1):118-127. doi: 10.1016/j.epsl.2009.01.026.
30. Williams GA, Turekian KK. The glacial–interglacial variation of seawater osmium isotopes as recorded in Santa Barbara Basin. *Earth Planet Sci Lett*. 2004;228(3):379-389. doi: 10.1016/j.epsl.2004.10.004.
31. Shimizu H, Tachikawa K, Masuda A, et al. Cerium and neodymium isotope ratios and REE patterns in seawater from the North Pacific Ocean. *Geochim Cosmochim Acta*. 1994;58(1):323-333. doi: 10.1016/0016-7037(94)90467-7.
32. Clark I, Fritz P. *Environmental Isotopes in Hydrogeology*. New York: CRC Press LLC; 1997.
33. Kohl DH, Shearer GB, Commoner B. Fertilizer Nitrogen: Contribution to Nitrate in Surface Water in a Corn Belt Watershed. *Sci*. 1971;174(4016):1331-1334. doi: 10.1126/science.174.4016.1331.
34. Shand P, Darbyshire DPF, Love AJ, et al. Sr isotopes in natural waters: Applications to source characterisation and water–rock interaction in contrasting landscapes. *Appl Geochem*. 2009;24(4):574-586. doi: 10.1016/j.apgeochem.2008.12.011.
35. Capo RC, Stewart BW, Chadwick OA. Strontium isotopes as tracers of ecosystem processes: Theory and methods. *Geoderma*. 1998;82(1-3):197-225. doi: 10.1016/s0016-7061(97)00102-x.
36. Yaroshevsky AA. Abundances of chemical elements in the Earth's crust. *Geochemistry International*. 2006;44(1):48-55. doi: 10.1134/s001670290601006x.
37. Holden N. Total half-lives for selected nuclides. *Pure and Applied Chemistry: International Union of Pure and Applied Chemistry*; 1990. p. 941-958.
38. Pawlewicz M, Steinhouser D, Gautier D. *Map Showing Geology, Oil and Gas Fields, and Geologic Provinces of Europe including Turkey*. U.S. Geological Survey; 1971.
39. Aberg G. The use of natural strontium isotopes as tracers in environmental studies. *Water, Air, Soil Pollut*. 1995;79(1-4):309-322. doi: 10.1007/bf01100444.
40. Flockhart D, Kyser T, Chipley D, et al. Experimental evidence shows no fractionation of strontium isotopes ( $^{87}\text{Sr}/^{86}\text{Sr}$ ) among soil, plants, and herbivores: implications for tracking wildlife and forensic science. *Isot Environ Health Stud*. 2015;51(3):372-381. doi: 10.1080/10256016.2015.1021345.
41. Faure G, Powell JL. *Strontium Isotope Geology*. Berlin Heidelberg New York: Springer Verlag; 1972.
42. Woods T, Fullagar P, Spruill R, et al. Strontium Isotopes and Major Elements As Tracers of Ground Water Evolution: Example from the Upper Castle Hayne Aquifer of

- North Carolina. *Groundwater*. 2000;38(5):762-771. doi: 10.1111/j.1745-6584.2000.tb02712.x.
43. Zitek A, Irrgeher J, Cervicek M, et al. Individual-specific transgenerational marking of common carp, *Cyprinus carpio* L., using  $^{86}\text{Sr}/^{84}\text{Sr}$  double spikes. *Mar Freshw Res*. 2014;65(11):978-986. doi: 10.1071/mf13235.
  44. Rodushkin I, Bergman T, Douglas G, et al. Authentication of Kalix (N.E. Sweden) vendace caviar using inductively coupled plasma-based analytical techniques: Evaluation of different approaches. *Anal Chim Acta*. 2007;583(2):310-318. doi: 10.1016/j.aca.2006.10.038.
  45. Zitek A, Sturm M, Waidbacher H, et al. Discrimination of wild and hatchery trout by natural chronological patterns of elements and isotopes in otoliths using LA-ICP-MS. *Fish Manage Ecol*. 2010;17(5):435-445. doi: 10.1111/j.1365-2400.2010.00742.x.
  46. Montgomery J, Evans JA, Wildman G.  $^{87}\text{Sr}/^{86}\text{Sr}$  isotope composition of bottled British mineral waters for environmental and forensic purposes. *Appl Geochem*. 2006;21(10):1626-1634. doi: 10.1016/j.apgeochem.2006.07.002.
  47. Ohno T, Hirata T. Simultaneous determination of mass-dependent isotopic fractionation and radiogenic isotope variation of strontium in geochemical samples by multiple collector-ICP-mass spectrometry. *Anal Sci*. 2007;23(11):1275-1280. doi: 10.2116/analsci.23.1275.
  48. Fietzke J, Eisenhauer A. Determination of temperature-dependent stable strontium isotope ( $^{88}\text{Sr}/^{86}\text{Sr}$ ) fractionation via bracketing standard MC-ICP-MS. *GGG*. 2006;7(8). doi: 10.1029/2006gc001243.
  49. Neymark LA, Premo WR, Mel'Nikov NN, et al. Precise determination of  $\delta^{88}\text{Sr}$  in rocks, minerals, and waters by double-spike TIMS: A powerful tool in the study of geological, hydrological and biological processes. *JAAS*. 2014;29(1):65-75. doi: 10.1039/c3ja50310k.
  50. Palmer MR, Edmond JM. Controls over the strontium isotope composition of river water. *Geochim Cosmochim Acta*. 1992;56(5):2099-2111. doi: 10.1016/0016-7037(92)90332-D.
  51. Campana SE. Otolith Elemental Composition as a Natural Marker of Fish Stocks. *Stock Identification Methods 2005*. p. 227-245.
  52. Kennedy BP, Blum JD, Folt CL, et al. Using natural strontium isotopic signatures as fish markers: methodology and application. *Can J Fish Aquat Sci*. 2000;57(11):2280-2292.
  53. Irrgeher J. *Strontium Isotope Ratios as Tracers of Biological Migration*. Vienna: University of Natural Resources and Life Sciences Vienna; 2013.
  54. Hegg JC, Kennedy BP, Fremier AK. Predicting strontium isotope variation and fish location with bedrock geology: Understanding the effects of geologic heterogeneity. *ChGeo*. 2013;360-361:89-98. doi: 10.1016/j.chemgeo.2013.10.010.
  55. Bowen GJ, West JB, Hoogewerff J. Isoscapes: Isotope mapping and its applications. *J Geochem Explor*. 2009;102(3):v-vii. doi: 10.1016/j.gexplo.2009.05.001.
  56. Yang C, Telmer K, Veizer J. Chemical dynamics of the "St. Lawrence" riverine system:  $\delta\text{D H}_2\text{O}$ ,  $\delta^{18}\text{O H}_2\text{O}$ ,  $\delta^{13}\text{C DIC}$ ,  $\delta^{34}\text{S sulfate}$ , and dissolved  $^{87}\text{Sr}/^{86}\text{Sr}$ . *Geochim Cosmochim Acta*. 1996;60:851-866. doi: 10.1016/0016-7037(95)00445-9.
  57. Evans JA, Montgomery J, Wildman G, et al. Spatial variations in biosphere  $^{87}\text{Sr}/^{86}\text{Sr}$  in Britain. *J Geol Soc London*. 2010;167(1):1-4. doi: 10.1144/0016-76492009-090.
  58. Voerkelius S, Lorenz GD, Rummel S, et al. Strontium isotopic signatures of natural mineral waters, the reference to a simple geological map and its potential for authentication of food. *Food Chem*. 2010;118(4):933-940. doi: 10.1016/j.foodchem.2009.04.125.

59. Irrgeher J, Zitek A, Cervicek M, et al. Analytical factors to be considered for the application of enriched strontium spikes to monitor biological systems [10.1039/C3JA50212K]. *JAAS*. 2014;29(1):193-200. doi: 10.1039/c3ja50212k.
60. Zitek A, Irrgeher J, Prohaska T. Applications of isotopes in analytical ecogeochemistry. *Anal Bioanal Chem*. 2016;408(2):341-343. doi: 10.1007/s00216-015-9037-z.
61. Skoog D, Leary J. Principles of instrumental analysis. 4th ed. USA: Saunders College Publishing; 1992.
62. Lajunen L, Perämäki P. Spectrochemical analysis by atomic absorption and emission. 2nd ed. Cambridge: Royal Society of Chemistry; 2004.
63. Hahn DW, Omenetto N. Laser-Induced Breakdown Spectroscopy (LIBS), Part II: Review of Instrumental and Methodological Approaches to Material Analysis and Applications to Different Fields. *ApSpe*. 2012;66(4):347-419. doi: 10.1366/11-06574.
64. Jakubowski N, Prohaska T, Rottmann L, et al. Inductively coupled plasma- and glow discharge plasma-sector field mass spectrometry Part I. Tutorial: Fundamentals and instrumentation. *JAAS*. 2011;26(4):693-726. doi: 10.1039/c0ja00161a.
65. Jakubowski N, Horsky M, Ross P, et al. Inductively Coupled Plasma Mass Spectrometry. In: Prohaska T, Irrgeher J, Zitek A, et al., editors. *Sector Field Mass Spectrometry for Elemental and Isotopic Analysis*. Cambridge: The Royal Society of Chemistry; 2015. p. 208-318.
66. Cuculić V, Frančišković-Bilinski S, Bilinski H, et al. Multi-methodological approach to evaluate trace elements and major components in wetland system with subsaline and freshwater characteristics. *Environ Earth Sci*. 2016;75(20):1351. doi: 10.1007/s12665-016-6156-6.
67. Watson J, Chow C. Particle and Gas Measurement on Filters. *Environmental Sampling for Trace Analysis*: VCH Publishers Inc; 1994.
68. Friedbacher G, Rosenberg E. Lecture on Analytische Chemie- Physikalische Analyse. 4th ed. Vienna: Vienna University of Technology, Institut of Chemical Technologies and Analytics; 2003. (LVA-Nr. 164.048).
69. Limbeck A. Lecture on Methoden der Verteilungs- und Durchschnittsanalyse. LVA-Nr. 151.042 Werkstoff- und Strukturanalytik. Vienna: Vienna University of Technology, Institut of Chemical Technologies and Analytics; 2011.
70. Becker JS. *Inorganic Mass Spectrometry: Principles and Applications*. John Wiley & Sons Ltd; 2007.
71. Nelms S. *Inductively coupled plasma mass spectrometry handbook*. Oxford: Blackwell; 2005.
72. Frick D. Laser Ablation Inductively Coupled Plasma Mass Spectrometry. Workshop on Laser Ablation Inductively Coupled Plasma Mass Spectrometry. Federal Institute for Materials Research and Testing: ICP-MS Usermeeting Berlin; 2018.
73. Jakubowski N, Prohaska T, Vanhaecke F, et al. Inductively coupled plasma- and glow discharge plasma-sector field mass spectrometry Part II. Applications. *JAAS*. 2011;26(4):727-757. doi: 10.1039/c0ja00007h.
74. Irrgeher J, Vogl J, Santner J, et al. Measurement Strategies. In: Prohaska T, Irrgeher J, Zitek A, et al., editors. *Sector Field Mass Spectrometry for Elemental and Isotopic Analysis*. Cambridge 2015. p. 126-152.
75. Bürger S, Boulyga SF. Lecture on Advanced Analytical Techniques for Elemental Trace and Isotope Analysis. Vienna: University of Natural Resources and Life Sciences Vienna, Department of Chemistry; 2011.
76. Yeghicheyan D, Bossy C, Bouhnik Le Coz M, et al. A Compilation of Silicon, Rare Earth Element and Twenty-One other Trace Element Concentrations in the Natural River Water Reference Material SLRS-5 (NRC-CNRC). *Geostand Geoanal Res*. 2013;37(4):449-467. doi: 10.1111/j.1751-908X.2013.00232.x.

77. Prohaska T. Interferences. In: Prohaska T, Irrgeher J, Zitek A, et al., editors. *Sector Field Mass Spectrometry for Elemental and Isotopic Analysis*. Cambridge 2015. p. 121-125.
78. Alves RIS, Machado CS, Beda CF, et al. Water Quality Assessment of the Pardo River Basin, Brazil: A Multivariate Approach Using Limnological Parameters, Metal Concentrations and Indicator Bacteria. *Arch Environ Contam Toxicol*. 2018;75(2):199-212. doi: 10.1007/s00244-017-0493-7.
79. Wojcieszek J, Szpunar J, Lobinski R. Speciation of technologically critical elements in the environment using chromatography with element and molecule specific detection. *TrAC*. 2018;104:42-53. doi: 10.1016/j.trac.2017.09.018.
80. Romanovskiy KA, Bolshov MA, Münz AV, et al. A novel photochemical vapor generator for ICP-MS determination of As, Bi, Hg, Sb, Se and Te. *Talanta*. 2018;187:370-378. doi: 10.1016/j.talanta.2018.05.052.
81. Gitari MW, Akinyemi SA, Ramugondo L, et al. Geochemical fractionation of metals and metalloids in tailings and appraisal of environmental pollution in the abandoned Musina Copper Mine, South Africa. *Environ Geochem Health*. 2018. doi: 10.1007/s10653-018-0109-9.
82. He J, Ma J, Zhao W, et al. Groundwater evolution and recharge determination of the Quaternary aquifer in the Shule River basin, Northwest China. *HydJ*. 2015;23(8):1745-1759. doi: 10.1007/s10040-015-1311-9.
83. Négrel P, Petelet-Giraud E, Widory D. Strontium isotope geochemistry of alluvial groundwater: A tracer for groundwater resources characterisation. *HESS*. 2004;8(5):959-972.
84. Liu K, Gao X, Li L, et al. Determination of ultra-trace Pt, Pd and Rh in seawater using an off-line pre-concentration method and inductively coupled plasma mass spectrometry. *Chemosphere*. 2018;212:429-437. doi: 10.1016/j.chemosphere.2018.08.098.
85. Søndergaard J, Asmund G, Larsen MM. Trace elements determination in seawater by ICP-MS with on-line pre-concentration on a Chelex-100 column using a 'standard' instrument setup. *MethodsX*. 2015;2:323-330. doi: 10.1016/j.mex.2015.06.003.
86. Yang L, Nadeau K, Meija J, et al. Inter-laboratory study for the certification of trace elements in seawater certified reference materials NASS-7 and CASS-6. *Anal Bioanal Chem*. 2018;410(18):4469-4479. doi: 10.1007/s00216-018-1102-y.
87. Vodopivec C, Curtosi A, Pelletier E, et al. Element concentrations of environmental concern in surface sediment samples from a broad marine area of 25 de Mayo (King George) Island, South Shetland Islands. *ScTEen*. 2019;646:757-769. doi: 10.1016/j.scitotenv.2018.07.174.
88. Alkinani M, Merkel B. Geochemistry of sediments of the Al-Batin alluvial fan, Southern Iraq. *Environmental Earth Sciences*. 2018;77(7):282. doi: 10.1007/s12665-018-7461-z.
89. Irrgeher J, Prohaska T, Sturgeon RE, et al. Determination of strontium isotope amount ratios in biological tissues using MC-ICPMS. *Anal Methods*. 2013;5(7):1687-1694. doi: 10.1039/C3AY00028A.
90. Fahrenholtz S, Griesel S, Pröfrock D, et al. Essential and non-essential elements in tissues of harbour porpoises (*Phocoena phocoena*) stranded on the coasts of the North and Baltic Seas between 2004–2006. *J Environ Monit*. 2009;11(5):1107-1113. doi: 10.1039/b821504a.
91. Prohaska T, Irrgeher J, Zitek A. Simultaneous multi-element and isotope ratio imaging of fish otoliths by laser ablation split stream ICP-MS/MC ICP-MS. *JAAS*. 2016;31(8):1612-1621. doi: 10.1039/c6ja00087h.

92. McGowan N, Fowler A, Parkinson K, et al. Beyond the transect: An alternative microchemical imaging method for fine scale analysis of trace elements in fish otoliths during early life. *ScTEen*. 2014;494:177-186. doi: 10.1016/j.scitotenv.2014.05.115.
93. Bentley RA. Strontium isotopes from the earth to the archaeological skeleton: A review. *J Archaeol Method Theory*. 2006;13(3):135-187. doi: 10.1007/s10816-006-9009-x.
94. Horsky M, Irrgeher J, Prohaska T. Evaluation strategies and uncertainty calculation of isotope amount ratios measured by MC ICP-MS on the example of Sr. *Anal Bioanal Chem*. 2016;408(2):351-367. doi: 10.1007/s00216-015-9003-9.
95. Bürger S, Vogl J, Kloetzli U, et al. Thermal Ionisation Mass Spectrometry. In: Prohaska T, Irrgeher J, Zitek A, et al., editors. *Sector Field Mass Spectrometry for Elemental and Isotopic Analysis*. Cambridge 2015. p. 381-439.
96. Irrgeher J, Prohaska T. Instrumental Isotopic Fractionation. In: Prohaska T, Irrgeher J, Zitek A, et al., editors. *Sector Field Mass Spectrometry for Elemental and Isotopic Analysis*. Cambridge 2015. p. 107-121.
97. Yang L. Accurate and precise determination of isotopic ratios by MC-ICP-MS: A review. *Mass Spectrom Rev*. 2009;28(6):990-1011. doi: doi:10.1002/mas.20251.
98. Sahoo SK, Masuda A. Precise measurement of zirconium isotopes by thermal ionization mass spectrometry. *ChGeo*. 1997;141(1):117-126. doi: 10.1016/S0009-2541(97)00024-7.
99. Yang Z, Fryer BJ, Longerich HP, et al. 785 nm femtosecond laser ablation for improved precision and reduction of interferences in Sr isotope analyses using MC-ICP-MS. *JAAS*. 2011;26(2):341-351. doi: 10.1039/c0ja00131g.
100. Irrgeher J, Prohaska T, Sturgeon RE, et al. Determination of strontium isotope amount ratios in biological tissues using MC-ICPMS. *Analytical Methods*. 2013;5(7):1687-1694. doi: 10.1039/C3AY00028A.
101. Horwitz PE, Chiarizia R, Dietz ML. A novel strontium-selective extraction chromatographic resin. *Solvent Extr Ion Exch*. 1992;10(2):313-336. doi: 10.1080/07366299208918107.
102. Retzmann A, Zimmermann T, Pröfrock D, et al. A fully automated simultaneous single-stage separation of Sr, Pb, and Nd using DGA Resin for the isotopic analysis of marine sediments [J]. *Anal Bioanal Chem*. 2017;409(23):5463-5480. doi: 10.1007/s00216-017-0468-6.
103. Andersson P, Lofvendahl R, Åberg G. Major element chemistry,  $\delta^2\text{H}$ ,  $\delta^{18}\text{O}$  and  $^{87}\text{Sr}/^{86}\text{Sr}$  in a snow profile across Central Scandinavia. *Atmospheric Environ*. 1990;24:2601-2608. doi: 10.1016/0960-1686(90)90138-d.
104. Souza GFD, Reynolds BC, Kiczka M, et al. Evidence for mass-dependent isotopic fractionation of strontium in a glaciated granitic watershed. *Geochim Cosmochim Acta*. 2010;74(9):2596-2614.
105. Pearce CR, Parkinson IJ, Gaillardet J, et al. Reassessing the stable ( $\delta^{88}/^{86}\text{Sr}$ ) and radiogenic ( $^{87}\text{Sr}/^{86}\text{Sr}$ ) strontium isotopic composition of marine inputs. *Geochim Cosmochim Acta*. 2015;157:125-146. doi: 10.1016/j.gca.2015.02.029.
106. Wei G, Ma J, Liu Y, et al. Seasonal changes in the radiogenic and stable strontium isotopic composition of Xijiang River water: Implications for chemical weathering. *ChGeo*. 2013;343:67-75. doi: 10.1016/j.chemgeo.2013.02.004.
107. Krabbenhöft A, Eisenhauer A, Böhm F, et al. Constraining the marine strontium budget with natural strontium isotope fractionations ( $^{87}\text{Sr}/^{86}\text{Sr}^*$ ,  $\delta^{88}/^{86}\text{Sr}$ ) of carbonates, hydrothermal solutions and river waters. *Geochim Cosmochim Acta*. 2010;74(14):4097-4109. doi: 10.1016/j.gca.2010.04.009.
108. Boger P, Faure G. Strontium-Isotope Stratigraphy of a Red Sea Core. *Geo*. 1974;2(4):181-183. doi: 10.1130/0091-7613(1974)2.
109. Krabbenhöft A, Fietzke J, Eisenhauer A, et al. Determination of radiogenic and stable strontium isotope ratios ( $^{87}\text{Sr}/^{86}\text{Sr}$ ;  $\delta^{88}/^{86}\text{Sr}$ ) by thermal ionization mass spectrometry



- applying an  $^{87}\text{Sr}/^{84}\text{Sr}$  double spike. *JAAS*. 2009;24(9):1267-1271. doi: 10.1039/b906292k.
110. Veizer J, Ala D, Azmy K, et al.  $^{87}\text{Sr}/^{86}\text{Sr}$ ,  $\delta^{13}\text{C}$  and  $\delta^{18}\text{O}$  evolution of Phanerozoic seawater. *ChGeo*. 1999;161(1-3):59-88. doi: 10.1016/S0009-2541(99)00081-9.
  111. Christensen JN, Halliday AN, Lee D-C, et al. In situ Sr isotopic analysis by laser ablation. *Earth Planet Sci Lett*. 1995;136(1):79-85.
  112. Outridge P, Chenery S, Babaluk J, et al. Analysis of geological Sr isotope markers in fish otoliths with subannual resolution using laser ablation-multicollector-ICP-mass spectrometry. *Environ Geol*. 2002;42(8):891-899. doi: 10.1007/s00254-002-0596-x.
  113. Ellison SLR, Williams A. *EURACHEM/CITAC Guide: Quantifying Uncertainty in Analytical Measurement*. 3rd ed. 2012.
  114. Irrgeher J, Prohaska T. Metrology. In: Prohaska T, Irrgeher J, Zitek A, et al., editors. *Sector Field Mass Spectrometry for Elemental and Isotopic Analysis*. Cambridge 2015. p. 183-199.
  115. Evaluation of measurement data- Guide to the expression of uncertainty in measurements, *JCGM 100:2008*, (2008).
  116. Kragten J. Tutorial review. Calculating standard deviations and confidence intervals with a universally applicable spreadsheet technique. *Analyst*. 1994;119(10):2161-2165. doi: 10.1039/an9941902161.
  117. Couto P, Damasceno J, De Oliveira S. Monte Carlo Simulations Applied to Uncertainty in Measurement. In: Chan WK, editor. *Theory and Applications of Monte Carlo Simulations*: IntechOpen; 2013.
  118. Varmuza K, Filzmoser P. *Introduction to multivariate statistical analysis in chemometrics*. Boca Raton: CRC Press; 2008.
  119. Brereton R. *Chemometrics- Data Analysis for the Laboratory and Chemical Plant*. John Wiley & Sons Ltd; 2003.
  120. Miller J, Miller J. *Statistics and Chemometrics for Analytical Chemistry*. 4th ed.: Prentice Hall; 2000.
  121. Rodriguez-Gonzalez P, Garcia Alonso JI. Recent advances in isotope dilution analysis for elemental speciation. *JAAS*. 2010;25(3):239-259. doi: 10.1039/b924261a.
  122. Rodriguez-Castrillon JA, Moldovan M, Garcia Alonso JI, et al. Isotope pattern deconvolution as a tool to study iron metabolism in plants. *Anal Bioanal Chem*. 2008;390(2):579-590. doi: 10.1007/s00216-007-1716-y.
  123. Rodriguez-Castrillon J, Reyes L, Marchante-Gayon J, et al. Internal correction of spectral interferences and mass bias in ICP-MS using isotope pattern deconvolution: Application to the determination of selenium in biological samples by isotope dilution analysis. *JAAS*. 2008;23(4):579-582. doi: 10.1039/b716785g.
  124. Carames-Pasaron I, Rodriguez-Castrillon JA, Moldovan M, et al. Development of a Dual-Isotope Procedure for the Tagging and Identification of Manufactured Products: Application to Explosives. *AnaCh*. 2012;84(1):121-126. doi: 10.1021/ac201945g.
  125. Rodriguez-Gonzalez P, Bouchet S, Monperrus M, et al. In situ experiments for element species-specific environmental reactivity of tin and mercury compounds using isotopic tracers and multiple linear regression. *Environ Sci Pollut Res Int*. 2013;20(3):1269-1280. doi: 10.1007/s11356-012-1019-5.
  126. Rizzini Ansari N, Fernandez Iglesias N, Cordeiro RC, et al. Determination and speciation of cadmium in microcosms with *Bunodosoma caissarum* and *Perna perna* using isotopically enriched  $^{116}\text{Cd}$ . *Mar Pollut Bull*. 2017;115(1-2):362-368. doi: 10.1016/j.marpolbul.2016.12.010.
  127. Rodriguez-Castrillon JA, Moldovan M, Ruiz Encinar J, et al. Isotope pattern deconvolution for internal mass bias correction in the characterisation of isotopically enriched spikes. *JAAS*. 2008;23(3):318-324. doi: 10.1039/b710595a.

128. Castillo A, Rodriguez-Gonzalez P, Centineo G, et al. Multiple spiking species-specific isotope dilution analysis by molecular mass spectrometry: Simultaneous determination of inorganic mercury and methylmercury in fish tissues. *AnaCh.* 2010;82(7):2773-2783. doi: 10.1021/ac9027033.
129. Huelga-Suarez G, Fernandez B, Moldovan M, et al. Detection of transgenerational barium dual-isotope marks in salmon otoliths by means of LA-ICP-MS. *Anal Bioanal Chem.* 2013;405(9):2901-2909. doi: 10.1007/s00216-012-6452-2.
130. Huelga-Suarez G, Moldovan M, Garcia-Valiente A, et al. Individual-specific transgenerational marking of fish populations based on a barium dual-isotope procedure. *AnaCh.* 2012;84(1):127-133. doi: 10.1021/ac201946k.

## Publications

### I. Isotope pattern deconvolution of different sources of stable strontium isotopes in natural systems

Anastassiya Tchaikovsky, Johanna Irrgeher, Andreas Zitek and Thomas Prohaska  
*Journal of Analytical Atomic Spectrometry*, 2017 (published)

### II. Chemometric tools for determining site-specific elemental and strontium isotopic fingerprints in sturgeon caviar

Anastassiya Tchaikovsky, Andreas Zitek, Johanna Irrgeher, Christine Opper, Rudolf Scheiber, Karl Moder, Leonardo Congiu and Thomas Prohaska  
*European Food Research and Technology*, 2019 (submitted)

### III. Analysis of $n(^{87}\text{Sr})/n(^{86}\text{Sr})$ , $\delta^{88}\text{Sr}/^{86}\text{Sr}_{\text{SRM987}}$ and elemental pattern to characterise groundwater and recharge of saline ponds in a clastic aquifer in East Austria

Anastassiya Tchaikovsky, Hermann Häusler, Martin Kralik, Andreas Zitek, Johanna Irrgeher and Thomas Prohaska  
*Isotopes in Environmental and Health Studies*, 2019 (published)

### IV. The $^{87}\text{Sr}/^{86}\text{Sr}$ river water isoscape of the Danube catchment

Andreas Zitek, Anastassiya Tchaikovsky, Johanna Irrgeher, Herwig Waidbacher and Thomas Prohaska  
*Joint Danube Survey 3*, 2014 (published)  
ISBN: 978-3-200-03795-3

### V. The potential of $^{87}\text{Sr}/^{86}\text{Sr}$ and Sr elemental mass fractions in fish otoliths as a fisheries management tool in a European pre-alpine river catchment

Andreas Zitek, Johannes Oehm, Johanna Irrgeher, Michael Schober, Anastassiya Tchaikovsky, Anika Retzmann, Barbara Thalinger, Michael Traugott and Thomas Prohaska (in preparation)

All publishers gave the permission to reproduce published articles.

**I. Isotope pattern deconvolution of different sources of stable strontium isotopes in natural systems**

*Anastassiya Tchaikovsky, Johanna Irrgeher, Andreas Zitek and Thomas Prohaska*

*Journal of Analytical Atomic Spectrometry, 2017 (published)*

<http://dx.doi.org/10.1039/C7JA00251C>



Cite this: DOI: 10.1039/c7ja00251c

## Isotope pattern deconvolution of different sources of stable strontium isotopes in natural systems†

A. Tchaikovsky,<sup>a</sup> J. Irrgeher,<sup>b</sup> A. Zitek<sup>a</sup> and T. Prohaska<sup>\*a</sup>

Isotope pattern deconvolution (IPD) was used to determine the contribution of different Sr sources to the Sr isotopic composition of natural samples using the examples of sturgeon caviar and otoliths. For this purpose, the Sr isotopic composition of raw and salted sturgeon caviar, and otoliths as well as water, fish feed and salt (representing the assumed main contributors to the final isotopic composition of strontium in caviar) was analyzed using MC ICP-MS. The molar fractions and their uncertainties were determined using multiple-linear regression modeling and linear algebra calculations. The optimized approach was applied to caviar and otolith samples of different origin. The Sr isotopic composition of raw caviar and otoliths was formed of  $79.8 \pm 4.3\%$  Sr from water and  $20.2 \pm 4.3\%$  Sr from fish feed (1 SD,  $n = 5$ , between site variations). Deconvolution was possible even when the isotopic difference of the  $n(^{87}\text{Sr})/n(^{86}\text{Sr})$  between sources was less than 0.1%. The influence of salting on the isotopic composition of processed caviar accounted for up to almost 80% for samples treated with salt containing high concentrations of Sr. The developed methodology provides the basis for the accurate origin determination of samples by  $n(^{87}\text{Sr})/n(^{86}\text{Sr})$  isotopic-amount ratios, in cases, where the initial natural signature is modified by known additives.

Received 21st July 2017  
Accepted 15th September 2017

DOI: 10.1039/c7ja00251c

rsc.li/jaas

### Introduction

Isotope pattern deconvolution (IPD) has developed into an important mathematical tool in organic<sup>1</sup> and inorganic mass spectrometry.<sup>2</sup> This technique allows for the determination of the fraction of a component in the chemical composition of a sample *via* the corresponding isotope pattern. Based on the solution of simple linear equation systems by multiple-linear regression modeling, IPD furthermore allows for the correction of *e.g.* instrumental isotopic fractionation or spectral interference. The variance of the modeling allows an estimation of uncertainty, as well, even though it does not cover a full uncertainty budget.<sup>3</sup> Due to these outstanding properties, isotope pattern deconvolution has been applied successfully in a variety of studies such as the deconvolution of complex organic mass spectra,<sup>4,5</sup> the quantification of organic<sup>6</sup> and inorganic<sup>7</sup> isotopically enriched spikes or the investigation of isotopically enriched tracers in biological,<sup>8–13</sup> forensic<sup>14</sup> or environmental studies.<sup>15–18</sup>

So far, the applications of IPD were either in conjunction with samples of synthetic origin or mixtures of natural samples

with isotopically enriched spikes. However, natural samples do not display such a distinct isotopic variation as compared to artificially prepared mixtures containing isotopically enriched materials.

To the best of our knowledge, no study on the application of IPD to deconvolute the composition of sole natural systems has been conducted so far. Here, IPD bears high potential for studying natural pathways and accumulation of elements displaying natural isotopic fractionation such as light stable isotopes (H, O, N, C, and S) or traditional geochemical isotope tracers (*e.g.* Pb, Sr, Nd, and Hf) opening the door to a variety of applications in the field of analytical ecogeochemistry.<sup>2</sup> The major challenge lies in resolving different sources with mostly small relative isotopic differences in natural samples.

In this study, the applicability of IPD to natural systems was tested on the example of the isotopic system of strontium (Sr). Sr consists of four naturally occurring stable isotopes <sup>84</sup>Sr, <sup>86</sup>Sr, <sup>87</sup>Sr and <sup>88</sup>Sr. An observed range of natural variations for each of the isotopic abundances is reported by the International Union of Pure and Applied Chemistry (IUPAC).<sup>19</sup> The isotope displaying the highest variability in natural abundance is <sup>87</sup>Sr, conventionally still expressed *via* the absolute isotope-amount ratio of  $n(^{87}\text{Sr})/n(^{86}\text{Sr})$ . Due to the radioactive  $\beta^-$ -decay of <sup>87</sup>Rb to <sup>87</sup>Sr, its relative amount in nature is a function of the Rb/Sr elemental ratio and the age of the geological material, with a reported  $n(^{87}\text{Sr})/n(^{86}\text{Sr})$  range between about 0.70 and 0.78<sup>20,21</sup> (corresponding to a  $\delta(^{87}\text{Sr}/^{86}\text{Sr})_{\text{NIST SRM 987}}$  range of  $-14.56$  to  $98.07\%$ ). In contrast, the variation of  $n(^{88}\text{Sr})/n(^{86}\text{Sr})$  is

<sup>a</sup>University of Natural Resources and Life Sciences Vienna, Department of Chemistry, Division of Analytical Chemistry, VIRIS Laboratory, Konrad-Lorenz-Strasse 24, 3430 Tulln, Austria. E-mail: thomas.prohaska@boku.ac.at

<sup>b</sup>Helmholtz-Centre for Materials and Coastal Research, Institute for Coastal Research, Dept. for Marine Bioanalytical Chemistry, Max-Planck Strasse 1, 21502 Geesthacht, Germany

† Electronic supplementary information (ESI) available. See DOI: 10.1039/c7ja00251c

comparably small being a result of mass-dependent fractionation only.<sup>22</sup> The isotope ratios of  $n(^{88}\text{Sr})/n(^{86}\text{Sr})$  are conventionally expressed in the  $\delta$ -notation relative to the certified reference material NIST SRM 987. Its total range of reported variations covers the values of  $\delta(^{88}\text{Sr}/^{86}\text{Sr})_{\text{NIST SRM 987}}$  ranging from about  $-1.1$  to  $1.4\%$ .<sup>23</sup> Natural variations of the  $\delta(^{84}\text{Sr}/^{86}\text{Sr})_{\text{NIST SRM 987}}$  isotope ratio of about  $-1.8$  to  $0.2\%$  were reported for *e.g.* bio(apatite),<sup>24</sup> fish otolith certified reference material FEBS-1<sup>25,26</sup> and lobster tissue certified reference material TORT-3.<sup>27</sup>

The  $n(^{87}\text{Sr})/n(^{86}\text{Sr})$  isotope-amount ratio is a well-established tracer for the origin determination of environmental,<sup>28</sup> archaeological<sup>29,30</sup> and food samples<sup>21,31,32</sup> as the bioavailable fraction of Sr is taken up and stored by living organisms from soil or water without significant isotopic fractionation. However, in the case of food, the isotopic composition of a primary agricultural product can be significantly altered by processing (*e.g.* salting<sup>33</sup>), rendering the attribution of the sample to its source difficult or impossible. As a consequence, this study addresses this challenge by the combination of isotope ratio measurements and IPD, allowing for the quantification of the perturbing component and subsequently correcting for its influence.

The aim of this work was to evaluate the applicability of isotope pattern deconvolution to determine the isotopic contribution of single sources to a mixed isotopic signature of natural samples using Sr isotopes. This work is based on an experimentally determined dataset of food samples consisting of two and three natural components. In the first example of use, the influence of Sr from water and fish feed on the Sr isotopic composition of raw sturgeon caviar and fish otoliths was investigated. In the second example, the influence of Sr from water, fish feed and salt on the Sr isotopic composition of salted, *i.e.* processed, sturgeon caviar was determined.

## Experimental

### Materials and methods

Experimental work was carried out at the University of Natural Resources and Life Science Vienna. Preparatory laboratory work was performed in an ISO class 8 clean room according to ISO 14644-1. Type I reagent-grade water (18 M $\Omega$  cm) (F+L GmbH, Vienna, Austria) was further purified by sub-boiling distillation (Milestone-MLS GmbH, Leutkirch, Germany). Analytical reagent-grade nitric acid (65% w/w, Merck-Millipore, Darmstadt, Germany) was purified by double sub-boiling using a DST-1000 sub-boiling distillation system (AHF Analysentechnik, Tübingen, Germany). All laboratory consumables (polyethylene bottles, tubes, and pipette tips) used for sampling, preparation and dilution of samples were pre-cleaned in a two-stage washing procedure using nitric acid (10% w/w and 1% w/w).

**Samples.** Samples of water, fish feed, salt, raw sturgeon caviar and salted sturgeon caviar were collected from one sturgeon farm in Salzburg, Austria (AT\_GRU) and two in North Italy (IT\_GOI and IT\_VIA), respectively. Water, fish feed and charr samples (*Salvelinus alpinus*) were collected from two fish farms in Carinthia (AT\_SIR) and Tyrol (AT\_LEU) in Austria.

**Preparation of samples for solution-based (MC) ICP-MS measurements.** Water collected from the fish farms was filtered using 0.45  $\mu\text{m}$  pore size filters (Sartorius, Göttingen, Germany) to obtain the dissolved elemental fraction and subsequently acidified with 2% HNO<sub>3</sub> (w/w) prepared from sub-boiled H<sub>2</sub>O and double sub-boiled HNO<sub>3</sub>. Fish feed was ground using an agate mortar, divided into aliquots of 0.4 g and digested by microwave-assisted acid digestion (Multiwave 3000, Anton Paar, Graz, Austria) using 6.7 mL conc. HNO<sub>3</sub> and 3.3 mL H<sub>2</sub>O<sub>2</sub> (30% suprapur, Merck, Darmstadt, Germany). Caviar samples were freeze dried (Christ Beta1-8 LD plus, Martin Christ Gefriertrocknungsanlagen GmbH, Osterode am Harz, Germany) before microwave-assisted acid digestion (Multiwave 3000) using 0.5 g of dry caviar and a reaction mixture of 9 mL of conc. HNO<sub>3</sub>/0.75 mL of H<sub>2</sub>O<sub>2</sub>. Salt was dissolved gravimetrically in 2% HNO<sub>3</sub> (w/w). All samples were prepared in triplicate. Prior to isotopic measurements, Sr/matrix separation of the samples was accomplished using a Sr specific extraction resin (Triskem, Bruz, France) following a routine separation procedure<sup>22</sup> (details are given in the ESI.1†). The certified isotope reference material strontium carbonate NIST SRM 987 (National Institute of Standards and Technology, Gaithersburg, USA,  $n = 12$ ) and matrix-matched reference material lobster tissue TORT-3 (National Research Council Canada, Ottawa, Canada,  $n = 7$ ) and seawater IAPSO (Batch num. P143, OSIL Ltd, Havant, UK,  $n = 2$ ) followed the same preparation procedure as the samples.

**Preparation of samples for laser ablation (MC) ICP-MS measurements.** Otoliths of seven charr from a fish farm in Carinthia and thirteen charr from a fish farm in Tyrol were extracted and prepared for LA-ICP-MS following the procedure by Zitek *et al.*<sup>34</sup> In this study, the sagitta was used. The certified reference materials fish otolith powder FEBS-1 (National Research Council of Canada, Ottawa, Canada,  $n = 4$ ) and calcium carbonate MACS-3 (USGS, Reston, USA,  $n = 4$ ) were used for elemental quantification and method evaluation.

### Instrumentation

Water and digests of fish feed, raw and salted caviar and salt samples were diluted as required and analyzed for their Sr content using a quadrupole ICP-MS (NexION 350 D, PerkinElmer, Waltham, USA) in standard mode. The isotope-amount ratios of  $n(^{84}\text{Sr})/n(^{86}\text{Sr})$ ,  $n(^{87}\text{Sr})/n(^{86}\text{Sr})$  and  $n(^{88}\text{Sr})/n(^{86}\text{Sr})$  were determined using a MC ICP-MS (Nu Plasma HR, Nu Instruments, Wrexham, UK) coupled to a desolvation unit (either DSN-100, Nu Instruments, Wrexham, UK or Aridus II, Cetac Technologies, Omaha, Nebraska) using a PFA nebulizer. Typical instrumental and data acquisition parameters are given elsewhere.<sup>22</sup> Laser ablation measurements of otolith samples were performed using split stream ICP-MS/MC ICP-MS according to Prohaska *et al.*<sup>35</sup> Samples were measured in line scan mode from the otolith core to the rim area.

### Data reduction strategies

**Elemental amount fractions.** Elemental amount fractions of Sr were determined following blank correction, normalization to indium as internal normalization standard (single element

ICP-MS standard, CertiPur, Merk, Darmstadt, Germany), and external calibration applying a 5-point calibration (multi elemental ICP-MS standard VI, CertiPur, Merk, Darmstadt, Germany). Results were validated using in-house quality control standards and certified reference materials TORT-3 and IAPSO.

**Isotope-amount ratios.** Isotope-amount ratios of  $n(^{84}\text{Sr})/n(^{86}\text{Sr})$ ,  $n(^{87}\text{Sr})/n(^{86}\text{Sr})$  and  $n(^{88}\text{Sr})/n(^{86}\text{Sr})$  were determined using on-peak blank corrected signals. The isobaric interference of  $^{87}\text{Rb}$  on  $^{87}\text{Sr}$  was corrected following the procedure described by Horsky *et al.*<sup>12</sup> These calculations were implemented in the Nu Instruments Calculation Editor routine (NICE, Nu Instruments Inc., Wrexham, UK), allowing for a point by point correction including outlier-elimination.

Different correction strategies for instrumental isotopic fractionation (IIF, also termed “mass bias” or “mass discrimination”) were compared for the determination of the isotope-amount ratios of  $n(^{84}\text{Sr})/n(^{86}\text{Sr})$ ,  $n(^{87}\text{Sr})/n(^{86}\text{Sr})$  and  $n(^{88}\text{Sr})/n(^{86}\text{Sr})$ :

(a) External intra-elemental correction (standard-sample-bracketing) using the  $n(^{88}\text{Sr})/n(^{86}\text{Sr})$  isotope-amount ratio of the isotope certified reference material NIST SRM 987 for IIF correction of all measured Sr isotope ratios in the sample – hereafter referred to as “SSB<sub>f(88Sr/86Sr)</sub>”.<sup>36</sup>

(b) External intra-elemental correction (standard-sample-bracketing) using the respective isotopic ratios of NIST SRM 987 for the IIF correction of the corresponding measured Sr isotopic ratios in the sample – hereafter referred to as “SSB”.<sup>36</sup>

(c) Internal inter-elemental correction using zirconium (single element ICP-MS standard, Inorganic Ventures, Christiansburg, USA) and standard-sample-bracketing with NIST SRM 987 using the respective Sr isotope ratios for the determination of the  $n(^{91}\text{Zr})/n(^{90}\text{Zr})$  isotope-amount ratio and the subsequent IIF correction of the respective Sr isotope ratios in the sample – hereafter referred to as “SSB-Zr<sub>corr</sub>”.<sup>27</sup>

All three methods are frequently applied for Sr isotope-amount ratio determination. Method a. has been routinely used for LA-MC ICP-MS in our laboratory.<sup>11,35</sup> Theoretical considerations and the practical application of these approaches for the IIF correction of Sr isotopic ratios are described in detail elsewhere.<sup>22</sup> IIF correction following an internal intra-elemental approach<sup>37</sup> traditionally applied for the IIF correction of  $n(^{87}\text{Sr})/n(^{86}\text{Sr})$  using  $n(^{88}\text{Sr})/n(^{86}\text{Sr})$  was considered inadequate in this study as all isotope-amount ratios of Sr were determined and taken into account for further IPD processing. Further, modeling of the theoretical IIF using the SOLVER add-in in Microsoft Excel<sup>®7</sup> was performed, but proved to be inferior to IIF correction based on experimentally determined IIF correction factors.

**Laser ablation (MC) ICP-MS measurements.** Data reduction for the determination of the Sr mass fraction in otoliths was performed according to Prohaska *et al.*<sup>35</sup> The isotope-amount ratios of  $n(^{84}\text{Sr})/n(^{86}\text{Sr})$ ,  $n(^{87}\text{Sr})/n(^{86}\text{Sr})$  and  $n(^{88}\text{Sr})/n(^{86}\text{Sr})$  were calculated based on Irrgeher *et al.*<sup>11</sup> by performing the  $^{87}\text{Rb}$  correction *via* peak stripping assuming similar instrumental isotopic fractionation behaviour of Rb and Sr and using the respective IIF factors for all Sr isotopic ratios determined from the NIST SRM 987 in a standard-sample-bracketing approach.

Subsequently, the individual isotopic abundances of all Sr isotopes were calculated from the measured isotope-amount ratios and used as input parameters for the IPD.

### Deconvolution of natural sources

In case that the isotopic composition of a sample results from the mixing of multiple natural sources with different isotopic compositions, the resulting isotopic pattern in the sample is a function of the isotopic composition of the individual sources and the relative amounts of Sr. This relationship can be expressed as a linear combination of the isotopic abundances  $A^i$  of isotope  $i$  of the element of interest and the molar fractions  $x_{\text{nat},n}$  of the respective natural sources (eqn (1)). A general procedure on the delineation of linear equations for isotopic pattern deconvolution calculations can be found elsewhere.<sup>3</sup>

$$A^i_{\text{sample}} = x_{\text{nat}_1} A^i_{\text{nat}_1} + x_{\text{nat}_2} A^i_{\text{nat}_2} + \dots + x_{\text{nat}_n} A^i_{\text{nat}_n} \quad (1)$$

The four stable isotopes of Sr allow the construction of four equations with four unknowns. The latter represents the molar fractions of the individual components in the natural sample. If three components (*i.e.* natural sources) are involved, the system is over-determined resulting in a system of four equations, three unknowns and an error vector  $e$ , as written in the matrix notation (eqn (2)):

$$\begin{bmatrix} A^84_{\text{sample}} \\ A^86_{\text{sample}} \\ A^87_{\text{sample}} \\ A^88_{\text{sample}} \end{bmatrix} = \begin{bmatrix} A^84_{\text{nat}_1} & A^84_{\text{nat}_2} & A^84_{\text{nat}_3} \\ A^86_{\text{nat}_1} & A^86_{\text{nat}_2} & A^86_{\text{nat}_3} \\ A^87_{\text{nat}_1} & A^87_{\text{nat}_2} & A^87_{\text{nat}_3} \\ A^88_{\text{nat}_1} & A^88_{\text{nat}_2} & A^88_{\text{nat}_3} \end{bmatrix} \times \begin{bmatrix} x_{\text{nat}_1} \\ x_{\text{nat}_2} \\ x_{\text{nat}_3} \end{bmatrix} + \begin{bmatrix} e^84 \\ e^86 \\ e^87 \\ e^88 \end{bmatrix} \quad (2)$$

The equation system can be solved by multiple-linear regression modeling using the LINEST-function in Microsoft Excel<sup>®</sup>. Alternatively, linear algebra calculations can be performed based on Cramer's rule.<sup>38</sup> These calculations can also be implemented in Microsoft Excel<sup>®</sup>,<sup>39</sup> but are easier to perform using computation software, *e.g.* Wolfram Alpha.<sup>40</sup> When applying Cramer's rule, the over-determined linear equation system needs to be reduced to an  $(n \times n)$  – matrix. In the case of a three-component system of Sr, the elimination of the  $^{84}\text{Sr}$  equation seems obvious, as the determination of  $^{84}\text{Sr}$  is usually associated with the highest uncertainty because of the low relative natural abundance and the resulting lowest signal intensities in MC ICP-MS measurements. In the case of a two-component system, the reduction to an  $^{86}\text{Sr}$  and  $^{87}\text{Sr}$  equation system is most useful, as the  $n(^{87}\text{Sr})/n(^{86}\text{Sr})$  is the isotope-abundance ratio with the highest variation in nature, thus representing the most useful parameter for sample characterization. Examples on the calculation using both approaches are given in ESI.2.1 and 2.2.†

### Uncertainty evaluation

The uncertainty of the molar fractions calculated by IPD was determined in four steps:

(1) The combined standard uncertainties of the isotope-amount ratios of  $n(^{84}\text{Sr})/n(^{86}\text{Sr})$ ,  $n(^{87}\text{Sr})/n(^{86}\text{Sr})$  and  $n(^{88}\text{Sr})/n(^{86}\text{Sr})$  were calculated according to Eurachem<sup>41</sup> using an adapted Kragten spreadsheet approach based on Horsky *et al.*<sup>22</sup> Therefore, the contributions of blank, measurement precision, instrumental isotopic fractionation correction, heterogeneity of the samples and  $^{87}\text{Rb}$  correction of the 87-ion beam signal were taken into account. The uncertainty of the  $n(^{86}\text{Sr})/n(^{86}\text{Sr})$  isotope-amount ratio was considered as zero.

(2) The standard combined uncertainties were transformed into the standard errors of the mean, in order to account for the heterogeneity of variances.

(3) The corresponding uncertainty was added to its respective Sr isotope ratio, followed by an IPD calculation. This step was performed in a separate spread sheet making a total number of twelve and sixteen IPD calculations for a two- and a three-component system, respectively. The resulting molar fractions were collected in a summary spread sheet.

(4) The uncertainty of the molar fraction corresponded to the square root of the sum of the error squares.<sup>17</sup> Examples on the uncertainty calculation using the regression modeling and linear algebra approach are given in ESI.2.1 and 2.2.†

## Results and discussion

### Data processing strategies

**Instrumental isotopic fractionation correction.** Accurate absolute isotope-amount ratios are the basis for isotopic pattern deconvolution. However, different evaluation strategies are prone to differences in the resulting isotope ratios and uncertainties.<sup>22</sup> In the case of Sr, most applied methods focus on the determination of the  $n(^{87}\text{Sr})/n(^{86}\text{Sr})$  isotope-amount ratio.<sup>36</sup> In this work, we considered all experimentally determined Sr isotope-amount ratios in the IPD calculations. Thus, a data processing method allowing for the accurate determination of  $n(^{84}\text{Sr})/n(^{86}\text{Sr})$ ,  $n(^{87}\text{Sr})/n(^{86}\text{Sr})$  and  $n(^{88}\text{Sr})/n(^{86}\text{Sr})$  isotope-amount ratios was required. Therefore, we applied three different data processing strategies described before.

Table 1 shows the resulting  $n(^{84}\text{Sr})/n(^{86}\text{Sr})$ ,  $n(^{87}\text{Sr})/n(^{86}\text{Sr})$  and  $n(^{88}\text{Sr})/n(^{86}\text{Sr})$  isotope-amount ratios and their expanded uncertainties ( $U, k = 2$ ) for a caviar dataset from one fish farm in Italy (IT\_GOI) and reference materials using the three investigated calibration strategies. For a given sample, all isotope-amount ratios overlapped within the limits of uncertainty, independent of the applied calibration method. Even though these ratios are not significantly different, IPD is very sensitive to small variations in the isotope amount ratios. The determined isotopic composition of the reference materials NIST SRM 987, TORT-3 and IAPSO was in agreement with the certified values<sup>27,42</sup> independent of the calibration strategy.

Best agreement between the experimental and certified values was achieved for data obtained by external intra-elemental correction (SSB) and internal inter-elemental correction using zirconium as an additional internal standard ( $\text{Zr}_{\text{corr}}$ ). Therefore, the data corrected *via* SSB were taken for the following considerations.

**Table 1** Determined isotope-amount ratios of Sr using three different calibration strategies for instrumental isotopic fractionation correction of a caviar dataset (IT\_GOI) and certified reference materials TORT-3, IAPSO and NIST SRM 987; uncertainties correspond to ( $U, k = 2$ )

Sample	SSB <sub>f(88Sr/86Sr)</sub>	SSB	SSB-Zr <sub>corr</sub>	Reference
<b><math>n(^{87}\text{Sr})/n(^{86}\text{Sr})</math></b>				
Water	0.70867 (19)	0.70860 (21)	0.70830 (20)	—
Fish feed	0.70936 (17)	0.70923 (21)	0.70932 (21)	—
Salt	0.70944 (18)	0.70931 (23)	0.70942 (21)	—
Caviar <sub>raw</sub>	0.70877 (16)	0.70869 (19)	0.70866 (25)	—
Caviar <sub>salted</sub>	0.70911 (17)	0.70902 (19)	0.70902 (20)	—
TORT-3	0.70944 (21)	0.70928 (25)	0.70937 (36)	0.70937 (10)
IAPSO	0.70921 (48)	0.70935 (24)	0.70924 (27)	0.70931 (30)
SRM 987	0.71031 (24)	0.71022 (23)	0.71029 (27)	0.71034 (26)
<b><math>n(^{88}\text{Sr})/n(^{86}\text{Sr})</math></b>				
Water	8.3759 (24)	8.3758 (25)	8.3714 (28)	—
Fish feed	8.3773 (24)	8.3774 (26)	8.3806 (30)	—
Salt	8.3802 (40)	8.3801 (42)	8.3827 (32)	—
Caviar <sub>raw</sub>	8.3763 (21)	8.3764 (23)	8.3781 (48)	—
Caviar <sub>salted</sub>	8.3791 (22)	8.3789 (23)	8.3800 (28)	—
TORT-3	8.378 (10)	8.378 (10)	8.381 (13)	8.3824 (12)
IAPSO	8.3805 (51)	8.3805 (54)	8.3817 (46)	8.3818 (30)
SRM 987	8.3768 (32)	8.3769 (33)	8.3793 (85)	8.3786 (33)
<b><math>n(^{84}\text{Sr})/n(^{86}\text{Sr})</math></b>				
Water	0.05644 (54)	0.05616 (34)	0.05619 (35)	—
Fish feed	0.05655 (18)	0.05656 (14)	0.05653 (18)	—
Salt	0.05647 (7)	0.05653 (9)	0.05651 (8)	—
Caviar <sub>raw</sub>	0.05654 (23)	0.05626 (15)	0.05656 (21)	—
Caviar <sub>salted</sub>	0.05658 (8)	0.05664 (7)	0.05665 (9)	—
TORT-3	0.05654 (20)	0.05653 (11)	0.05653 (12)	0.056526 (48)
IAPSO	0.05644 (26)	0.05650 (17)	0.05646 (12)	—
SRM 987	0.05654 (11)	0.05656 (13)	0.05654 (16)	0.05655 (14)

**Measurement uncertainty.** The calculated uncertainties for the different calibration strategies for IIF correction were in a comparable range. Fig. 1 shows the contributors to the variances of the Sr isotope-amount ratios for the SSB calibration of

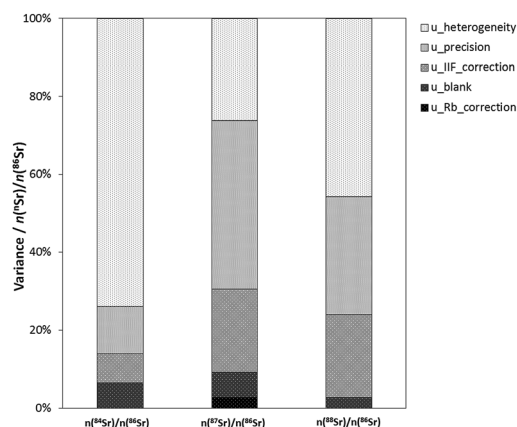


**Fig. 1** Relative contribution of the heterogeneity, measurement precision, IIF correction, blank and  $^{87}\text{Rb}$  interference correction to the variance of the  $n(^{84}\text{Sr})/n(^{86}\text{Sr})$ ,  $n(^{87}\text{Sr})/n(^{86}\text{Sr})$  and  $n(^{88}\text{Sr})/n(^{86}\text{Sr})$  isotope-amount ratios of a fish feed sample from a caviar dataset (IT\_GOI).



a selected fish feed sample from the dataset in Table 1. The heterogeneity of the sample was the main contributor to the total standard combined uncertainty of the  $n(^{84}\text{Sr})/n(^{86}\text{Sr})$  and the  $n(^{88}\text{Sr})/n(^{86}\text{Sr})$  isotope-amount ratios followed by measurement precision, instrumental isotopic fractionation correction and blank contributions. In contrast, in the case of the  $n(^{87}\text{Sr})/n(^{86}\text{Sr})$  isotope-amount ratios, the precision represented the main source of uncertainty. Overall, the relative expanded combined uncertainties ( $U_{\text{rel}}$ ,  $k = 2$ ) correspond to 0.13%, 0.03% and 0.03% for the  $n(^{84}\text{Sr})/n(^{86}\text{Sr})$ ,  $n(^{87}\text{Sr})/n(^{86}\text{Sr})$  and  $n(^{88}\text{Sr})/n(^{86}\text{Sr})$  isotope-amount ratios, respectively. For the latter two ratios the obtained values are in good agreement with published data,<sup>22,43</sup> while due to the low abundance of  $^{84}\text{Sr}$ , measurements of the  $n(^{84}\text{Sr})/n(^{86}\text{Sr})$  represent an analytical challenge. Details about the chosen uncertainty parameters are discussed elsewhere.<sup>22</sup>

### Deconvolution of the isotopic composition of natural samples

**Two-component system.** One dataset of raw caviar from one fish farm in Italy (IT\_GOI) was chosen as a model of a two-component system. Therefore, the molar fractions of water ( $x_{\text{water}}$ ) and fish feed ( $x_{\text{fish feed}}$ ) as the two natural sources contributing to the Sr isotopic composition were calculated using multiple-linear regression modeling and linear algebra calculations (*via* Cramer's rule). The resulting molar fractions correspond to percentage fractions. Table 2 shows that using both IPD calculation techniques the average Sr isotopic composition of raw caviar is formed of about 85% Sr from water and 15% Sr from fish feed. These values are in accordance with findings by Campana<sup>44</sup> and Doubleday.<sup>45</sup> The relative combined standard uncertainties ( $u_c$ ,  $k = 1$ ) of 13% for both molar fractions showed that each component contributes equally to the total variance of the isotopic composition.

IPD was applied to two additional caviar datasets from Italy (IT\_VIA) and Austria (AT\_GRU) measured by solution based-MC ICP-MS as well as otoliths from two other fish farms in Austria (AT\_SIR and AT\_LEU) measured by LA-MC ICP-MS. Isotope-amount ratios of the samples, the certified reference materials otolith powered FEBS-1 and calcium carbonate MACS-1 as well as the corresponding reference values<sup>26,46</sup> are given in ESI.3.1.† IPD *via* multiple-linear regression was performed on these samples allowing for easier and faster data processing in comparison to linear algebra calculation where the use of additional software is necessary. Table 3 summarises the obtained molar fractions of raw caviar and otoliths. The average contribution of water and fish feed to the Sr isotopic

**Table 2** Comparison of the molar fractions of water and fish feed as the two natural sources to the isotopic composition of raw caviar (IT\_GOI) obtained by IPD using regression modeling and linear algebra calculations according to Cramer's rule; uncertainties correspond to  $u_c$

IPD method	$x_{\text{water}}$	$x_{\text{fish feed}}$	Parameters
Regression modeling	$0.84 \pm 0.13$	$0.16 \pm 0.13$	$^{84}\text{Sr}$ , $^{86}\text{Sr}$ , $^{87}\text{Sr}$ , $^{88}\text{Sr}$
Cramer's rule	$0.86 \pm 0.13$	$0.14 \pm 0.13$	$^{86}\text{Sr}$ , $^{87}\text{Sr}$

**Table 3** Molar fractions of the constituents of raw caviar (IT\_VIA and AT\_GRU) and otoliths (AT\_SIR and AT\_LEU), uncertainties correspond to  $u_c$

Sample	Origin	$x_{\text{water}}$	$x_{\text{fish feed}}$
Caviar <sub>raw</sub>	IT_VIA	$0.84 \pm 0.16$	$0.16 \pm 0.16$
Caviar <sub>raw</sub>	AT_GRU	$0.77 \pm 0.81$	$0.23 \pm 0.81$
Otoliths	AT_SIR	$0.76 \pm 0.02$	$0.24 \pm 0.02$
Otoliths	AT_LEU	$0.77 \pm 0.07$	$0.23 \pm 0.07$

composition of the samples accounted for  $79.8 \pm 4.3\%$  and for  $20.2 \pm 4.3\%$  (1 SD, between site variations for  $n = 5$ ). These results are in accordance with the literature.<sup>45,47</sup>

The results obtained using linear algebra calculations suggest that the experimentally determined  $n(^{87}\text{Sr})/n(^{86}\text{Sr})$  isotope-amount ratio is suitable to deconvolute the composition of a two-component system, as only two of the four available parameters are needed to solve the linear equation system. To test whether this hypothesis is also true for IPD calculations using multiple-linear regression, the experimentally determined  $n(^{84}\text{Sr})/n(^{86}\text{Sr})$  and  $n(^{88}\text{Sr})/n(^{86}\text{Sr})$  isotope-amount ratios were kept constant using the theoretical values of 0.05655 and 8.37861 of the NIST SRM 987 for raw caviar and otoliths. Subsequently, IPD calculations using multiple-regression modeling were performed. The results given in ESI.3.2† show that only for two datasets (IT\_GOI and IT\_VIA) the resulting molar fractions were in accordance with previous findings when all experimentally determined parameters were used for the IPD calculations. This result allows the assumption that all experimentally determined isotope-amount ratios have to be taken into consideration, when performing IPD using multiple-linear regression. In turn, as four parameters are available, a linear equation system consisting of up to four unknowns (sources to the isotopic composition of the sample) can theoretically be solved.

**Three-component system.** The above described calculations were applied to salted sturgeon caviar (IT\_GOI, IT\_VIA, and AT\_GRU) as a model for a three-component system (Sr isotope amount ratios are given in Table 1 and ESI.3.1†). The Sr isotopic composition of salted caviar is influenced by water, fish feed and salt representing the major Sr sources. Table 4 shows the resulting molar fractions of water ( $x_{\text{water}}$ ), fish feed ( $x_{\text{fish feed}}$ ) and salt ( $x_{\text{salt}}$ ) calculated *via* multiple-regression modeling.

Linear algebra calculations failed to deconvolute the three-component system, as negative molar fractions for fish feed were obtained independent of the calibration strategy used for

**Table 4** Molar fractions of water, fish feed and salt as three sources contributing to the isotopic composition of salted caviar obtained by IPD calculations using multiple-linear regression modeling; uncertainties correspond to  $u_c$

Sample	Origin	$x_{\text{water}}$	$x_{\text{fish feed}}$	$x_{\text{salt}}$
Caviar <sub>salted</sub>	IT_GOI	$0.19 \pm 0.11$	$0.03 \pm 0.42$	$0.77 \pm 0.38$
Caviar <sub>salted</sub>	IT_VIA	$0.19 \pm 0.20$	$0.05 \pm 0.87$	$0.76 \pm 0.68$
Caviar <sub>salted</sub>	AT_GRU	$1.57 \pm 0.99$	$-0.14 \pm 0.68$	$-0.44 \pm 0.36$

IIF correction. This can be explained by the use of exact values when linear algebra calculations are applied compared to multiple-linear regression, where data fitting represents a generic feature of the method.

IPD calculations showed that the addition of salt accounted for 76 and 77% of the total Sr isotopic composition of salted sturgeon caviar from Italian fish farms (IT\_GOI and IT\_VIA). The remaining 24% corresponds to the molar fraction of Sr from raw caviar, which in turn consists of about 85% of Sr from water and 15% of Sr from fish feed, as shown in the previous section. These two fish farms belong to the same caviar producer where salt with high Sr content ( $26.3 \mu\text{g g}^{-1}$  for IT\_GOI and  $24.6 \mu\text{g g}^{-1}$  for IT\_VIA) is used for processing raw caviar. In contrast, IPD calculations of salted caviar from the Austrian fish farm AT\_GRU did not lead to useful results. Salt used for caviar processing contained about 35-times less Sr ( $0.7 \mu\text{g g}^{-1}$ ), compared to the other two cases (IT\_VIA and IT\_GOI) and did not alter the isotopic composition of caviar (compare the  $n(^{87}\text{Sr})/n(^{86}\text{Sr})$  of  $0.70908 \pm 0.00027$  of caviar<sub>raw</sub> and  $0.70907 \pm 0.00022$  of caviar<sub>salted</sub>,  $\text{ESI.3.1}\dagger$ ). Consequently, if using salt as a variable in the IPD calculations, its contribution is considered equal to water and fish feed, leading to mathematically valid, but stoichiometrically wrong results. This shows a limitation of the IPD method, suggesting that the sources have to be chosen thoughtfully taking into account their actual contribution to the isotopic composition of the sample (*i.e.* considering the Sr content and the Sr isotopic composition).

**Uncertainty contributors to the molar fractions.** No uniform procedure for the calculation of uncertainties of the molar fractions obtained by IPD is available in the literature. A common approach is the performance of the IIF correction within the multiple-linear regression modeling and using the standard deviation or the standard error of the mean of the measured isotopic ratios in combination with the regression variance to state the combined standard uncertainty.<sup>7,48,49</sup> This approach does not account for the contribution of the blank, the precision of the measurement or interference correction.

In this study, all contributors to the standard uncertainty of the strontium isotope-amount ratios (blank, measurement precision, IIF correction, heterogeneity of the samples, the  $^{87}\text{Rb}$  correction and the heterogeneity of variances) were considered.<sup>22</sup> IIF correction within the IPD was not applicable as the samples were measured on different days, thus being subject to different IIF factors. The respective uncertainties were propagated to the isotopic ratios of the sources and the samples in a Kragten approach followed by the calculation of the molar fractions by IPD. The resulting molar fractions were then subtracted from the IPD result without error propagation. Subsequently, the sum of the squared differences represented the variance of the individual component. The regression variance of the fitting was lower than  $1 \times 10^{-6}\%$  for all calibration approaches and can therefore be considered negligible (see  $\text{ESI.1}$  for more details<sup>†</sup>).

The resulting uncertainty of the molar fractions is a function of the uncertainty of the isotope-amount ratios and the proportion between the sources and the sample. Fig. 2 shows the relationship between the uncertainty of the molar fractions

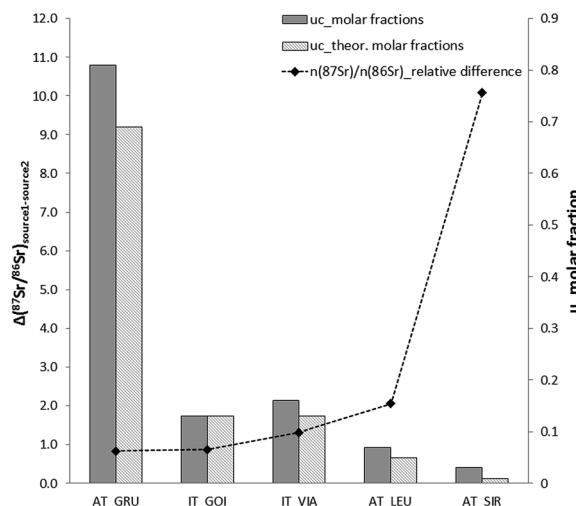


Fig. 2 Relationship of the standard combined uncertainty of the molar fractions (filled bars) of raw caviar (AT\_GRU, IT\_GOI, and IT\_VIA) and otoliths (AT\_LEU and AT\_SIR) and the differences in the  $n(^{87}\text{Sr})/n(^{86}\text{Sr})$  isotopic composition between the natural sources water and fish feed (black diamonds); striped bars correspond to molar fractions obtained by a theoretical calculation when propagating the same uncertainties to all samples.

(filled bars) of raw caviar and otoliths and the relative difference of the isotope-amount ratios of  $n(^{87}\text{Sr})/n(^{86}\text{Sr})$  (filled diamonds) between the corresponding sources water and fish feed. The sample with the smallest relative isotopic differences of  $\Delta(^{87}\text{Sr}/^{86}\text{Sr})_{\text{source1-source2}}$  of 0.84‰ (AT\_GRU) displayed the highest uncertainties of the molar fractions. In turn, the sample with the largest isotopic differences of  $\Delta(^{87}\text{Sr}/^{86}\text{Sr})_{\text{source1-source2}}$  of 10.1‰ (AT\_SIR) displayed the lowest uncertainties of the molar fractions. A theoretical calculation propagating the uncertainty of the  $n(^{84}\text{Sr})/n(^{86}\text{Sr})$ ,  $n(^{87}\text{Sr})/n(^{86}\text{Sr})$  and  $n(^{88}\text{Sr})/n(^{86}\text{Sr})$  isotope-amount ratios of the sampling site IT\_GOI to the isotope-amount ratios of AT\_GRU, IT\_VIA, AT\_LEU and AT\_SIR instead of the original values showed that the overall pattern of the uncertainties of the molar fractions (striped bars) remained the same. This allows the conclusion that the uncertainty substantially depends on the relative isotopic difference between the sources. The molar fractions of the constituents of all samples were in accordance with the literature.

## Conclusions

This study demonstrated the successful application of isotope pattern deconvolution as a powerful mathematical tool for the determination of the individual contributions of different sources to the strontium isotopic composition of two- and three-component natural biological samples. Therefore, all isotopic ratios of Sr have to be determined accurately and used as input parameters to the subsequent mathematical calculations, where the best results were achieved using multiple-linear regression modeling. The calculations following the SSB approach were considered as the most accurate in regard to

stoichiometry and uncertainty for a two- as well as a three-component system for both solution-based as well as LA-MC ICP-MS.

Correct deconvolution of the molar fractions of constituents was possible for isotopic differences ( $\Delta(^{87}\text{Sr}/^{86}\text{Sr})_{\text{source1-source2}}$ ) of the sources down to 0.83‰ corresponding to two-times the expanded combined uncertainty of the sample. However, these samples showed the highest uncertainties in the molar fractions.

The applicability of the presented method can be extended to other isotopic systems, accordingly.

## Conflicts of interest

There are no conflicts of interest to declare.

## Acknowledgements

The authors would like to acknowledge the Federal Ministry of Science, Research and Economy for funding the research within the Sparkling Science program (Project “CSI:Trace your Food”). Furthermore, we gratefully thank the project cooperation partners Wolfgang Grill (Grill, Gröding, Austria), Mario Pazzaglia (Agroittica Lombarda SpA) and Leonardo Congiu (University of Padova, Italy) for providing the samples, Christine Opper and Sabrina van der Oeven for their support with sample preparation, as well as Johannes Tintner (University of Natural Resources and Life Sciences Vienna, Institute of Wood Technology and Renewable Materials), Rui Vasconcelos and Kirill Khurstalev for their support with mathematical considerations.

## References

- 1 P. Rodriguez-Gonzalez and J. I. Garcia Alonso, *J. Anal. At. Spectrom.*, 2010, **25**, 239–259.
- 2 J. Irrgeher and T. Prohaska, *Anal. Bioanal. Chem.*, 2016, **408**, 369–385.
- 3 J. I. Garcia Alonso and P. Rodriguez-Gonzalez, *Isotope Dilution Mass Spectrometry*, Royal Society of Chemistry, Cambridge, UK, 2013.
- 4 S. G. Roussis and R. Proulx, *Anal. Chem.*, 2003, **75**, 1470–1482.
- 5 J. Meija and J. A. Caruso, *J. Am. Soc. Mass Spectrom.*, 2004, **15**, 654–658.
- 6 A. Gonzalez-Gago, J. M. Marchante-Gayon, M. Ferrero and J. I. Garcia Alonso, *Anal. Chem.*, 2010, **82**, 2879–2887.
- 7 J. A. Rodriguez-Castrillon, M. Moldovan, J. Ruiz Encinar and J. I. Garcia Alonso, *J. Anal. At. Spectrom.*, 2008, **23**, 318–324.
- 8 J. Draxler, E. Martinelli, A. M. Weinberg, A. Zitek, J. Irrgeher, M. Meischel, S. E. Stanzl-Tschegg, B. Mingler and T. Prohaska, *Acta Biomater.*, 2017, **51**, 526–536.
- 9 S. Fernandez-Menendez, M. L. Fernandez-Sanchez, H. Gonzalez-Iglesias, B. Fernandez-Colomer, J. Lopez-Sastre and A. Sanz-Medel, *Eur. J. Nutr.*, 2016, DOI: 10.1007/s00394-016-1325-7.
- 10 J. A. Rodriguez-Castrillon, M. Moldovan, J. I. Garcia Alonso, J. J. Lucena, M. L. Garcia-Tome and L. Hernandez-Apaolaza, *Anal. Bioanal. Chem.*, 2008, **390**, 579–590.
- 11 J. Irrgeher, A. Zitek, M. Cervicek and T. Prohaska, *J. Anal. At. Spectrom.*, 2014, **29**, 193–200.
- 12 A. Zitek, J. Irrgeher, M. Cervicek, M. Horsky, M. Kletzl, T. Weismann and T. Prohaska, *Mar. Freshwater Res.*, 2014, **65**, 978–986.
- 13 J. Giner Martinez-Sierra, F. Moreno Sanz, P. Herrero Espilez, J. M. Marchante Gayon and J. I. Garcia Alonso, *J. Anal. At. Spectrom.*, 2007, **22**, 1105–1112.
- 14 I. Carames-Pasaron, J. A. Rodriguez-Castrillon, M. Moldovan and J. I. Garcia Alonso, *Anal. Chem.*, 2012, **84**, 121–126.
- 15 P. Rodriguez-Gonzalez, S. Bouchet, M. Monperrus, E. Tessier and D. Amouroux, *Environ. Sci. Pollut. Res.*, 2013, **20**, 1269–1280.
- 16 N. Rizzini Ansari, N. Fernandez Iglesias, R. C. Cordeiro, M. A. Fernandez and J. Bettmer, *Mar. Pollut. Bull.*, 2017, **115**, 362–368.
- 17 J. A. Rodriguez-Castrillon, M. Moldovan and J. I. Garcia Alonso, *Anal. Bioanal. Chem.*, 2009, **394**, 351–362.
- 18 A. Castillo, P. Rodriguez-Gonzalez, G. Centineo, A. F. Roig-Navarro and J. I. Garcia Alonso, *Anal. Chem.*, 2010, **82**, 2773–2783.
- 19 J. Meija, T. B. Coplen, M. Berglund, W. A. Brand, P. De Bièvre, M. Gröning, N. E. Holden, J. Irrgeher, R. D. Loss, T. Walczyk and T. Prohaska, *Isotopic Compositions of the Elements 2013 (IUPAC Technical Report)*, 2013.
- 20 R. A. Bentley, *J. Archaeol. Method Th.*, 2006, **13**, 135–187.
- 21 S. Voerkelius, G. D. Lorenz, S. Rummel, C. R. Quétel, G. Heiss, M. Baxter, C. Brach-Papa, P. Deters-Itzelsberger, S. Hoelzl, J. Hoogewerff, E. Ponzevera, M. Van Bockstaele and H. Ueckermann, *Food Chem.*, 2010, **118**, 933–940.
- 22 M. Horsky, J. Irrgeher and T. Prohaska, *Anal. Bioanal. Chem.*, 2016, **408**, 351–367.
- 23 L. A. Neymark, W. R. Premo, N. N. Mel’Nikov and P. Emsbo, *J. Anal. At. Spectrom.*, 2014, **29**, 65–75.
- 24 W. Müller and R. Anczkiewicz, *J. Anal. At. Spectrom.*, 2016, **31**, 259–269.
- 25 J. F. Carter, U. Tinggi, X. Yang and B. Fry, *Food Chem.*, 2015, **170**, 241–248.
- 26 Z. Yang, B. J. Fryer, H. P. Longrich, J. E. Gagnon and I. M. Samson, *J. Anal. At. Spectrom.*, 2011, **26**, 341–351.
- 27 J. Irrgeher, T. Prohaska, R. E. Sturgeon, Z. Mester and L. Yang, *Anal. Methods*, 2013, **5**, 1687–1694.
- 28 T. Nakano, *Proc. Jpn. Acad. Ser. B Phys. Biol. Sci.*, 2016, **92**, 167–184.
- 29 C. Latkoczy, T. Prohaska, M. Watkins, M. Teschler-Nicola and G. Stingeder, *J. Anal. At. Spectrom.*, 2001, **16**, 806–811.
- 30 J. Montgomery, *Ann. Hum. Biol.*, 2010, **37**, 325–346.
- 31 G. Fortunato, K. Mumic, S. Wunderli, L. Pillonel, J. O. Bosset and G. Gremaud, *J. Anal. At. Spectrom.*, 2004, **19**, 227–234.
- 32 S. Swoboda, M. Brunner, S. F. Boulyga, P. Galler, M. Horacek and T. Prohaska, *Anal. Bioanal. Chem.*, 2008, **390**, 487–494.
- 33 A. Tchaikovskiy, A. Zitek, J. Irrgeher, C. Opper, R. Scheiber and T. Prohaska, *Presented in Part at the European Winter*

- Conference on Plasma Spectrochemistry*, Sankt Anton am Arlberg, 19–24th February, 2017.
- 34 A. Zitek, M. Sturm, H. Waidbacher and T. Prohaska, *Fish. Manag. Ecol.*, 2010, **17**, 435–445.
- 35 T. Prohaska, J. Irrgeher and A. Zitek, *J. Anal. At. Spectrom.*, 2016, **31**, 1612–1621.
- 36 J. Irrgeher, J. Vogel, J. Santner and T. Prohaska, in *Sector Field Mass Spectrometry for Elemental and Isotopic Analysis*, ed. T. Prohaska, J. Irrgeher, A. Zitek and N. Jakubowski, Cambridge, 2015, pp. 126–149.
- 37 T. Waight, J. Baker and D. Peate, *Int. J. Mass Spectrom.*, 2002, **221**, 229–244.
- 38 W. Cheney and D. Kincaid, *Linear Algebra – Theory and Applications*, Jones & Bartlett Learning, Sudury, Massachusetts, 2011.
- 39 D. Kleitman, <http://www-math.mit.edu>, (accessed 5/26/2017).
- 40 W. Research, <https://www.wolframalpha.com>, (accessed 9/05/2017).
- 41 S. L. R. Ellison and A. Williams, *EURACHEM/CITAC Guide: Quantifying Uncertainty in Analytical Measurement*, 2012.
- 42 A. Krabbenhöft, J. Fietzke, A. Eisenhauer, V. Liebetrau, F. Böhm and H. Vollstaedt, *J. Anal. At. Spectrom.*, 2009, **24**, 1267–1271.
- 43 E. Paredes, D. G. Asfaha and C. R. Quétel, *J. Anal. At. Spectrom.*, 2013, **28**, 320–326.
- 44 S. E. Campana, *Mar. Ecol.: Prog. Ser.*, 1999, **188**, 263–297.
- 45 Z. A. Doubleday, C. Izzo, S. H. Woodcock and B. M. Gillanders, *Aquat. Biol.*, 2013, **18**, 271–280.
- 46 U. S. G. Survey, [https://crustal.usgs.gov/geochemical\\_reference\\_standards/microanalytical\\_RM.html](https://crustal.usgs.gov/geochemical_reference_standards/microanalytical_RM.html), (accessed 07/08/2017).
- 47 S. E. Campana, in *Stock Identification Methods*, 2005, pp. 227–245, DOI: 10.1016/b978-012154351-8/50013-7.
- 48 G. Huelga-Suarez, M. Moldovan, A. Garcia-Valiente, E. Garcia-Vazquez and J. I. Garcia Alonso, *Anal. Chem.*, 2012, **84**, 127–133.
- 49 G. Huelga-Suarez, B. Fernandez, M. Moldovan and J. I. Garcia Alonso, *Anal. Bioanal. Chem.*, 2013, **405**, 2901–2909.

## Isotope pattern deconvolution of different sources of stable strontium isotopes in natural systems

A. Tchaikovsky, J. Irrgeher, A. Zitek and T. Prohaska

Electronic Supplementary Material 1 Sr/matrix separation scheme for extraction chromatography using Sr Resin (Triskem, Bruz, France)

<b>Step</b>	<b>Reagent</b>	<b>Volume ml</b>
column	Sr Resin in 0.3 mol L <sup>-1</sup>	
packing	HNO <sub>3</sub>	0.5
cleaning	6 mol L <sup>-1</sup> HNO <sub>3</sub>	3
	subb. H <sub>2</sub> O	3
	6 mol L <sup>-1</sup> HCl	2
	subb. H <sub>2</sub> O	3
conditioning	8 mol L <sup>-1</sup> HNO <sub>3</sub>	3
sample loading	sample in 8 mol L <sup>-1</sup> HNO <sub>3</sub>	3
washing	8 mol L <sup>-1</sup> HNO <sub>3</sub>	8
elution	subb. H <sub>2</sub> O	2

## Isotope pattern deconvolution of different sources of stable strontium isotopes in natural systems

A. Tchaikovsky, J. Irrgeher, A. Zitek and T. Prohaska

Electronic Supplementary Material 3.1 Strontium elemental and isotopic composition of water, fish feed, salt, raw and salted caviar from two sampling sites in Italy (IT\_GOI, IT\_VIA) and one in Austria (AT\_GRU) measured by solution based (MC) ICP-MS and two otolith datasets from Austria (AT\_SIR, AT\_LEU) as well as the certified reference materials otolith powder FEBS-1 and carbonate MACS-3 measured by laser ablation (MC) ICP-MS; uncertainties of the Sr elemental amount fractions equal to 10 % ( $U, k=2$ ), uncertainties of the solution based isotopic ratios correspond to the expanded combined standard uncertainty ( $U, k=2$ ), uncertainties of the experimentally determined otoliths and FEBS-1 and MACS-3 correspond to 2  $SD$  of the replicates

Method	Sample	Origin	Replicates	Sr $\mu\text{g g}^{-1}$	$n(^{87}\text{Sr})/n(^{86}\text{Sr})$	$U, k=2$	$n(^{88}\text{Sr})/n(^{86}\text{Sr})$	$U, k=2$	$n(^{84}\text{Sr})/n(^{86}\text{Sr})$	$U, k=2$
SB-(MC) ICP-MS	Water	IT_GOI	n=3	0.15	0.70861	0.00021	8.3758	0.0025	0.05616	0.00034
SB-(MC) ICP-MS	Fish feed	IT_GOI	n=3	47.2	0.70923	0.00021	8.3774	0.0026	0.05656	0.00014
SB-(MC) ICP-MS	Salt	IT_GOI	n=3	26.3	0.70931	0.00023	8.3801	0.0042	0.05653	0.00009
SB-(MC) ICP-MS	Caviar <sub>raw</sub>	IT_GOI	n=3	0.91	0.70869	0.00019	8.3764	0.0023	0.05626	0.00015
SB-(MC) ICP-MS	Caviar <sub>salted</sub>	IT_GOI	n=3	2.59	0.70902	0.00019	8.3789	0.0023	0.05664	0.00007
SB-(MC) ICP-MS	Water	IT_VIA	n=3	0.46	0.70838	0.00023	8.3748	0.0027	0.05676	0.00030
SB-(MC) ICP-MS	Fish feed	IT_VIA	n=3	36.60	0.70931	0.00020	8.3798	0.0028	0.05655	0.00008
SB-(MC) ICP-MS	Salt	IT_VIA	n=3	24.59	0.70952	0.00020	8.3822	0.0023	0.05652	0.00008
SB-(MC) ICP-MS	Caviar <sub>raw</sub>	IT_VIA	n=3	0.69	0.70849	0.00032	8.3734	0.0041	0.05637	0.00049
SB-(MC) ICP-MS	Caviar <sub>salted</sub>	IT_VIA	n=3	2.43	0.70927	0.00022	8.3806	0.0022	0.05652	0.00007
SB-(MC) ICP-MS	Water	AT_GRU	n=3	0.09	0.70866	0.00023	8.3783	0.0032	0.05666	0.00008
SB-(MC) ICP-MS	Fish feed	AT_GRU	n=3	32.34	0.70925	0.00023	8.3812	0.0030	0.05658	0.00010
SB-(MC) ICP-MS	Salt	AT_GRU	n=3	0.73	0.70790	0.00020	8.3786	0.0024	0.05735	0.00218
SB-(MC) ICP-MS	Caviar <sub>raw</sub>	AT_GRU	n=3	0.74	0.70908	0.00027	8.3733	0.0026	0.05683	0.00025
SB-(MC) ICP-MS	Caviar <sub>salted</sub>	AT_GRU	n=3	0.74	0.70907	0.00022	8.3762	0.0028	0.05670	0.00008
SB-(MC) ICP-MS	Water	AT_SIR	n=3	0.08	0.71640	0.00018	8.3807	0.0030	0.05663	0.00007
SB-(MC) ICP-MS	Fish feed	AT_SIR	n=3	26.89	0.70926	0.00019	8.3768	0.0022	0.05667	0.00007
LA-(MC) ICP-MS	Otoliths	AT_SIR	n=7	876.40	0.71423	0.00056	8.3740	0.0025	0.05724	0.00014
SB-(MC) ICP-MS	Water	AT_LEU	n=3	0.09	0.70791	0.00014	8.3821	0.0024	0.05664	0.00008
SB-(MC) ICP-MS	Fish feed	AT_LEU	n=3	33.03	0.70937	0.00028	8.3776	0.0049	0.05667	0.00008
LA-(MC) ICP-MS	Otoliths	AT_LEU	n=13	2144.91	0.70796	0.00031	8.3786	0.0071	0.05666	0.00121
LA-(MC) ICP-MS	FEBS-1	CRM	n=4	-	0.70969	0.00005	8.3691	0.0013	0.05694	0.00012
LA-(MC) ICP-MS	MACS-3	CRM	n=4	-	0.70820	0.00023	8.3715	0.0027	0.05676	0.00014
reference value	FEBS-1 <sup>1</sup>	CRM	-	-	0.70917	0.00001	-	-	0.056525	0.000003
reference value	MACS-3 <sup>2</sup>	CRM	-	-	0.70759	0.00001	-	-	-	-

<sup>1</sup> Reference value and uncertainty (1  $SD$ ) of FEBS-1 according to Yang *et al.* IIF correction was performed using internal correction via the  $^{88}\text{Sr}/^{86}\text{Sr}$  ratio, being a possible reason for lower isotopic ratios than measured in this experiment where external-intra elemental correction via the  $^{87}\text{Sr}/^{86}\text{Sr}$  ratio was used.

<sup>2</sup> Reference value and uncertainty for MACS-3 according to certificate (no statement on IIF correction or uncertainty calculation was available).

## Isotope pattern deconvolution of different sources of stable strontium isotopes in natural systems

A. Tchaikovsky, J. Irrgeher, A. Zitek and T. Prohaska

Electronic Supplementary Material 3.2 Molar fractions of water and fish feed obtained by model calculations, where the measured  $n(^{84}\text{Sr})/n(^{86}\text{Sr})$  and  $n(^{88}\text{Sr})/n(^{86}\text{Sr})$  isotope ratios were replaced by theoretical values of the NIST SRM 987 in all samples, uncertainties correspond to  $u_c$

<b>Sample</b>	<b>Origin</b>	<b><math>x_{\text{water}}</math></b>	<b><math>x_{\text{fish feed}}</math></b>
Caviar <sub>raw</sub>	IT_GOI	0.84 ± 0.13	0.16 ± 0.13
Caviar <sub>raw</sub>	IT_VIA	0.88 ± 0.12	0.12 ± 0.12
Caviar <sub>raw</sub>	AT_GRU	0.29 ± 0.15	0.71 ± 0.15
Otoliths	AT_SIR	0.70 ± 0.02	0.30 ± 0.02
Otoliths	AT_LEU	0.98 ± 0.06	0.01 ± 0.06

## **II. Chemometric tools for determining site-specific elemental and strontium isotopic fingerprints in sturgeon caviar**

*Anastassiya Tchaikovsky, Andreas Zitek, Johanna Irrgeher, Christine Opper, Rudolf Scheiber, Karl Moder, Leonardo Congiu and Thomas Prohaska*

*European Food Research and Technology, 2019 (submitted)*



# **Chemometric tools for determining site-specific elemental and strontium isotopic fingerprints in sturgeon caviar**

**Anastassiya Tchaikovsky<sup>1,†</sup>, Andreas Zitek<sup>1,2\*</sup>, Johanna Irrgeher<sup>3,‡</sup>, Christine Opper<sup>2,‡</sup>, Rudolf Scheiber<sup>2</sup>, Karl Moder<sup>4</sup>, Leonardo Congiu<sup>5</sup> and Thomas Prohaska<sup>2,‡</sup>**

<sup>1</sup> FFoQSI GmbH - Austrian Competence Centre for Feed and Food Quality, Safety & Innovation, Technopark 1C, 3430 Tulln

<sup>2</sup> University of Natural Resources and Life Sciences, Vienna, Department of Chemistry – VIRIS Laboratory, Konrad-Lorenz-Strasse 24, 3430 Tulln, Austria

<sup>3</sup> Helmholtz-Centre for Materials and Coastal Research, Institute for Coastal Research, Department of Marine Bioanalytical Chemistry, Max-Planck Straße 1, 21502 Geesthacht, Germany

<sup>4</sup> University of Natural Resources and Life Sciences, Vienna, Institute of Applied Statistics and Computing, Peter-Jordan-Strasse 82/I, 1190 Vienna, Austria

<sup>5</sup> University of Padova, Department of Biology, Via Ugo Bassi 58/b, 35121 Padova, Italy

<sup>†</sup> Present address: University of Vienna, Department of Analytical Chemistry, Währingerstraße 38, 1090 Vienna, Austria

<sup>‡</sup> Present address: Montanuniversität Leoben, Chair of General and Analytical Chemistry, Franz Josef- Straße 18, 8700 Leoben, Austria

\* Corresponding author: [andreas.zitek@ffoqsi.at](mailto:andreas.zitek@ffoqsi.at)

## Abstract

This study presents a chemometric protocol for the determination of site-specific elemental and strontium isotopic fingerprints in sturgeon caviar. The elemental and strontium isotopic composition of water, fish feed, salt, raw (*i.e.* unsalted) and salted sturgeon caviar from six fish farms in Europe and Iran was analyzed by (MC) ICP-MS. Multiple linear regression revealed six site-specific markers absorbed from water into sturgeon caviar ( $n(^{87}\text{Sr})/n(^{86}\text{Sr})$ ) isotope ratio and content of Na, Mn, Cu, Mo, Fe/Ca). Salting significantly changed the chemical composition of four ( $n(^{87}\text{Sr})/n(^{86}\text{Sr})$ , Na, Mn, Fe/Ca) of the six site-specific markers. Washing of salted caviar could not fully recover the initial site-specific tag. Therefore, a novel mathematical procedure based on mass balance calculations was developed for determining the theoretical  $n(^{87}\text{Sr})/n(^{86}\text{Sr})$  isotope ratio absorbed from water into sturgeon caviar. The resulting variable is a proxy for the environmental strontium isotopic signal and independent of the production process. Hierarchical cluster analysis showed that the combination of the theoretical  $n(^{87}\text{Sr})/n(^{86}\text{Sr})$  isotope ratio and two site-specific markers, which were not affected by salting (Cu, Mo), could differentiate salted caviar samples from six sites into five distinct clusters. The proposed combination of statistical and mathematical tools provides the basis for origin determination of salted sturgeon caviar using site-specific elemental and strontium isotopic fingerprints, even in cases where the initial environmental signature was altered by the production process.

**Keywords:** Food traceability; strontium isotopes; forensics; food processing; isotope pattern deconvolution; mixing models; inductively coupled plasma mass spectrometry

## 1. Introduction

Sturgeon caviar, the processed unfertilized eggs (roe) of Acipenseriformes species, is one of the most expensive food commodities in the world [1]. High consumer demand along with poaching and illegal caviar trade led to severe overexploitation of wild sturgeons [2,3]. To protect wild stocks, the trade in sturgeon caviar was put under regulation by the Convention on International Trade in Endangered Species of Wild Fauna and Flora (CITES) [4]. These measures include catch quotas, fostering of aquaculture production and legal caviar identification using a uniform labelling system. However, industry practices such as re-packing of caviar for domestic markets or re-export from intermediate countries have created possibilities for smuggling of caviar from illegal sources [3,5,6]. Consequently, methods for unambiguous verification of sturgeon caviar origin are required.

One of the most promising approaches for origin determination is the use of the chemical composition of caviar. It can be specific for a region of production or a production process, thus represents an intrinsic 'chemical fingerprint' which is difficult to counterfeit. However, previous studies on origin determination of sturgeon caviar showed that characteristic properties of processed (*i.e.* salted) caviar such as water, lipid or protein content did not differ between origins [7]. Gessner *et al.* observed a decreased absolute fatty acids content as well as higher levels of eicosapentaenoic acid (C20:5n3) in caviar produced in aquacultures in comparison to wild caviar, which they attributed to differences in the diet [7]. DePeters *et al.* confirmed these findings, but pointed out that other environmental factors such as water temperature, season, age and sexual maturity of the fish are controlling the fatty acid composition of caviar [8]. In other studies, the elemental composition of sturgeon caviar was determined on wet weight basis [9,7,8,10,11]. As the water content of the roe significantly depends on the amount of salt added for conservation and flavoring [7,12], these results are not suitable for a direct comparison of roe of different origin. The analysis of the  $\delta^{15}\text{N}/^{14}\text{N}$  and  $\delta^{13}\text{C}/^{12}\text{C}$  composition of commercially available caviar from different countries showed a large spread of the obtained results within caviar from the same water body [13]. As a consequence, a more targeted approach and a specific set of chemical markers are necessary for unambiguous caviar origin determination.

The  $n(^{87}\text{Sr})/n(^{86}\text{Sr})$  isotope ratio<sup>1</sup> is a well-established tracer for origin determination of food [16-25]. Strontium is a natural non-toxic element ubiquitous in the environment [26]. The  $n(^{87}\text{Sr})/n(^{86}\text{Sr})$  isotope ratio varies in nature due to the radioactive decay of  $^{87}\text{Rb}$  to  $^{87}\text{Sr}$ . This natural reaction occurs mainly in rocks with a half-life of about 50 billion years [27]. Thus, old

---

<sup>1</sup>The  $n(^i\text{Sr})/n(^j\text{Sr})$  isotope notation is recommended by the Commission on Isotopic Abundances and Atomic Weights of the International Union of Pure and Applied Chemistry (IUPAC) and will be used throughout the publication [14,15]

rocks are rich in  $^{87}\text{Sr}$ , while younger rocks show comparably lower  $n(^{87}\text{Sr})/n(^{86}\text{Sr})$  isotopic compositions. Chemical weathering releases strontium from bedrocks to water [26]. Consequently, water in different geologic areas has different strontium isotopic compositions [28]. Fish absorb the  $n(^{87}\text{Sr})/n(^{86}\text{Sr})$  isotope ratio from ambient water and store it in their tissue without significant isotopic fractionation [29,30]. Hence the  $n(^{87}\text{Sr})/n(^{86}\text{Sr})$  isotope ratio represents a site-specific marker, which allows to link fish to their water body of origin [30].

The analysis of elemental pattern in food provides additional information for traceability studies [31-34]. Kerr and Campana described the use of strontium isotopes and elemental pattern to discriminate between fish stocks [35]. Rodushkin *et al.* combined the  $n(^{87}\text{Sr})/n(^{86}\text{Sr})$  isotope and Sr/Ca, Sr/Mg and Sr/Ba elemental amount ratios to differentiate Swedish vendace (Kalix) caviar from vendace caviar of other origin [21]. This approach uses either direct comparison of single variables or multi-variate statistical methods to discriminate between samples of different origin based on their strontium isotopic and elemental composition.

Alternatively, site-specific markers can be used to link samples to their environment of origin [36,37]. Zitek *et al.* determined a significant correlation of the  $n(^{87}\text{Sr})/n(^{86}\text{Sr})$  isotope and Sr/Ca elemental amount ratio between water and fish otoliths. In a subsequent step, they used these site-specific markers in combination with Na/Ca elemental amount ratios to attribute fish to their water body of origin by a discriminant analysis based on habitat clusters characterized by similar chemical parameters [22].

Food processing can significantly alter the composition of site-specific markers [17]. Epova *et al.* reported that the  $n(^{87}\text{Sr})/n(^{86}\text{Sr})$  isotopic composition of Bayonne ham is directly related to the salt used for curing [33]. Edura *et al.* found significant differences between the elemental content of Mg, P, Ca, Mn, Fe, Zn, Rb and Sr in raw and processed wakame (*i.e.* edible seaweed; [38]). Thus, the chemical composition of the investigated samples was a combination of the site-specific tag and salt used for processing. Consequently, the influence of salt on the  $n(^{87}\text{Sr})/n(^{86}\text{Sr})$  isotopic and elemental composition of sturgeon caviar needs to be investigated in order to select markers which are independent of the production process.

The aim of this paper was the development of a chemometric protocol for the determination of site-specific chemical fingerprints in salted sturgeon caviar. The calculations are based on experimentally determined strontium isotopic and elemental data in water, fish feed, salt, raw (*i.e.* not salted) and salted sturgeon caviar from six fish farms in Europe and Iran. Furthermore, a novel mathematical method for calculating the theoretical  $n(^{87}\text{Sr})/n(^{86}\text{Sr})$  isotope ratio of water in raw and salted sturgeon caviar is presented.

## 2. Materials and methods

Preparatory laboratory work was performed in an ISO class 8 clean room according to ISO 14644-1. Laboratory water type I (18 M $\Omega$  cm, F+L GmbH, Vienna, Austria) was further purified using a sub-boiling distillation system (Milestone-MLS GmbH, Leutkirch, Germany). Nitric acid (p.a., 65 % w/w, Merck-Millipore, Darmstadt, Germany) was double sub-boiled in a DST-1000 sub-boiling distillation system (AHF Analystechnik, Tübingen, Germany). All laboratory consumables were pre-cleaned before use.

### 2.1 Samples

The investigated samples comprised of fish farm pool water, fish feed, salt, raw (*i.e.* not salted) and salted sturgeon caviar from one fish farm in Austria, four fish farms in North Italy and one fish farm in the Islamic Republic of Iran (no raw caviar was available from this farm). Table 1 gives details on the production plants and their CITES code used for identification. Water samples were collected in pre-cleaned 100 mL polyethylene bottles from fish farm pools in triplicates. (The Iranian farm provided one water sample, analyzed in triplicates.) Raw and salted caviar samples represented a randomized subset of the current production batch of the investigated fish farm, respectively. Raw caviar was sampled in pre-cleaned 100 mL polyethylene bottles. Salted caviar was obtained in commercial glass containers with metal lids or in metal cans. Fish feed and salt were collected in polyethylene zip-bags and kept refrigerated until further treatment. Water and caviar samples were frozen to -20°C.

Country	Sample Type	Company	CITES code	Latitude	Longitude	Fish farm	Sample ID
Austria	water, fish feed, salt, raw caviar, salted caviar	Grüll GmbH	0001	47.774130	13.061140	Grüll	GRU
Italy	water, fish feed, salt, raw caviar, salted caviar	Agro Ittica	384/IT0004	45.224814	10.698914	Goito	GOI
Italy	water, fish feed, salt, raw caviar, salted caviar	Agro Ittica	384/IT0004	45.366563	10.319548	Malpaga	MAL
Italy	water, fish feed, salt, raw caviar, salted caviar	Agro Ittica	384/IT0004	45.325253	10.395025	Viadana	VIA
Italy	water, fish feed, salt, raw caviar, salted caviar	Agro Ittica	384/IT0004	45.382434	8.829054	Ticino Park	TIC
Iran	water, fish feed, salt, salted caviar	Sari Aquaculture	943	36.611138	53.113259	Sari	SAR

Table 1. Sample list of fish farm pool water, fish feed, salt, raw and salted caviar from six sturgeon farms in Europe and Iran

### 2.2 Sample preparation

Water samples were defrosted, filtered using a 0.45  $\mu$ m pore size filter (Sartorius, Göttingen, Germany) to obtain the dissolved elemental fraction and acidified to 2 % HNO<sub>3</sub> (w/w). Raw and salted caviar samples were allowed to thaw at room temperature. Raw caviar was divided into three aliquots of about 10 g (wet weight) per sampling site. Salted caviar represented a blend of

raw caviar and salt. Salted caviar was divided into 3 x 3 aliquots of about 10 g (wet weight) per sampling site in order to investigate if it is possible to remove salt by washing and the efficacy of this procedure: (1) Three aliquots were used as such (salted caviar). (2) Three aliquots were washed twice by adding 50 mL of sub-boiled water, slewing and decanting of the supernatant solution (salted caviar two-times washed). (3) Three aliquots were washed four times (salted caviar four-times washed). All caviar samples were freeze-dried (either by Christ Beta 1-8 LD plus or Christ Alpha 1-s LD, Martin Christ Gefriertrocknungsanlagen GmbH, Osterode am Harz, Germany) before microwave-assisted (Multiwave 3000, Anton Paar, Graz, Austria) acid digestion using 0.5 g dry caviar and a reaction mixture of 9 mL sub-boiled conc.  $\text{HNO}_3$  and 0.75 mL of  $\text{H}_2\text{O}_2$  (30 % w/w, suprapur, Merck). Fish feed pellets were ground using an agate mortar, divided into triplicates per sampling site and microwave digested using 0.2 g of fish feed and a reaction mixture of 6.67 mL of sub-boiled conc.  $\text{HNO}_3$  and 3.33 mL of  $\text{H}_2\text{O}_2$  (30 % w/w, suprapur, Merck). Digested caviar and fish feed samples were diluted with sub-boiled water to 2 %  $\text{HNO}_3$  (w/w). Salt was dissolved gravimetrically in 2 %  $\text{HNO}_3$  (w/w). Water, salt solutes and digests of feed, raw and salted caviar samples underwent Sr/matrix separation using a strontium specific extraction resin (Triskem, Bruz, France) according to [39] prior to strontium isotopic measurements.

### 2.3 Analytical measurements

The elemental composition of water, fish feed, salt, raw caviar and salted caviar was measured using an inductively coupled plasma quadrupole mass spectrometer (ICP-QMS, NexION 350 D or Elan DRC-e, PerkinElmer, Waltham, USA) using a PFA (perfluoroalkoxy) nebulizer (Microflow ST Nebulizer, Elemental Scientific Inc., Nebraska, USA) in combination with a cyclonic spray chamber (PerkinElmer, Waltham, USA). Elemental mass fractions of Li, Be, B, Na, Mg, Al, K, Ca, V, Cr, Mn, Fe, Ni, Co, Cu, Zn, Ga, As, Se, Rb, Sr, Mo, Ag, Cd, Te, Ba, Tl, Pb, Bi and U were determined following blank correction, normalization to indium (single element ICP-MS standard, CertiPur, Merck, Darmstadt, Germany) and external calibration applying a 5-point calibration (multi-elemental ICP-MS standard VI, CertiPur, Merck, Darmstadt, Germany). Samples were diluted as required for the working range of the calibration. The elemental mass fraction of Na was not analyzed in salt and salted caviar samples.

The limit of quantification (LOQ) was calculated as equivalent to ten times the standard deviation of the process blank taking into account dilution factors and the initial weight of the samples, respectively. Results were validated using in-house quality control standards and reference materials SLRS-5 river water, TORT-3 lobster hepatopancreas (both from the National Research

Council, Ontario, Canada) as well as IAPSO seawater standard (Batch num. P143, OSIL Ltd, Havant, UK).

The  $n(^{87}\text{Sr})/n(^{86}\text{Sr})$ ,  $n(^{88}\text{Sr})/n(^{86}\text{Sr})$  and  $n(^{84}\text{Sr})/n(^{86}\text{Sr})$  isotope ratio measurements were assessed on a multi-collector inductively coupled plasma mass spectrometer (MC ICP-MS, Nu Plasma HR, Nu Instruments Ltd., Wrexham, UK). Samples were introduced using a membrane desolvation introduction system (either DSN-100, Nu Instruments, Wrexham, UK or Aridus II, Cetac Technologies, Omaha, Nebraska, USA). Strontium isotope ratios were corrected for blank, residual  $^{87}\text{Rb}$  and instrumental isotopic fractionation following the procedure by Horsky *et al.* [40]. Instrumental isotopic fractionation of the  $n(^{87}\text{Sr})/n(^{86}\text{Sr})$ ,  $n(^{88}\text{Sr})/n(^{86}\text{Sr})$  and  $n(^{84}\text{Sr})/n(^{86}\text{Sr})$  isotope ratios was corrected in an external intra-elemental approach (standard-sample-bracketing) using NIST SRM 987 (National Institute of Standards and Technology, Gaithersburg, USA)[41]. The reference materials TORT-3 and IAPSO followed the same preparation procedure as the samples. Furthermore, the NIST SRM 987 was separated in order to monitor potential on-column fractionation.

## 2.4 Measurement uncertainty

The measurement uncertainty indicates the quality of the analytical result. It represents the combination of all uncertainties (*e.g.* heterogeneity of the sample, blank, measurement precision, etc.) contributing to the measurement result [42]. All uncertainties in this study were determined in a Kragten approach [43] following EURACHEM guidelines [42]. The combined standard uncertainties of the  $n(^{87}\text{Sr})/n(^{86}\text{Sr})$ ,  $n(^{88}\text{Sr})/n(^{86}\text{Sr})$  and  $n(^{84}\text{Sr})/n(^{86}\text{Sr})$  isotope ratios, were calculated based on the procedure by Horsky *et al.* [40] including the contribution of the blank, measurement precision, instrumental isotopic fractionation correction, heterogeneity of the samples and  $^{87}\text{Rb}$ -correction. Calculations of the uncertainty of molar fractions obtained by isotope pattern deconvolution are discussed in detail by Tchaikovsky *et al.* [39]. If not stated otherwise, all uncertainties in this work correspond to the expanded uncertainty ( $U$ ,  $k=2$ ) corresponding to a coverage factor of 95 %. The heterogeneity of the sample represented the major source to the uncertainty. In accordance to EURACHEM guidelines, measurement values have to be considered equal when they overlap within limits of uncertainty [42].

## 2.5 Isotope pattern deconvolution

The contributions of water, fish feed and salt to the  $n(^{87}\text{Sr})/n(^{86}\text{Sr})$  isotope ratio of salted caviar was calculated using isotope pattern deconvolution (IPD). This mathematical procedure is used in multiple-spike isotope dilution mass spectrometry (IDMS)[44], but can also be applied for the

calculation of the contribution of natural sources to the strontium isotopic composition of fish tissue [39]. Therefore, the experimentally assessed  $n(^{87}\text{Sr})/n(^{86}\text{Sr})$ ,  $n(^{88}\text{Sr})/n(^{86}\text{Sr})$  and  $n(^{84}\text{Sr})/n(^{86}\text{Sr})$  isotope ratios of water, fish feed, salt and salted caviar were converted into isotopic abundances  $A$  of the isotope  $i$  and used as input variables in a set of simple linear equations (Equation 1). The molar fractions of the individual components  $x_n$  to the  $n(^{87}\text{Sr})/n(^{86}\text{Sr})$  isotope ratio of salted caviar were calculated by multiple-linear regression modelling by minimizing the error vector  $e$  using the LINEST-function in Microsoft Excel®. Similar to IDMS calculations, IPD does not require the strontium elemental content of the individual components for the calculation of the molar fractions.

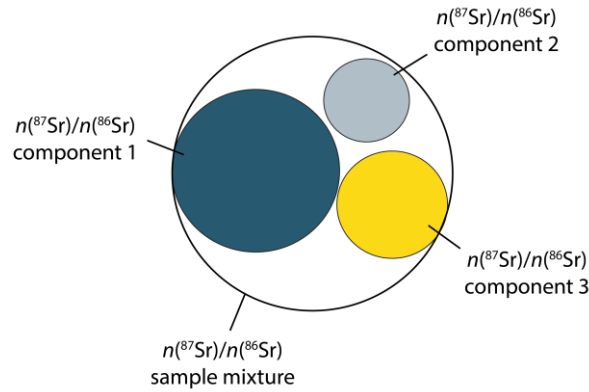
$$\begin{bmatrix} A_{\text{salted caviar}}^{84} \\ A_{\text{salted caviar}}^{86} \\ A_{\text{salted caviar}}^{87} \\ A_{\text{salted caviar}}^{88} \end{bmatrix} = \begin{bmatrix} A_{\text{water}}^{84} & A_{\text{feed}}^{84} & A_{\text{salt}}^{84} \\ A_{\text{water}}^{86} & A_{\text{feed}}^{86} & A_{\text{salt}}^{86} \\ A_{\text{water}}^{87} & A_{\text{feed}}^{87} & A_{\text{salt}}^{87} \\ A_{\text{water}}^{88} & A_{\text{feed}}^{88} & A_{\text{salt}}^{88} \end{bmatrix} \times \begin{bmatrix} x_{\text{water}} \\ x_{\text{feed}} \\ x_{\text{salt}} \end{bmatrix} + \begin{bmatrix} e^{84} \\ e^{86} \\ e^{87} \\ e^{88} \end{bmatrix} \quad \text{Eq.1}$$

The contribution of water and fish feed to the  $n(^{87}\text{Sr})/n(^{86}\text{Sr})$  isotope ratio of raw caviar was determined in our previous study [39]. Table S1 supplementary material summarizes the used input variables for the calculation of the contribution of water, fish feed and salt to the  $n(^{87}\text{Sr})/n(^{86}\text{Sr})$  isotope ratio of salted caviar from the fish farms GRU, MAL, TIC and SAR. Molar fractions of the individual components of the strontium isotopic composition of salted caviar from the fish farms GOI and VIA correspond to results reported previously [39]. An example of the determination of the contribution of water, fish feed and salt to the  $n(^{87}\text{Sr})/n(^{86}\text{Sr})$  isotope ratio of salted caviar by IPD using Microsoft Excel® is given in Tchaikovsky *et al.* [39].

## 2.6 Reverse-mixing model calculation

Reverse-mixing models are a novel mathematical method based on mixing model calculations by Faure and Powell [27]. It uses mass balance equations to calculate the  $n(^{87}\text{Sr})/n(^{86}\text{Sr})$  isotope ratio of an unknown component in a sample mixture. This method is particularly useful to calculate the theoretical  $n(^{87}\text{Sr})/n(^{86}\text{Sr})$  isotope ratio absorbed from water into sturgeon caviar. The  $n(^{87}\text{Sr})/n(^{86}\text{Sr})$  isotope ratio in water depends mainly on local geology and has the potential to link sturgeon caviar to its environment of origin. In a natural habitat, water and feed have the same isotopic signature. However, in aquaculture production the  $n(^{87}\text{Sr})/n(^{86}\text{Sr})$  isotopic composition of raw caviar is a mixture of water and fish feed [39], which is in most cases of non-local origin.





$$A_{sample\ mix}^i = x_{comp1} A_{comp1}^i + x_{comp2} A_{comp2}^i + x_{comp3} A_{comp3}^i$$

Figure 1. The isotopic composition of a sample is determined by the isotopic abundances  $A^i$  and the molar fractions  $x_n$  of the individual components [27,44]

Moreover, commercially available sturgeon caviar is salted, which represent a third source to the strontium isotopic composition of the sample (Figure 1). Accordingly, the environmental strontium isotopic signature in the sample mixture can only be determined by mathematical methods. The theoretical  $n(^{87}\text{Sr})/n(^{86}\text{Sr})$  isotopic composition of water in raw caviar was calculated using Equation 2. The  $n(^{87}\text{Sr})/n(^{86}\text{Sr})$  isotopic composition of raw caviar and fish feed were determined experimentally and converted into strontium isotopic abundance of raw caviar  $A_{raw\ caviar}^i$  and fish feed  $A_{feed}^i$ . The molar fraction of feed  $x_{feed}$  was calculated by IPD in our previous study and accounted to  $0.20 \pm 0.08$  (2 SD; [39]).

$$n(^{87}\text{Sr})/n(^{86}\text{Sr})_{water,calc.A} = \frac{A_{raw\ caviar}^{87} - x_{feed} \cdot A_{feed}^{87}}{A_{raw\ caviar}^{86} - x_{feed} \cdot A_{feed}^{86}} \quad \text{Eq.2}$$

The determination of the theoretical  $n(^{87}\text{Sr})/n(^{86}\text{Sr})$  isotope ratio of water in salted sturgeon caviar requires the experimentally determined  $n(^{87}\text{Sr})/n(^{86}\text{Sr})$  isotopic composition of salted caviar, salt and fish feed along with molar fractions of salt and fish feed determined by IPD (Equation 3).

$$n(^{87}\text{Sr})/n(^{86}\text{Sr})_{water,calc.B} = \frac{A_{salted\ caviar}^{87} - (x_{salt} \cdot A_{salt}^{87}) - (x_{feed} \cdot A_{feed}^{87})}{A_{salted\ caviar}^{86} - (x_{salt} \cdot A_{salt}^{86}) - (x_{feed} \cdot A_{feed}^{86})} \quad \text{Eq.3}$$

If salt had no significant influence on the  $n(^{87}\text{Sr})/n(^{86}\text{Sr})$  isotopic composition of salted caviar, the theoretical  $n(^{87}\text{Sr})/n(^{86}\text{Sr})$  isotope ratio of water in salted caviar can be calculated by Equation 4.

Therefore, the experimentally determined  $n(^{87}\text{Sr})/n(^{86}\text{Sr})$  isotope ratios of salted caviar and fish feed along with  $x_{feed}$  of  $0.20 \pm 0.08$  (2 SD; [39]) were used.

$$n(^{87}\text{Sr})/n(^{86}\text{Sr})_{water,calc.C} = \frac{A_{salted\ caviar}^{87} - x_{feed} \cdot A_{feed}^{87}}{A_{salted\ caviar}^{86} - x_{feed} \cdot A_{feed}^{86}} \quad \text{Eq.4}$$

An example of reverse-mixing model calculations for the determination of the  $n(^{87}\text{Sr})/n(^{86}\text{Sr})$  isotope ratio of water in salted caviar using Microsoft Excel® is given in the supplementary material 2, worksheet 'Water\_calc\_B'.

## 2.6 Statistical data analysis

A Kolmogorov-Smirnov test showed non-normal data distribution of most  $n(^{87}\text{Sr})/n(^{86}\text{Sr})$  isotope ratios, element/Ca amount ratios and elemental mass fractions of water, feed and raw caviar samples. Consequently, a Kruskal-Wallis test was used to assess significant differences of these variables of water, feed and raw caviar from different fish farms, respectively. Multiple linear regression analysis was applied to investigate the influence of water and fish feed on the strontium isotopic and elemental composition of raw caviar. Variables which showed a significant relationship between water and raw caviar were considered as site-specific markers. A pairwise t-test for dependant samples was used to determine the influence of salt on the site-specific markers. Therefore, the chemical site-specific markers and their constituents in raw and salted caviar from five of the six investigated fish farms (GRU, GOI, MAL, VIA, TIC) was compared. No raw caviar was available from the Iranian fish farm SAR. A Spearman rank correlation analysis was used to verify the compliance of the theoretical  $n(^{87}\text{Sr})/n(^{86}\text{Sr})$  isotope ratios of water in raw and salted caviar calculated by reverse-mixing models to the experimentally determined  $n(^{87}\text{Sr})/n(^{86}\text{Sr})$  isotope ratios of fish farm pool water. The potential of site-specific markers in salted caviar to form a fish farm-specific chemical fingerprint was investigated by hierarchical cluster analysis (Ward's method, Euclidean distance; Nearest neighbour and Within-groups linkage, Squared Euclidean distance; standardized values). These procedures were applied to the same dataset using variables which were a) not influenced by salting and b) determined by reverse-mixing models ( $n(^{87}\text{Sr})/n(^{86}\text{Sr})_{theoretical}$ ) in order to provide more confidence in cluster separation. A similarity dendrogram along with the knee criterion served to delineate the number of salted caviar clusters. The statistical significance level for all analysis corresponded to  $\alpha=0.05$ . Statistical data evaluation was performed using SPSS® (IBM SPSS Statistics 24, Armonk, USA).

Sample ID	LOQ	GRU	GOI	MAL	VIA	TIC	SAR	
<b>water</b>								
$n(^{87}\text{Sr})/n(^{86}\text{Sr})$		0.70866 (23)	0.70861 (22)	0.70858 (21)	0.70838 (23)	0.70945 (28)	0.70843 (23)	
Ca	mg g <sup>-1</sup>	3.84E-04	0.103 (13)	0.052 (9)	0.111 (11)	0.112 (12)	0.030 (4)	0.106 (11)
Na	mg g <sup>-1</sup>	2.20E-04	0.0102 (10)	0.0045 (10)	0.0069 (11)	0.0065 (6)	0.0055 (6)	0.058 (6)
Mg	mg g <sup>-1</sup>	7.04E-05	0.0285 (27)	0.0091 (27)	0.0229 (32)	0.0270 (27)	0.0064 (7)	0.0306 (33)
Mn	mg g <sup>-1</sup>	4.62E-05	0.00060 (10)	0.0025 (15)	0.0085 (9)	<LOQ	0.0051 (6)	0.00039 (15)
K	μg g <sup>-1</sup>	4.66E-02	1.71 (18)	1.36 (35)	2.68 (29)	3.01 (33)	1.43 (34)	3.5 (9)
Fe	μg g <sup>-1</sup>	1.32E-02	0.234 (33)	0.120 (31)	0.272 (27)	0.233 (25)	0.079 (10)	0.45 (4)
Sr	μg g <sup>-1</sup>	2.34E-04	0.104 (12)	0.15 (4)	0.43 (4)	0.46 (5)	0.219 (22)	1.53 (15)
Co	ng g <sup>-1</sup>	4.97E-03	0.123 (13)	0.089 (21)	0.188 (21)	0.203 (22)	0.065 (9)	0.54 (5)
Cu	ng g <sup>-1</sup>	7.72E-02	0.51 (6)	0.97 (12)	0.68 (8)	0.68 (17)	0.68 (17)	0.68 (7)
As	ng g <sup>-1</sup>	1.85E-03	0.125 (14)	1.27 (16)	0.75 (9)	0.56 (6)	1.54 (17)	<LOQ
Rb	ng g <sup>-1</sup>	1.85E-03	0.47 (5)	1.06 (14)	0.53 (6)	1.34 (14)	1.21 (12)	1.15 (11)
Mo	ng g <sup>-1</sup>	3.36E-02	<LOQ	1.37 (32)	2.20 (28)	2.22 (22)	0.53 (6)	1.45 (15)
<b>fish feed</b>								
$n(^{87}\text{Sr})/n(^{86}\text{Sr})$		0.70925 (23)	0.70924 (22)	0.70938 (30)	0.70931 (20)	0.70937 (20)	0.7092 (4)	
K	g g <sup>-1</sup>	1.18E-05	0.0115 (13)	0.0103 (13)	0.0108 (11)	0.0124 (13)	0.0108 (13)	0.0093 (9)
Ca	g g <sup>-1</sup>	5.46E-05	0.0121 (14)	0.0262 (28)	0.0114 (12)	0.0134 (14)	0.0124 (13)	0.0152 (18)
Na	g g <sup>-1</sup>	1.23E-05	0.0039 (4)	0.0050 (5)	0.0050 (5)	0.0050 (5)	0.0051 (6)	0.016 (16)
Mg	mg g <sup>-1</sup>	2.01E-03	2.04 (22)	2.40 (29)	2.62 (30)	2.41 (24)	2.68 (29)	2.79 (30)
Mn	mg g <sup>-1</sup>	4.93E-05	0.048 (6)	0.058 (10)	0.098 (10)	0.118 (13)	0.110 (13)	0.045 (15)
Fe	mg g <sup>-1</sup>	7.12E-03	0.66 (10)	0.51 (7)	0.73 (9)	0.72 (9)	0.72 (12)	0.46 (7)
Cu	mg g <sup>-1</sup>	1.34E-02	0.0151 (17)	0.0184 (25)	0.0246 (25)	0.0278 (32)	0.0269 (28)	0.0134 (15)
Sr	mg g <sup>-1</sup>	1.02E-04	0.032 (4)	0.047 (7)	0.032 (4)	0.037 (4)	0.035 (4)	0.037 (4)
Co	μg g <sup>-1</sup>	5.05E-03	0.151 (28)	0.192 (23)	0.135 (15)	0.256 (26)	0.233 (25)	0.16 (6)
As	μg g <sup>-1</sup>	7.12E-02	1.98 (22)	1.40 (14)	1.34 (18)	1.50 (15)	1.44 (21)	2.45 (27)
Rb	μg g <sup>-1</sup>	8.42E-03	6.7 (7)	9.9 (9)	8.5 (9)	903 (9)	8.2 (9)	4.1 (4)
Mo	μg g <sup>-1</sup>	2.46E-02	1.63 (21)	1.59 (16)	2.58 (26)	2.55 (26)	2.61 (27)	0.85 (10)
<b>raw caviar</b>								
$n(^{87}\text{Sr})/n(^{86}\text{Sr})$		0.70908 (27)	0.70869 (19)	0.70847 (22)	0.70850 (31)	0.70899 (25)	-	
Na	mg g <sup>-1</sup>	1.23E-02	1.32 (13)	0.56 (6)	0.88 (11)	1.22 (12)	1.29 (14)	-
Mg	mg g <sup>-1</sup>	2.01E-03	0.95 (10)	0.73 (8)	0.80 (9)	0.65 (7)	0.60 (6)	-
K	mg g <sup>-1</sup>	1.18E-02	4.6 (5)	2.95 (30)	3.7 (5)	3.5 (4)	2.84 (28)	-
Ca	mg g <sup>-1</sup>	5.46E-02	0.41 (4)	0.34 (4)	0.31 (4)	0.258 (28)	0.243 (26)	-
Fe	mg g <sup>-1</sup>	7.12E-03	0.067 (9)	0.061 (6)	0.072 (10)	0.051 (10)	0.058 (7)	-
Mn	μg g <sup>-1</sup>	4.93E-02	2.89 (32)	1.83 (21)	1.90 (22)	2.31 (24)	1.78 (19)	-
Co	μg g <sup>-1</sup>	5.05E-03	0.044 (5)	0.0327 (35)	0.0303 (32)	0.034 (4)	0.0301 (31)	-
Cu	μg g <sup>-1</sup>	3.71E-01	4.2 (4)	7.8 (9)	6.9 (9)	6.8 (8)	2.82 (32)	-
As	μg g <sup>-1</sup>	7.12E-02	0.37 (4)	0.60 (6)	0.55 (8)	0.49 (6)	0.33 (4)	-
Rb	μg g <sup>-1</sup>	8.42E-03	4.2 (4)	2.07 (23)	2.57 (30)	2.79 (30)	2.68 (27)	-
Sr	μg g <sup>-1</sup>	1.02E-01	0.72 (9)	0.91 (11)	1.00 (13)	0.69 (7)	0.61 (6)	-
Mo	μg g <sup>-1</sup>	2.46E-02	0.051 (19)	0.072 (9)	0.124 (15)	0.120 (14)	<LOQ	-
<b>salted caviar</b>								
$n(^{87}\text{Sr})/n(^{86}\text{Sr})$		0.70907 (22)	0.70902(20)	0.70907 (27)	0.70927 (22)	0.70878 (30)	0.70823 (24)	
K	g g <sup>-1</sup>	1.18E-05	0.0051 (8)	0.00282 (32)	0.0043 (8)	0.0041 (20)	0.0025 (14)	0.0034 (7)
Mg	mg g <sup>-1</sup>	2.01E-03	0.87 (13)	0.65 (8)	0.93 (15)	0.7 (4)	0.5 (4)	0.82 (18)
Ca	mg g <sup>-1</sup>	5.46E-02	0.35 (4)	0.39 (15)	0.40 (5)	0.31 (4)	0.15 (4)	0.27 (5)
Fe	mg g <sup>-1</sup>	7.12E-03	0.115 (19)	0.058 (7)	0.085 (17)	0.053 (8)	0.042 (4)	0.043 (12)
Cu	mg g <sup>-1</sup>	3.71E-04	0.0042 (6)	0.0073 (7)	0.0075 (9)	0.0070 (9)	0.0024 (15)	0.0024 (6)
Mn	μg g <sup>-1</sup>	4.93E-02	3.3 (4)	2.22 (26)	2.7 (4)	3.09 (32)	2.2 (9)	2.2 (4)
Co	μg g <sup>-1</sup>	5.05E-03	0.042 (4)	0.033 (4)	0.035 (6)	0.038 (4)	0.02681 (31)	0.050 (12)
As	μg g <sup>-1</sup>	7.12E-02	0.72 (7)	0.60 (7)	0.63 (8)	0.74 (8)	0.31 (17)	0.24 (18)
Rb	μg g <sup>-1</sup>	8.42E-03	3.1 (5)	1.82 (18)	2.6 (4)	2.61 (28)	2.1 (9)	2.6 (5)
Sr	μg g <sup>-1</sup>	1.02E-01	0.74 (7)	2.6 (5)	3.2 (4)	2.44 (25)	0.89 (12)	1.8 (4)
Mo	μg g <sup>-1</sup>	2.46E-02	0.064 (12)	0.068 (11)	0.123 (16)	0.121 (14)	<LOQ	0.092 (29)
<b>salt</b>								
$n(^{87}\text{Sr})/n(^{86}\text{Sr})$		0.70790 (20)	0.70931 (23)	0.70924 (19)	0.70952 (20)	0.70713 (19)	0.70843 (27)	
K	mg g <sup>-1</sup>	2.33E-04	1.15 (12)	0.160 (17)	0.174 (24)	0.187 (19)	0.072 (8)	0.0136 (21)
Ca	mg g <sup>-1</sup>	2.04E-04	0.013 (4)	0.46 (5)	0.42 (4)	0.43 (4)	0.046 (6)	0.44 (5)
Mg	mg g <sup>-1</sup>	2.18E-05	0.0002 (5)	0.206 (21)	0.228 (31)	0.303 (33)	0.0150 (22)	0.0041 (4)
Sr	mg g <sup>-1</sup>	9.72E-07	0.00073 (7)	0.0263 (26)	0.0267 (27)	0.0246 (25)	0.00156 (16)	0.0037 (4)
Rb	μg g <sup>-1</sup>	7.08E-05	0.69 (7)	0.0283 (29)	0.0299 (32)	0.0341 (34)	0.0096 (10)	0.0194 (32)
Mo	ng g <sup>-1</sup>	1.31E+00	<LOQ	11.7 (9)	11.3 (9)	32 (4)	<LOQ	2.0 (4)

Table 2. The  $n(^{87}\text{Sr})/n(^{86}\text{Sr})$  isotopic and elemental composition of investigated samples from six fish farms (GRU, GOI, MAL, VIA, TIC and SAR); uncertainties correspond to  $U$ ,  $k=2$ ; significant numbers of digits are given according to EURACHEM guidelines

### 3. Results and discussion

#### 3.1 Pre-selection of variables for statistical analysis

In order to investigate the influence of water, fish feed and salt on the elemental and strontium isotopic composition of raw and salted sturgeon caviar, only variables that fulfilled the following two requirements were selected: 1) the elemental mass fraction of an element had to be above the LOQ in at least two-thirds of the investigated water, feed, salt, raw and salted caviar samples, respectively; and 2) the measured values of both the strontium isotope ratios and elemental mass fraction of the reference materials and in-house quality-control standards had to be in agreement with their respective certified or target values (Table S2 supplementary material; [45-48]). These criteria were fulfilled by the  $n(^{87}\text{Sr})/n(^{86}\text{Sr})$  isotope ratio and the elemental mass fractions of Na, Mg, K, Ca, Mn, Fe, Co, Cu, As, Rb, Sr and Mo in water, fish feed, raw and salted caviar as well as the  $n(^{87}\text{Sr})/n(^{86}\text{Sr})$  isotope ratios and the elemental mass fractions of Mg, K, Ca, Rb, Sr and Mo in salt (Table 2).

#### 3.2 Influence of water and feed on the strontium isotopic and elemental composition of raw caviar

Fish farm pool water and fish feed were assumed to be the main sources of the  $n(^{87}\text{Sr})/n(^{86}\text{Sr})$  isotopic and elemental composition of raw (*i.e.* unsalted) sturgeon caviar [49]. Variance analysis revealed significant differences of all pre-selected variables and their element/Ca mass amount ratios of water, fish feed and raw caviar samples, respectively (Kruskal-Wallis test,  $P < 0.05$ ) with the exception of the  $n(^{87}\text{Sr})/n(^{86}\text{Sr})$  isotope ratios of fish feed (Kruskal-Wallis test,  $P > 0.05$ ). The average  $n(^{87}\text{Sr})/n(^{86}\text{Sr})$  isotope ratio of fish feed in this study accounted to  $0.70930 \pm 0.00025$  ( $n=6$ ;  $U$ ,  $k=2$ ). This strontium isotope ratio was in accordance to seawater [46], which suggested marine origin of the investigated fish feed. Multiple linear regression analysis showed that fish farm pool water significantly determined the  $n(^{87}\text{Sr})/n(^{86}\text{Sr})$  isotope ratio, the Na, Mn, Cu and Mo mass fraction as well as the elemental amount ratio of Fe/Ca of raw caviar. Fish feed significantly influenced the Mg, As, Rb, Mg/Ca, K/Ca and the Co/Ca composition of raw caviar (Table 3).

The relationship of the  $n(^{87}\text{Sr})/n(^{86}\text{Sr})$  isotope ratios of raw caviar and water confirmed previous findings that water is the main contributor to the strontium elemental mass fraction of raw sturgeon caviar [39]. Furthermore, as the strontium isotope ratios of fish feed showed no significant difference between sampling sites, the contribution of fish feed to the variation of the  $n(^{87}\text{Sr})/n(^{86}\text{Sr})$  isotopic composition of raw caviar was negligible.

Source	Variable	Stat. significance
water	$n(^{87}\text{Sr})/n(^{86}\text{Sr})$	0.006
	Na	0.049
	Mn	0.020
	Cu	0.029
	Mo	0.000
	Fe/Ca	0.015
fish feed	Mg	0.018
	As	0.008
	Rb	0.000
	Mg/Ca	0.000
	K/Ca	0.000
	Co/Ca	0.000

Table 3. Variables in water and fish feed determining the chemical composition of raw caviar along with the statistical significance of the regression coefficient

The link between the elemental composition of water, fish feed and raw caviar was not discussed in literature yet, as most studies focused on the analysis of salted caviar only. In this context, Rudoshkin *et al.* reported variations of the Mg, K, Ca, Mn, Fe, Cu, As, Rb and Mo elemental mass fractions in processed vendace caviar of various geographic sources [21]. Analysing metal contaminants in commercial sturgeon caviar, Wang *et al.* confirmed the variation of the Mo and Co elemental content in products of different geographic origin, which can arise from both anthropogenic and natural sources [10]. The elemental mass fraction of Cu of  $1.42 \mu\text{g g}^{-1} \pm 0.22 \mu\text{g g}^{-1}$  (1 SD) in salted sturgeon caviar reported by Sobhanardakani *et al.* [11] was significantly lower than the Cu mass fraction determined in salted caviar from one Austrian (GRU) and three Italian fish farms (GOI, MAL, VIA; compare Table 2). Yet, little is known about Mo, Co and Cu metabolism in Acipenseriformes species. The moderate but still significant relationship of the elemental mass fraction of Na in raw sturgeon caviar and water could be advantageous to improve discrimination between raw caviar from sturgeons reared in freshwater pools in comparison to cage production or wild anadromous species due to the higher sodium content of seawater.

Other variables, such as the Sr/Ca elemental amount ratio used by Rodushkin *et al.* for differentiation between salted vendace caviar from different producers were not identified as chemical markers in raw sturgeon caviar in this study. The variation of the Sr/Ca elemental amount ratios between different vendace caviar products might have been influenced by salt used for processing.

These findings suggested that the  $n(^{87}\text{Sr})/n(^{86}\text{Sr})$  isotopic and the Na, Mn, Cu, Mo and Fe/Ca elemental pattern were absorbed from fish farm pool water into sturgeon caviar. These variables are influenced by the chemical composition of fish farm pool water, which is predominantly

determined by geological settings. They represent site-specific chemical markers, which have the potential to link sturgeon caviar to its environment of origin and were used for further data analysis hereafter.

### 3.3 Influence of salting on the site-specific chemical markers

Table 4 shows the results of a pairwise t-test used to investigate the influence of salting on site-specific chemical markers. Salting significantly changed the  $n(^{87}\text{Sr})/n(^{86}\text{Sr})$  isotope ratio, the Fe/Ca elemental amount ratio and the Mn elemental mass fractions of some fish farms (Figure 2 and Figure 3a, 3b). The alteration of the Fe/Ca elemental amount ratio was governed by the shift of the Fe mass fraction towards higher values (Figure 3c). The elemental mass fraction of Ca of all investigated raw and salted caviar samples overlapped within limits of uncertainty (Figure 3d). According to the EURACHEM guidelines these values have to be considered equal [42]. Therefore, the Ca composition of caviar was considered not affected by salting. Salting had no significant effect on the Cu and Mo elemental composition of caviar (Table 4; pairwise t-test,  $P>0.05$ ). The elemental content of Na was not analysed in salted caviar as sodium is one of the main elements in table salt which comprises about 7 - 8 % of the total weight of commercial “malossol” (*i.e.* less salty) type caviar [10].

Figure 2 shows that the difference between the  $n(^{87}\text{Sr})/n(^{86}\text{Sr})$  isotope ratios of raw and salted caviar was largest for samples from the fish farms GOI, MAL and VIA. Salt from these fish farms showed the highest strontium mass fraction of 25 – 27  $\mu\text{g g}^{-1}$  and  $n(^{87}\text{Sr})/n(^{86}\text{Sr})$  isotope ratios of about 0.7093 (Table 2), which were in the range of the strontium isotopic composition of seawater [46]. This result indicated that the used salt might have been sea salt.

Variables	GRU	GOI	MAL	VIA	TIC
$n(^{87}\text{Sr})/n(^{86}\text{Sr})$	-	sig. diff.*	<b>sig. diff.</b>	<b>sig. diff.</b>	-
Fe/Ca	<b>sig. diff.</b>	-	-	-	sig. diff.*
Ca	sig. diff.*	-	sig. diff.*	sig. diff.*	-
Fe	<b>sig. diff.</b>	sig. diff.*	-	-	equal
Mn	sig. diff.*	sig. diff.*	<b>sig. diff.</b>	<b>sig. diff.</b>	-
Cu	-	-	-	-	-
Mo	-	-	-	-	<LOQ

Table 4. Pairwise comparison of site-specific markers and constituents of the elemental amount ratio of Fe/Ca in raw and salted caviar before and after salting (paired t-test); bold values denote significant differences according to test statistics and uncertainty calculations; empty cells (-) correspond to values showing no differences according to both concepts; \*denotes values which overlap within limits of uncertainty, but show statistically significant differences; ‘equal’ denotes values that do not overlap within limits of uncertainty, but are statistically not significant

In comparison, raw caviar from the sampling site TIC and GRU was mixed with salt showing significantly lower  $n(^{87}\text{Sr})/n(^{86}\text{Sr})$  isotope ratios (compare Figure 2) and strontium mass fractions ( $1.56 \mu\text{g g}^{-1} \pm 0.16 \mu\text{g g}^{-1}$  and  $0.73 \mu\text{g g}^{-1} \pm 0.07 \mu\text{g g}^{-1}$ , respectively). These salts did not significantly change the strontium isotopic composition of the caviar samples. In this study all caviar samples were of type “malossol” ( $w_{\text{salt}} 7 - 8 \%$ ). Thus, the amount of salt used for processing was comparable. Consequently, the alteration of the  $n(^{87}\text{Sr})/n(^{86}\text{Sr})$  isotopic composition of caviar by salt was influenced by a) the strontium isotopic composition of salt and b) the strontium elemental mass fraction of salt.

In order to estimate the influence of salt on the  $n(^{87}\text{Sr})/n(^{86}\text{Sr})$  isotope ratio of salted sturgeon caviar further knowledge about possible salt sources has to be collected accordingly. The original strontium mass fraction of sea salt is in the range of  $200 \mu\text{g g}^{-1} - 500 \mu\text{g g}^{-1}$  total dissolved solids. Processing of sea salt or rock salt to produce table salt results in a substantial reduction of the strontium elemental mass fraction of  $<1 \mu\text{g g}^{-1}$  to  $205 \mu\text{g g}^{-1}$  ([33,50,51]; this study). Therefore, a prediction of the contribution of salt to the strontium isotopic composition of salted caviar remains a challenge and requires solid information on salt used in caviar processing at specific fish farms.

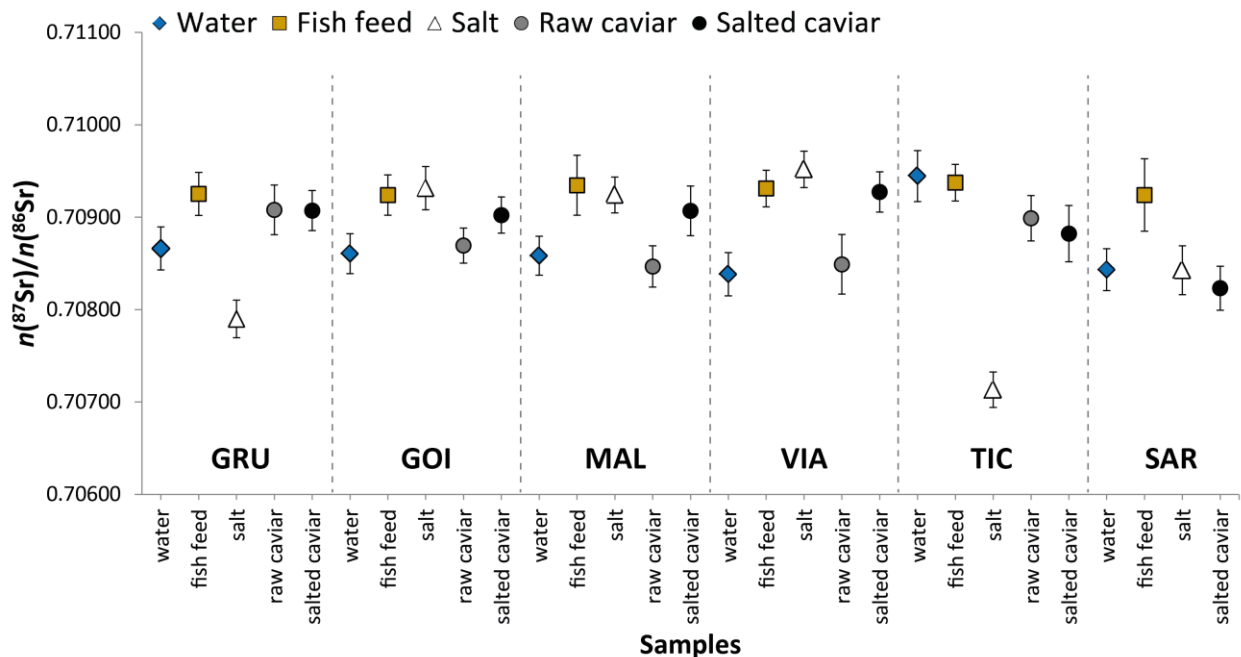


Figure 2. The  $n(^{87}\text{Sr})/n(^{86}\text{Sr})$  isotopic composition of water (blue diamonds), fish feed (brown squares), salt (white triangles), raw caviar (grey circles) and salted caviar (black circles) of six investigated fish farms (GRU, GOI, MAL, VIA, TIC, SAR); error bars correspond to the expanded uncertainty  $U$ ,  $k = 2$

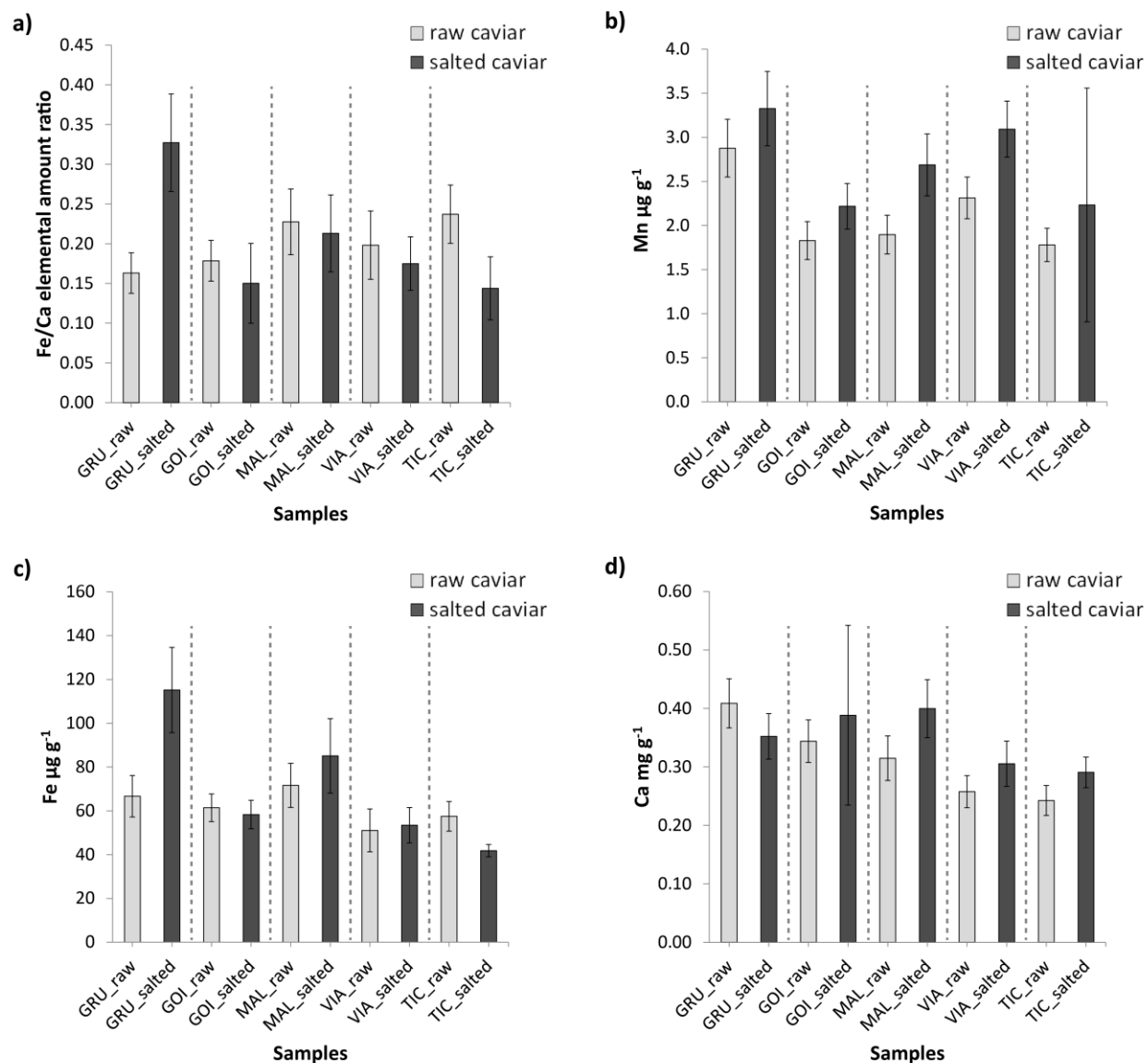


Figure 3. Comparison of the elemental amount ratio of Fe/Ca (a) and elemental mass fractions of Mn (b), Fe (c) and Ca (d) of raw caviar (light grey bars) and salted caviar (dark grey bars) from five sturgeon farms; error bars correspond to the expanded uncertainty  $U, k = 2$

The alteration of Fe and Mn elemental mass fractions of caviar by salting might be a result of the addition of salt that contains high amounts of these particular elements. This assumption was supported by comparison of the Fe and Mn elemental mass fractions of the investigated raw caviar samples (Fe ca.  $0.06 \mu\text{g g}^{-1}$  and Mn ca.  $2 \mu\text{g g}^{-1}$ ) to reported values of salt used for food processing [33]. Increased Fe and Mn content in salted caviar could also result from other sources such as possible contaminations of the samples during preparation and/or originate from the storage containers. However, these effects were not assessed in this study. Considering the low elemental mass fraction of Mo in salt (compare Table 2) as well as reported



values of Cu in various types of salt used for food processing [33], the total amount of these elements added to raw caviar by salting could be neglected. The elemental mass fraction of Ca in caviar was substantially higher than in salt, therefore salting did not significantly change the Ca content of caviar (compare Ca in salt of about  $13 \mu\text{g g}^{-1}$  and Ca in raw caviar of about  $410 \mu\text{g g}^{-1}$ , sampling site GRU; Table 2).

### **3.4 Washing of salted caviar to recover the initial composition of the site-specific markers**

Assuming that most salt is on the outside of the fish eggs, a multi-step washing procedure should remove salt from the caviar. Thus, the initial composition of the site-specific markers, which were altered by salting of caviar ( $n(^{87}\text{Sr})/n(^{86}\text{Sr})$ , Fe/Ca, Na and Mn) should be recovered. Figure S1 supplementary material shows that washing reduced the influence of salt on the strontium isotopic composition of caviar samples, which were salted with salt of high strontium content ( $>25 \mu\text{g g}^{-1}$ ; fish farms GOI, MAL, VIA). However, the initial  $n(^{87}\text{Sr})/n(^{86}\text{Sr})$  isotope ratio could not be recovered for all samples.

Salting significantly altered the Mn elemental mass fraction of caviar from the fish farms MAL and VIA (compare Table 4). Four-times washing of salted caviar from these fish farms decreased the elemental mass fractions of Mn of salted caviar to initial levels before salting (Figure S2a supplementary material). However, neither two-times washed nor four-times washed salted caviar showed elemental mass fractions of Na comparable to raw caviar (Figure S2b supplementary material). Furthermore, washing could not recover the initial elemental mass fraction of Fe from the sampling site GRU (Figure S2c supplementary material). These results showed that washing of salted caviar could not fully remove the influence of salt on most of the affected site-specific markers. Therefore, washing of caviar was not considered further.

### **3.5 Reverse-mixing models for predicting the strontium isotopic ratio of water in sturgeon caviar**

#### *3.5.1 Step 1 – Calculation of the contribution of individual components to the $n(^{87}\text{Sr})/n(^{86}\text{Sr})$ isotope ratio of caviar*

In the first step, the contribution of individual natural components such as water, fish feed and salt to the  $n(^{87}\text{Sr})/n(^{86}\text{Sr})$  isotope ratio of raw and salted caviar was determined by isotope pattern deconvolution (IPD). Water contributed to  $80 \pm 8 \%$  and fish feed to  $20 \pm 8 \%$  of the  $n(^{87}\text{Sr})/n(^{86}\text{Sr})$  isotope ratio of raw caviar (2 SD, data from [39]). The  $n(^{87}\text{Sr})/n(^{86}\text{Sr})$  isotope ratio of salted caviar was made up of 73 % salt, 22 % water and 5 % fish feed for caviar samples from fish farms GOI, VIA and MAL (average values; Table 5). In contrast, water was the main

contributor to the  $n(^{87}\text{Sr})/n(^{86}\text{Sr})$  isotope ratio of salted caviar from fish farm TIC (about 67 %). Caviar from this fish farm was salted with salt containing 15-times less strontium. Thus its contribution to the strontium isotope ratio of salted caviar from this fish farm was comparably low (see chapter 3.3).

Sample ID	Replicates	$X_{\text{water}}$	$X_{\text{fish feed}}$	$X_{\text{salt}}$
GOI	$n=3$	$0.19 \pm 0.11$	$0.03 \pm 0.42$	$0.78 \pm 0.38$
VIA	$n=3$	$0.19 \pm 0.20$	$0.05 \pm 0.87$	$0.76 \pm 0.68$
MAL	$n=3$	$0.27 \pm 0.13$	$0.07 \pm 0.42$	$0.67 \pm 0.46$
TIC	$n=3$	$0.67 \pm 0.27$	$0.07 \pm 0.29$	$0.27 \pm 0.05$
GRU	$n=3$	$1.57 \pm 0.99$	$-0.14 \pm 0.68$	$-0.44 \pm 0.36$
SAR	$n=3$	$2.17 \pm 11.94$	$-0.25 \pm 0.27$	$-0.92 \pm 11.78$

Table 5. Molar fractions of the individual sources of strontium to the final  $n(^{87}\text{Sr})/n(^{86}\text{Sr})$  isotopic composition of salted caviar calculated using IPD; uncertainties correspond to the combined uncertainty  $u_c$

Molar fractions of water, fish feed and salt of the  $n(^{87}\text{Sr})/n(^{86}\text{Sr})$  isotopic composition of salted caviar from the sampling sites GRU and SAR were negative or greater than one. Figure 2 suggests that these molar fractions were a result of inexistent effect of salting on the strontium isotope ratio of salted caviar due to low strontium content in salt (GRU) and similar  $n(^{87}\text{Sr})/n(^{86}\text{Sr})$  isotopic composition of salted caviar and salt (SAR). Accordingly, if taking salt as an input variable into the IPD calculation, its contribution is considered equal to those of water and fish feed. This leads to mathematically valid, but stoichiometrically wrong results. Consequently, these molar fractions were not used in the subsequent reverse-mixing model calculations.

### 3.5.2 Step 2 - Calculation of the theoretical $n(^{87}\text{Sr})/n(^{86}\text{Sr})$ isotope ratio of water in sturgeon caviar

In the second step, the theoretical  $n(^{87}\text{Sr})/n(^{86}\text{Sr})$  isotope ratio of water in sturgeon caviar was calculated by reverse-mixing models. First, the theoretical  $n(^{87}\text{Sr})/n(^{86}\text{Sr})$  isotope ratio of water was inferred from raw sturgeon caviar and fish feed using Equation 2. Figure 4 shows the calculated  $n(^{87}\text{Sr})/n(^{86}\text{Sr})$  isotope ratios of water in raw caviar (water calc. A) to be in agreement with the experimentally determined strontium isotopic composition of fish farm water. These findings were supported by correlation analysis showing a significant relationship of the theoretical  $n(^{87}\text{Sr})/n(^{86}\text{Sr})$  isotope ratios of water in raw caviar to the experimentally determined  $n(^{87}\text{Sr})/n(^{86}\text{Sr})$  isotopic composition of fish farm pool water (fish farms GRU, GOI, MAL, VIA, TIC;  $r_s= 0.64$ ;  $P=0.011$ ).

The theoretical  $n(^{87}\text{Sr})/n(^{86}\text{Sr})$  isotope ratio of water in salted sturgeon caviar (water calc. B, C) overlapped within limits of uncertainty with the experimentally determined  $n(^{87}\text{Sr})/n(^{86}\text{Sr})$  isotope ratio of fish farm pool water from the sampling sites GRU, MAL, VIA, TIC and SAR (Figure 4). The calculated  $n(^{87}\text{Sr})/n(^{86}\text{Sr})$  isotope ratio of water in salted sturgeon caviar from fish farm GOI was significantly lower than the corresponding measured strontium isotope ratio. This result suggested that the molar fraction of salt determined by IPD was potentially higher than the actual contribution of salt to the  $n(^{87}\text{Sr})/n(^{86}\text{Sr})$  isotopic composition of salted caviar from this farm. A major reason is the high sensitivity of IPD to little fluctuations in the measured strontium isotope ratios. Despite the result for fish farm GOI, correlation analysis showed a significant relationship between the theoretical  $n(^{87}\text{Sr})/n(^{86}\text{Sr})$  isotope ratios of water inferred from salted caviar and the experimentally determined  $n(^{87}\text{Sr})/n(^{86}\text{Sr})$  isotope composition of fish farm pool water (fish farms GRU, GOI, MAL, VIA, TIC, SAR;  $r_s=0.61$ ;  $P=0.007$ ).

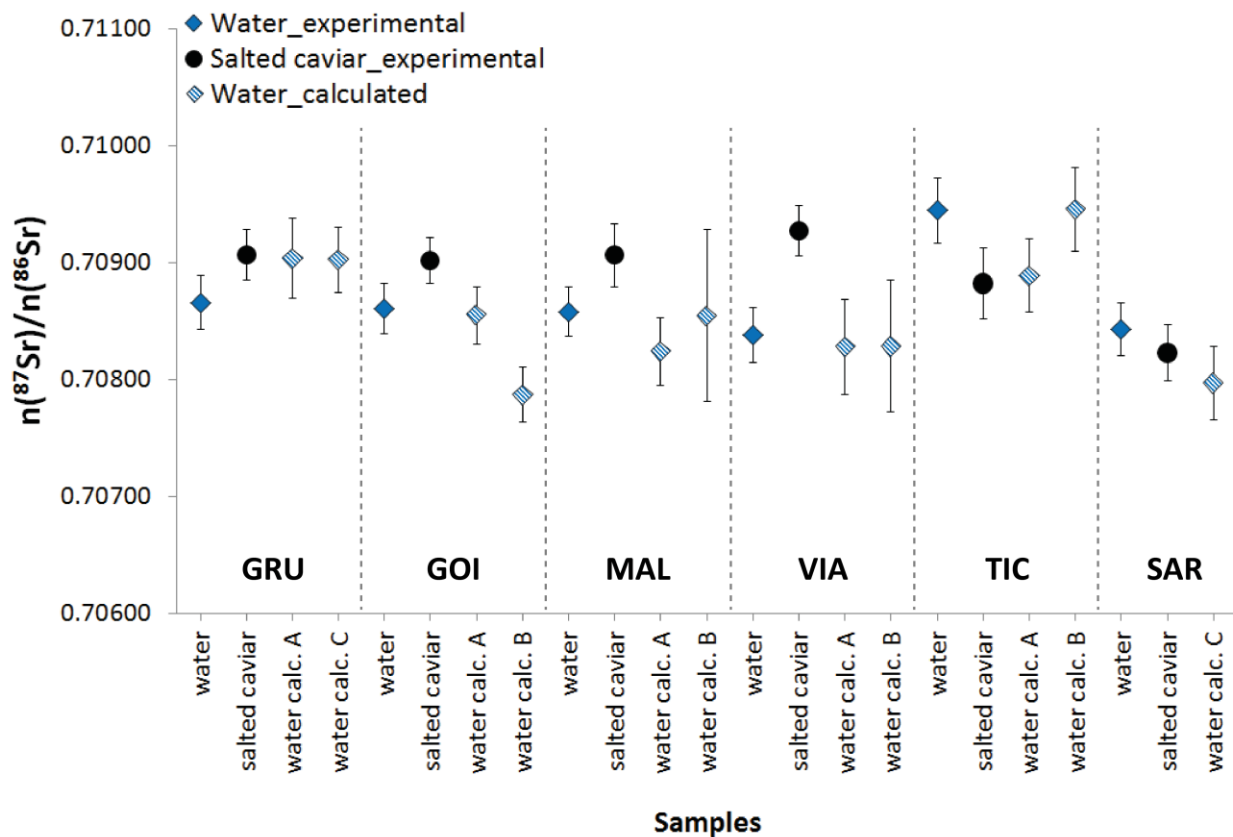


Figure 4. Comparison of experimentally determined  $n(^{87}\text{Sr})/n(^{86}\text{Sr})$  isotope ratios of water (blue diamonds) and salted caviar (black circles) to  $n(^{87}\text{Sr})/n(^{86}\text{Sr})$  isotope ratios of water calculated via reverse-mixing models using approach A, B and C (striped blue diamonds) of six sturgeon farms (GRU, GOI, MAL, VIA, TIC, SAR); error bars of the  $n(^{87}\text{Sr})/n(^{86}\text{Sr})$  isotope ratios of water, salted caviar and water calculated by approach A and C correspond to the expanded uncertainty  $U$ ,  $k=2$ ; error bars of the  $n(^{87}\text{Sr})/n(^{86}\text{Sr})$  isotope ratios of water calculated by approach B correspond to  $2\text{ SD}$  ( $n=3$ )

### 3.6 Combination of site-specific markers

The combination of site-specific markers in sturgeon caviar has the potential to form a unique chemical fingerprint. Salting can significantly alter this site-specific tag. Therefore, only markers, which were a) not affected by salting (Cu, Mo); or b) determined by reverse-mixing models ( $n(^{87}\text{Sr})/n(^{86}\text{Sr})_{\text{theoretical}}$ ), were considered as reliable carriers of the environmental information. Using these three site-specific markers, hierarchical cluster analysis using the Ward's method could differentiate salted caviar samples from six sites into five distinct clusters (Figure 5). This result was supported by Nearest neighbour and Within-groups linkage cluster analysis (Figure S3 and S4 supplementary material). These findings should be further fostered by a higher samples size, which was not possible to obtain in this pilot study due to the high prize of sturgeon caviar. Salted caviar samples from the fish farms MAL and VIA formed one cluster. These two fish farms are 7 km apart from each other sharing the same geologic environment [52]. This might be the reason for similar  $n(^{87}\text{Sr})/n(^{86}\text{Sr})$  isotopic and elemental composition of the fish farm pool water and sturgeon caviar from these two fish farms (MAL, VIA; compare Table 2).

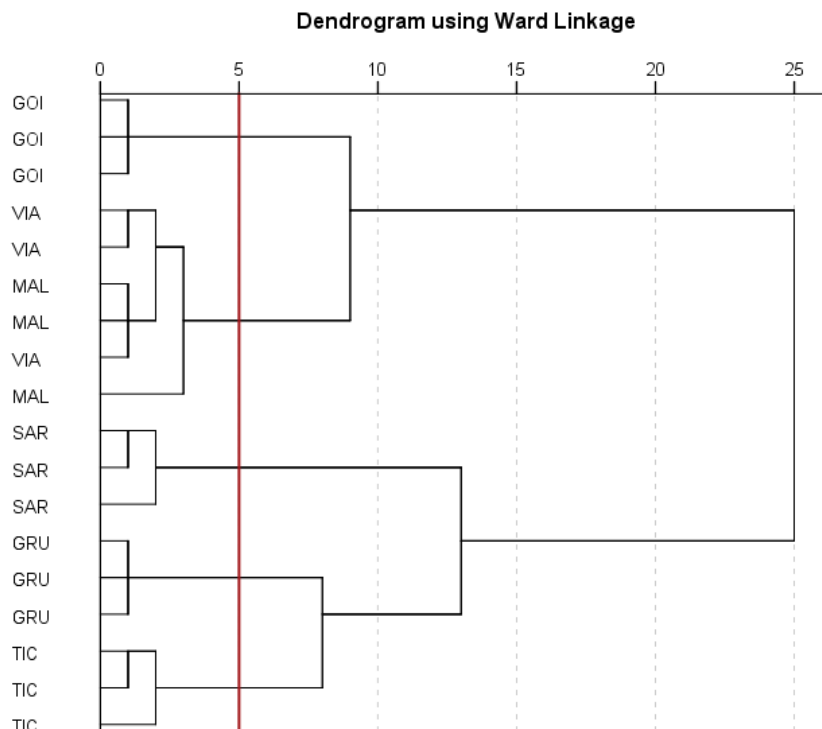


Figure 5. Cluster analysis of salted caviar samples from six investigated fish farms (GOI, VIA, MAL, SAR, GRU, TIC) using mathematically determined  $n(^{87}\text{Sr})/n(^{86}\text{Sr})$  isotope ratios of water in salted caviar and experimentally assessed elemental mass fractions of Cu and Mo of salted caviar using Ward's method on standardized values

#### **4. Conclusion**

Multiple linear regression revealed a significant relationship of six variables between ambient water and raw caviar ( $n(^{87}\text{Sr})/n(^{86}\text{Sr})$ , Na, Mn, Cu, Mo, Fe/Ca). These site-specific markers were assumed to reflect the water composition of the fish farm, which is mainly influenced by minerals forming the local bedrock material. Salting significantly altered the chemical composition of four ( $n(^{87}\text{Sr})/n(^{86}\text{Sr})$ , Na, Mn, Fe/Ca) of the six site-specific markers whereas Cu and Mo were not affected. Washing of salted caviar was ineffective in fully recovering the initial site-specific tag in caviar.

The results suggested that reverse-mixing models allowed calculating the theoretical  $n(^{87}\text{Sr})/n(^{86}\text{Sr})$  isotope ratio of water in raw and salted sturgeon caviar. The theoretical  $n(^{87}\text{Sr})/n(^{86}\text{Sr})$  isotope ratio of water in raw and salted sturgeon caviar represents a valuable proxy for the environmental tag absorbed from water into caviar, which is independent of the production process (feeding, salting). Once such a system is fully characterised, the data can be used to predict the theoretical  $n(^{87}\text{Sr})/n(^{86}\text{Sr})$  isotope ratio of water in raw and salted sturgeon caviar of test samples from the same production site.

Therefore, strontium isotopic and elemental pattern in sturgeon caviar proved to have an important potential to provide a site-specific chemical fingerprint allowing to link sturgeon caviar to its production site. The results of this study form the basis for establishing a systematic control tool for verifying the geographic origin of salted sturgeon caviar. The applicability of the presented chemometric protocol can be extended to other food commodities, accordingly.

#### **Conflicts of interest**

There are no conflicts of interest to declare.

#### **Acknowledgements**

The authors acknowledge the Federal Ministry of Science, Research and Economy for funding the research within the Sparkling Science program (Project „CSI:Trace your Food“, SPA 05\_052). We acknowledge the support of the project by the COMET-K1 competence centre FFoQSI. The COMET-K1 competence centre FFoQSI is funded by the Austrian ministries BMVIT, BMDW and the Austrian provinces Niederoesterreich, Upper Austria and Vienna within

the scope of COMET - Competence Centers for Excellent Technologies. The programme COMET is handled by the Austrian Research Promotion Agency FFG.

We gratefully thank the project cooperation partners Wolfgang Gröll (Gröll GmbH, Gröding, Austria), Mario Pazzaglia (Agroittica Lombarda SpA, Italy) and Shima Bakhshalizadeh (University of Gulian, Iran) for providing the samples, Jennifer Sarne and Melanie Diesner for their support with sample preparation as well as David Markvica for proofreading.

## References

1. Engler M, Knapp A. Briefing on the evolution of the caviar trade and range State implementation of Resolution Conf. 12.7 (Rev. CoP14). Brussels, Belgium 2008.
2. Ludwig A. Identification of *Acipenseriformes* species in trade. *J Appl Ichthyol*. 2008;24:2-19. doi: 10.1111/j.1439-0426.2008.01085.x.
3. Fain SR, Straughan DJ, Hamlin BC, et al. Forensic genetic identification of sturgeon caviars traveling in world trade. *Conserv Genet*. 2013;14(4):855-874. doi: 10.1007/s10592-013-0481-z.
4. CITES. Resolution Conf. 12.7 (Rev. CoP16): Convention on International Trade in Endangered Species of Wild Fauna and Flora; 2000 [03/05/2018]. Available from: <https://cites.org/eng/res/12/12-07R17.php>
5. Amangeldiyev DA. The experience of taking control over the illegal turnover of the sturgeon fishes, committed by forms of organized crime, applied abroad. *Journal of Advanced Research in Law and Economics*. 2015;6(2):270-276. doi: 10.14505/jarle.v6.2(12).01.
6. Ludwig A, Lieckfeldt D, Jahrl J. Mislabeled and counterfeit sturgeon caviar from Bulgaria and Romania. *J Appl Ichthyol*. 2015;31(4):587-591. doi: 10.1111/jai.12856.
7. Gessner J, Wirth M, Kirschbaum F, et al. Caviar composition in wild and cultured sturgeons - Impact of food sources on fatty acid composition and contaminant load. *J Appl Ichthyol*. 2002;18(4-6):665-672. doi: 10.1046/j.1439-0426.2002.00366.x.
8. DePeters EJ, Puschner B, Taylor SJ, et al. Can fatty acid and mineral compositions of sturgeon eggs distinguish between farm-raised versus wild white (*Acipenser transmontanus*) sturgeon origins in California? Preliminary report. *Forensic Sci Int*. 2013;229(1-3):128-132. doi: 10.1016/j.forsciint.2013.04.003.
9. Hosseini SV, Sobhanardakani S, Tahergorabi R, et al. Selected heavy metals analysis of persian sturgeon's (*Acipenser persicus*) caviar from southern caspian sea. *Biol Trace Elem Res*. 2013;154(3):357-362. doi: 10.1007/s12011-013-9740-6.
10. Wang W, Batterman S, Chernyak S, et al. Concentrations and risks of organic and metal contaminants in Eurasian caviar. *Ecotoxicol Environ Saf*. 2008;71(1):138-148. doi: 10.1016/j.ecoenv.2007.06.007.
11. Sobhanardakani S, Tayebi L, Hosseini SV. Health risk assessment of arsenic and heavy metals (Cd, Cu, Co, Pb, and Sn) through consumption of caviar of *Acipenser persicus* from Southern Caspian Sea. *Environ Sci Pollut R*. 2018;25(3):2664-2671. doi: 10.1007/s11356-017-0705-8.
12. Wirth M, Kirschbaum F, Gessner J, et al. Chemical and biochemical composition of caviar from different sturgeon species and origins. *Nahrung - Food*. 2000;44(4):233-237.
13. Rehbein H, Molkentin J, Schubring R, et al. Development of advanced analytical tools to determine the origin of caviar. *J Appl Ichthyol*. 2008;24:65-70. doi: 10.1111/j.1439-0426.2008.01091.x.
14. Coplen TB. Guidelines and recommended terms for expression of stable-isotope-ratio and gas-ratio measurement results. *Rapid Commun Mass Spectrom*. 2011;25(17):2538-2560. doi: 10.1002/rcm.5129.
15. Wieser M, Holden N, Coplen T, et al. Atomic weights of the elements 2011 (IUPAC Technical Report). *Pure Appl Chem*. 2013;85(5):pp. 1047–1078. doi: 10.1351/PAC-REP-13-03-02.
16. Fortunato G, Mucic K, Wunderli S, et al. Application of strontium isotope abundance ratios measured by MC-ICP-MS for food authentication. *JAAS*. 2004;19(2):227-234. doi: 10.1039/b307068a.
17. Kelly S, Heaton K, Hoogewerff J. Tracing the geographical origin of food: The application of multi-element and multi-isotope analysis. *Trends Food Sci Technol*. 2005;16(12):555-567. doi: 10.1016/j.tifs.2005.08.008.

18. Swoboda S, Brunner M, Boulyga SF, et al. Identification of Marchfeld asparagus using Sr isotope ratio measurements by MC-ICP-MS. *Anal Bioanal Chem.* 2008;390(2):487-494. doi: 10.1007/s00216-007-1582-7.
19. Brunner M, Katona R, Stefánka Z, et al. Determination of the geographical origin of processed spice using multielement and isotopic pattern on the example of Szegedi paprika. *Eur Food Res Technol.* 2010;231(4):623-634. doi: 10.1007/s00217-010-1314-7.
20. Rodrigues C, Brunner M, Steiman S, et al. Isotopes as tracers of the Hawaiian coffee-producing regions. *J Agric Food Chem.* 2011;59(18):10239-10246.
21. Rodushkin I, Bergman T, Douglas G, et al. Authentication of Kalix (N.E. Sweden) vendace caviar using inductively coupled plasma-based analytical techniques: Evaluation of different approaches. *Anal Chim Acta.* 2007;583(2):310-318. doi: 10.1016/j.aca.2006.10.038.
22. Zitek A, Sturm M, Waidbacher H, et al. Discrimination of wild and hatchery trout by natural chronological patterns of elements and isotopes in otoliths using LA-ICP-MS. *Fish Manage Ecol.* 2010;17(5):435-445. doi: 10.1111/j.1365-2400.2010.00742.x.
23. Liu H, Wei Y, Lu H, et al. The determination and application of  $^{87}\text{Sr}/^{86}\text{Sr}$  ratio in verifying geographical origin of wheat. *J Mass Spectrom.* 2017;52(4):248-253. doi: 10.1002/jms.3930.
24. Techer I, Medini S, Janin M, et al. Impact of agricultural practice on the Sr isotopic composition of food products: Application to discriminate the geographic origin of olives and olive oil. *Appl Geochem.* 2017;82:1-14. doi: 10.1016/j.apgeochem.2017.05.010.
25. Durante C, Bertacchini L, Cocchi M, et al. Development of  $^{87}\text{Sr}/^{86}\text{Sr}$  maps as targeted strategy to support wine quality. *Food Chem.* 2018;255:139-146. doi: 10.1016/j.foodchem.2018.02.084.
26. Capo RC, Stewart BW, Chadwick OA. Strontium isotopes as tracers of ecosystem processes: Theory and methods. *Geoderma.* 1998;82(1-3):197-225. doi: 10.1016/s0016-7061(97)00102-x.
27. Faure G, Powell JL. *Strontium Isotope Geology.* Berlin Heidelberg New York: Springer Verlag; 1972.
28. Faure G, Mensing T. *Isotopes: principles and applications.* 3rd ed. Hoboken, New Jersey: John Wiley & Sons; 2005.
29. Flockhart D, Kyser T, Chipley D, et al. Experimental evidence shows no fractionation of strontium isotopes ( $^{87}\text{Sr}/^{86}\text{Sr}$ ) among soil, plants, and herbivores: implications for tracking wildlife and forensic science. *Isot Environ Health Stud.* 2015;51(3):372-381. doi: 10.1080/10256016.2015.1021345.
30. Campana SE. Chemistry and composition of fish otoliths: Pathways, mechanisms and applications. *Mar Ecol Prog Ser.* 1999;188:263-297. doi: 10.3354/meps188263.
31. Bertacchini L, Cocchi M, Li Vigni M, et al. Chapter 10 - The Impact of Chemometrics on Food Traceability. In: Marini F, editor. *Data Handling in Science and Technology.* Vol. 28: Elsevier; 2013. p. 371-410.
32. Reguera-Galan A, Moldovan M, Garcia Alonso JI. The combined measurement of  $^{87}\text{Sr}/^{86}\text{Sr}$  isotope ratios and  $^{88}\text{Sr}/^{85}\text{Rb}$  elemental ratios using laser ablation MC-ICP-MS and its application for food provenance studies: the case for Asturian beans. *JAAS.* 2018;33(5):867-875. doi: 10.1039/c8ja00061a.
33. Epova EN, Bérail S, Zuliani T, et al.  $^{87}\text{Sr}/^{86}\text{Sr}$  isotope Ratio And Multielemental Signatures As Indicators Of Origin Of European Cured Hams: The Role Of Salt. *Food Chem.* 2017. doi: 10.1016/j.foodchem.2017.10.143.
34. Chang C-T, You C-F, Aggarwal SK, et al. Boron and strontium isotope ratios and major/trace elements concentrations in tea leaves at four major tea growing gardens in Taiwan. *Environ Geochem Health.* 2016;38(3):737-748. doi: 10.1007/s10653-015-9757-1.



35. Kerr L, Campana S. Chemical Composition of Fish Hard Parts as a Natural Marker of Fish Stocks. In: Cadrin S, Kerr LA, Mariani S, editors. Stock Identification Methods. 2nd ed. San Diego: Academic Press; 2014. p. 205-234.
36. Willmes M, McMorow L, Kinsley L, et al. The IRHUM (Isotopic Reconstruction of Human Migration) database - Bioavailable strontium isotope ratios for geochemical fingerprinting in France. Earth System Science Data. 2014;6(1):117-122. doi: 10.5194/essd-6-117-2014.
37. West JB, Bowen GJ, Dawson TE, et al. Isoscapes: Understanding movement, pattern, and process on earth through isotope mapping. Springer; 2010.
38. Edera T, Kokubun A, Abe H, et al. Tracing the geographical origin of raw, boiled and salted, and dried wakame (*undaria pinnatifida*) using trace element compositions resistant to manufacturing processes. Japanese Society for Food Science and Technology. 2016;63(9):427-432. doi: 10.3136/nskkk.
39. Tchaikovskiy A, Irrgeher J, Zitek A, et al. Isotope pattern deconvolution of different sources of stable strontium isotopes in natural systems JAAS. 2017;32:2300-2307 doi: 10.1039/C7JA00251C.
40. Horsky M, Irrgeher J, Prohaska T. Evaluation strategies and uncertainty calculation of isotope amount ratios measured by MC ICP-MS on the example of Sr. Anal Bioanal Chem. 2016;408(2):351-367. doi: 10.1007/s00216-015-9003-9.
41. Irrgeher J, Vogel J, Santner J, et al. In: Prohaska T, Irrgeher J, Zitek A, et al., editors. Sector Field Mass Spectrometry for Elemental and Isotopic Analysis. Cambridge 2015. p. 126-149.
42. Ellison SLR, Williams A. EURACHEM/CITAC Guide: Quantifying Uncertainty in Analytical Measurement. 3rd ed. 2012.
43. Kragten J. Tutorial review. Calculating standard deviations and confidence intervals with a universally applicable spreadsheet technique. Analyst. 1994;119(10):2161-2165. doi: 10.1039/an9941902161.
44. Garcia Alonso JI, Rodriguez-Gonzalez P. Isotope Dilution Mass Spectrometry. Cambridge, UK: Royal Society of Chemistry; 2013.
45. Irrgeher J, Prohaska T, Sturgeon RE, et al. Determination of strontium isotope amount ratios in biological tissues using MC-ICPMS. Analytical Methods. 2013;5(7):1687-1694. doi: 10.1039/C3AY00028A.
46. Krabbenhöft A, Fietzke J, Eisenhauer A, et al. Determination of radiogenic and stable strontium isotope ratios ( $^{87}\text{Sr}/^{86}\text{Sr}$ ;  $\delta^{88}/^{86}\text{Sr}$ ) by thermal ionization mass spectrometry applying an  $^{87}\text{Sr}/^{84}\text{Sr}$  double spike. JAAS. 2009;24(9):1267-1271. doi: 10.1039/b906292k.
47. Burton J. The ocean: a global geochemical system. In: Summerhayes C, Thorpe S, editors. Oceanography: An Illustrated Guide. London: Manson; 1996. p. 165-181.
48. Yeghicheyan D, Bossy C, Bouhnik Le Coz M, et al. A Compilation of Silicon, Rare Earth Element and Twenty-One other Trace Element Concentrations in the Natural River Water Reference Material SLRS-5 (NRC-CNRC). Geostand Geoanal Res. 2013;37(4):449-467. doi: 10.1111/j.1751-908X.2013.00232.x.
49. Gabriellson RM, Kim J, Reid MR, et al. Does the trace element composition of brown trout *Salmo trutta* eggs remain unchanged in spawning redds? J Fish Biol. 2012;81(6):1871-1879. doi: 10.1111/j.1095-8649.2012.03396.x.
50. Kuhnlein H. The trace element content of indigenous salts compared with commercially refined substitutes. Ecol Food Nutr. 2010;10:2:113-121. doi: 10.1080/03670244.1980.9990626.
51. Atkinson M, Bingman C. Elemental composition of commercial seasalts. J Aquaricult Aquat Sci. 1997;VIII(2):39-43.

52. Carta Geologica d'Italia: Istituto Superiore per La Protezione e la Ricerca Ambientale; [03/07/2019]. Available from:  
[http://193.206.192.231/carta\\_geologica\\_italia/tavoletta.php?foglio=47](http://193.206.192.231/carta_geologica_italia/tavoletta.php?foglio=47)

# Chemometric tools for determining site-specific elemental and strontium isotopic fingerprints in sturgeon caviar

A. Tchaikovsky, A. Zitek, J. Irrgeher, C. Opper, R. Scheiber, K. Moder, L. Congiu and T. Prohaska

## Supplementary material 1

- Table S1 Input variables for the isotope pattern deconvolution in this work  
 Table S2 Comparison of measured to certified values of the investigated CRM and QC standards  
 Figure S1 Efficacy of the washing procedure on the strontium isotope ratio of salted caviar  
 Figure S2 Efficacy of the washing procedure on the Na, Fe, Mn elemental content of salted caviar  
 Figure S3 Cluster analysis of salted sturgeon caviar using the Nearest neighbour method  
 Figure S4 Cluster analysis of salted sturgeon caviar using the Within-groups linkage method

Sample ID	Sample type	Replicates	$n(^{87}\text{Sr})/n(^{86}\text{Sr})$	$n(^{88}\text{Sr})/n(^{86}\text{Sr})$	$n(^{84}\text{Sr})/n(^{86}\text{Sr})$
GRU	Water	$n=3$	0.70866 (23)	8.3783 (32)	0.056659 (84)
	Fish feed	$n=3$	0.70925 (23)	8.3812 (30)	0.05658 (10)
	Salt	$n=3$	0.70790 (20)	8.3786 (24)	0.0573 (22)
	Raw caviar	$n=3$	0.70908 (27)	8.3733 (26)	0.05683 (25)
	Salted caviar	$n=3$	0.70907 (22)	8.3762 (28)	0.056696 (81)
MAL	Water	$n=3$	0.70858 (21)	8.3787 (28)	0.05645 (52)
	Fish feed	$n=3$	0.70935 (33)	8.3792 (28)	0.05649 (11)
	Salt	$n=3$	0.70924 (19)	8.3814 (29)	0.056516 (96)
	Raw caviar	$n=3$	0.70847 (22)	8.3721 (29)	0.05658 (58)
	Salted caviar	$n=3$	0.70907 (27)	8.3805 (32)	0.056540 (92)
TIC	Water	$n=3$	0.70945 (28)	8.3753 (33)	0.05658 (90)
	Fish feed	$n=3$	0.70937 (20)	8.3806 (27)	0.056530 (72)
	Salt	$n=3$	0.70713 (19)	8.3774 (31)	0.056578 (73)
	Raw caviar	$n=3$	0.70899 (25)	8.3718 (36)	0.05675 (23)
	Salted caviar	$n=3$	0.70882 (30)	8.3762 (39)	0.056574 (75)
SAR	Water	$n=3$	0.70843 (23)	8.3800 (41)	0.056536 (84)
	Fish feed	$n=3$	0.70924 (39)	8.3824 (31)	0.056506 (74)
	Salt	$n=3$	0.70843 (27)	8.3811 (40)	0.056520 (90)
	Salted caviar	$n=3$	0.70823 (24)	8.3785 (22)	0.056520 (73)

Table S1. The  $n(^{87}\text{Sr})/n(^{86}\text{Sr})$ ,  $n(^{88}\text{Sr})/n(^{86}\text{Sr})$  and  $n(^{84}\text{Sr})/n(^{86}\text{Sr})$  strontium isotope ratios of water, fish feed, salt, raw and salted caviar used as input variables for the isotopic pattern deconvolution; uncertainties correspond to the expanded uncertainty  $U$ ,  $k=2$  and are stated to two significant figures

## Chemometric tools for determining site-specific elemental and strontium isotopic fingerprints in sturgeon caviar

A. Tchaikovskiy, A. Zitek, J. Irrgeher, C. Opper, R. Scheiber, K. Moder, L. Congiu and T. Prohaska

Sample ID	LOQ	measured value	reference value
<b>SRM 987</b>			
$n(^{87}\text{Sr})/n(^{86}\text{Sr})$		0.71022 (23)	0.71034 (26)
$n(^{88}\text{Sr})/n(^{86}\text{Sr})$		8.3769 (33)	8.3786 (33)
$n(^{84}\text{Sr})/n(^{86}\text{Sr})$		0.05656 (13)	0.05655 (14)
<b>TORT-3</b>			
$n(^{87}\text{Sr})/n(^{86}\text{Sr})$		0.70928 (25)	0.70937 (10)
$n(^{88}\text{Sr})/n(^{86}\text{Sr})$		8.378 (10)	8.3824 (12)
$n(^{84}\text{Sr})/n(^{86}\text{Sr})$		0.05653 (11)	0.05653 (4)
Fe	mg g <sup>-1</sup>	7.12E-03	0.17 (4)
Cu	mg g <sup>-1</sup>	1.34E-02	0.52 (5)
Mn	mg g <sup>-1</sup>	4.93E-05	0.0158 (27)
Sr	mg g <sup>-1</sup>	1.02E-04	0.036 (6)
Co	µg g <sup>-1</sup>	5.05E-03	1.11 (18)
As	µg g <sup>-1</sup>	7.12E-02	61 (12)
Mo	µg g <sup>-1</sup>	2.46E-02	3.7 (4)
<b>IAPSO</b>			
$n(^{87}\text{Sr})/n(^{86}\text{Sr})$		0.70935 (24)	0.70931 (30)
$n(^{88}\text{Sr})/n(^{86}\text{Sr})$		8.381 (5)	8.3818 (30)
$n(^{84}\text{Sr})/n(^{86}\text{Sr})$		0.05650 (17)	-
Mg	mg g <sup>-1</sup>	2.18E-05	1.45 (28)
K	mg g <sup>-1</sup>	2.33E-04	0.41 (10)
Ca	mg g <sup>-1</sup>	2.04E-04	0.40 (7)
Rb	µg g <sup>-1</sup>	7.08E-05	1.115 (12)
Sr	µg g <sup>-1</sup>	9.72E-04	7.6 (7)
Mo	µg g <sup>-1</sup>	1.31E+00	12.94 (30)
<b>SLRS-5</b>			
Na	µg g <sup>-1</sup>	2.20E-01	5.4 (7)
Mg	µg g <sup>-1</sup>	7.04E-02	2.8 (4)
K	µg g <sup>-1</sup>	4.66E-02	0.86 (10)
Ca	µg g <sup>-1</sup>	3.84E-01	10.2 (9)
Fe	µg g <sup>-1</sup>	1.32E-02	0.103 (15)
Cu	µg g <sup>-1</sup>	7.72E-05	0.0185 (20)
Sr	µg g <sup>-1</sup>	2.34E-04	0.050 (5)
Mn	ng g <sup>-1</sup>	4.62E-02	3.8 (7)
Co	ng g <sup>-1</sup>	4.97E-03	0.063 (6)
As	ng g <sup>-1</sup>	1.85E-03	0.53 (8)
Mo	ng g <sup>-1</sup>	3.36E-02	0.20 (6)
<b>VIRIS QC Standard</b>			
Mg	µg g <sup>-1</sup>	1.29E-03	0.116 (12)
K	µg g <sup>-1</sup>	4.96E-03	0.108 (13)
Ca	µg g <sup>-1</sup>	2.15E-02	0.98 (11)
Mn	µg g <sup>-1</sup>	4.92E-05	0.079 (10)
Fe	µg g <sup>-1</sup>	2.04E-02	0.168 (23)
As	µg g <sup>-1</sup>	1.69E-04	0.029 (4)
Rb	µg g <sup>-1</sup>	1.34E-05	0.0238 (26)
Sr	µg g <sup>-1</sup>	1.91E-05	0.0244 (29)
Na	ng g <sup>-1</sup>	6.30E+00	43 (5)
Co	ng g <sup>-1</sup>	2.69E-02	3.0 (4)
Cu	ng g <sup>-1</sup>	9.56E-02	3.1 (4)
Mo	ng g <sup>-1</sup>	6.31E-02	3.0 (4)

Table S2. Comparison of measured values to reference values of the strontium isotope ratios of the reference materials SRM 987, TORT-3 and IAPSO as well as the elemental amount fractions of TORT-3, IAPSO, SLRS-5 and in-house quality control standard VIRIS QC Standard; \* denotes information values; Mo in the IAPSO standard was determined using CASS-4, CASS-5, NASS-6 (all from the National Research Council, Ontario, Canada) and BCR-403 (Institute for Reference Materials and Measurements, Geel, Belgium) seawater standards; uncertainties correspond to the expanded uncertainty  $U$ ,  $k=2$ ; significant numbers of digits are given according to EURACHEM guidelines

## Chemometric tools for determining site-specific elemental and strontium isotopic fingerprints in sturgeon caviar

A. Tchaikovsky, A. Zitek, J. Irrgeher, C. Opper, R. Scheiber, K. Moder, L. Congiu and T. Prohaska

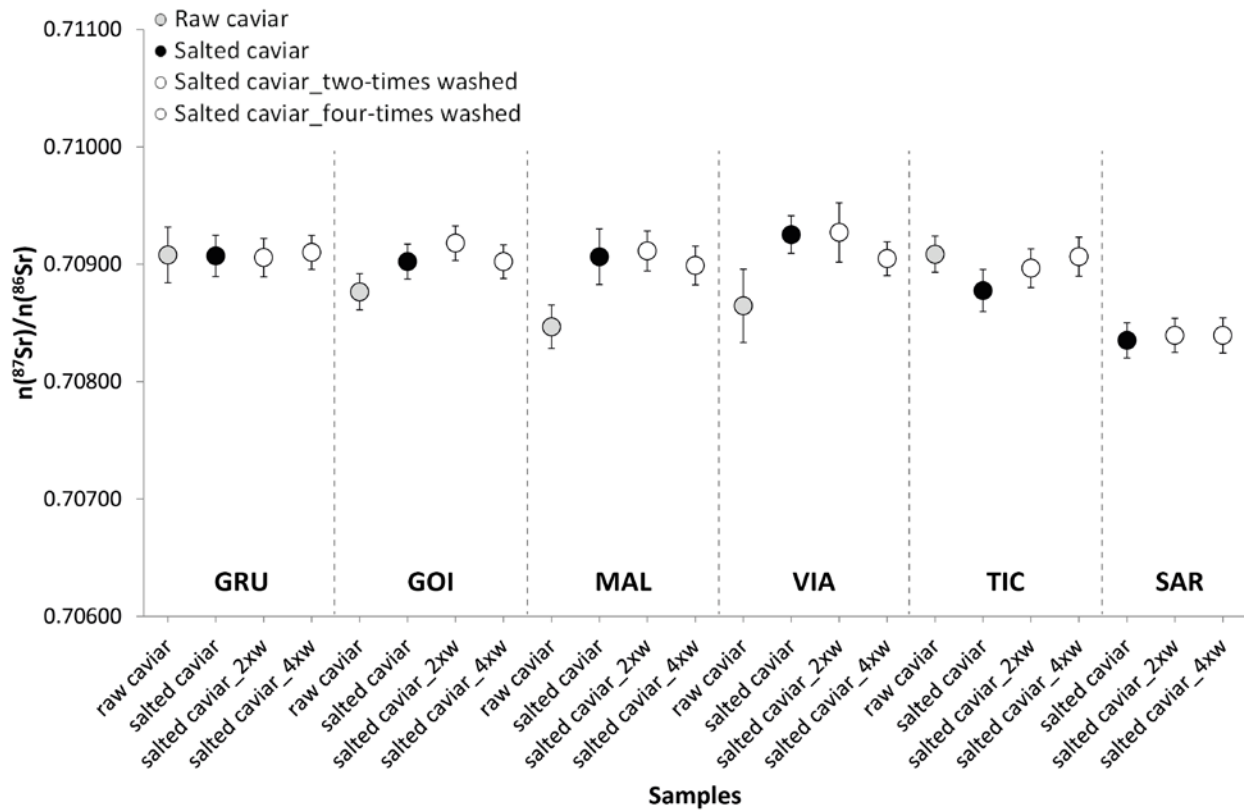


Figure S1. The  $n(^{87}\text{Sr})/n(^{86}\text{Sr})$  isotopic composition of raw caviar (grey circles), salted caviar (black circles) and washed salted caviar (white circles) of six investigated sturgeon farms; error bars correspond to the expanded uncertainty  $U, k=2$

## Chemometric tools for determining site-specific elemental and strontium isotopic fingerprints in sturgeon caviar

A. Tchaikovsky, A. Zitek, J. Irrgeher, C. Opper, R. Scheiber, K. Moder, L. Congiu and T. Prohaska

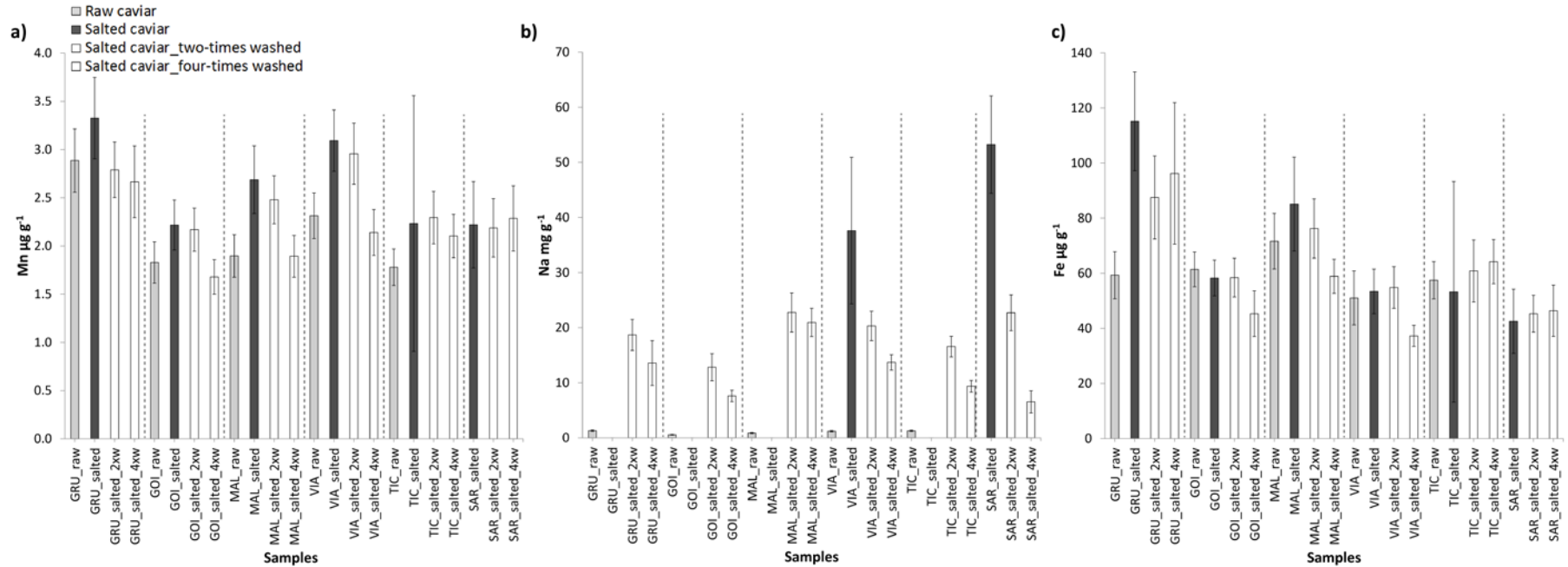


Figure S2. Comparison of the elemental mass fractions of Mn (a), Na (b) and Fe (c) of raw caviar (light grey bars), salted caviar (dark grey bars) and washed salted caviar (white bars) of six investigated sturgeon farms; no raw caviar was available from the sampling site SAR; error bars correspond to the expanded uncertainty  $U, k=2$

# Chemometric tools for determining site-specific elemental and strontium isotopic fingerprints in sturgeon caviar

A. Tchaikovsky, A. Zitek, J. Irrgeher, C. Opper, R. Scheiber, K. Moder, L. Congiu and T. Prohaska

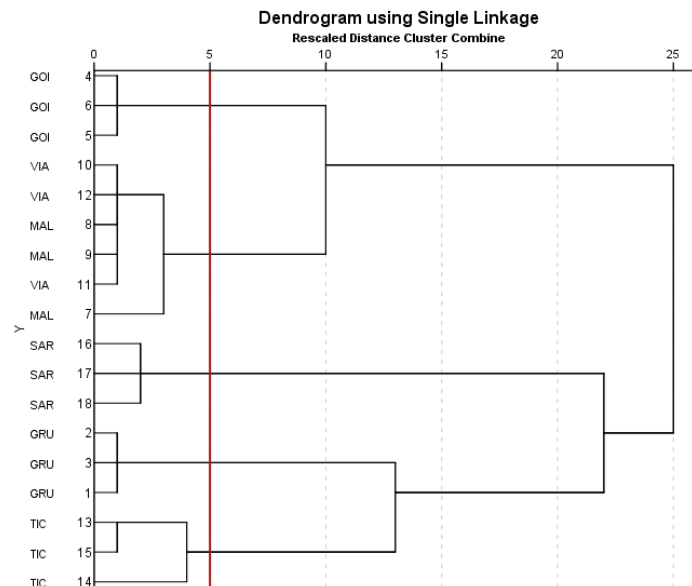


Figure S3. Cluster analysis of salted caviar samples from six investigated fish farms (GOI, VIA, MAL, SAR, GRU, TIC) using mathematically determined  $n(^{87}\text{Sr})/n(^{86}\text{Sr})$  isotope ratios of water in salted caviar and experimentally assessed elemental mass fractions of Cu and Mo of salted caviar using Nearest neighbour analysis on standardized values

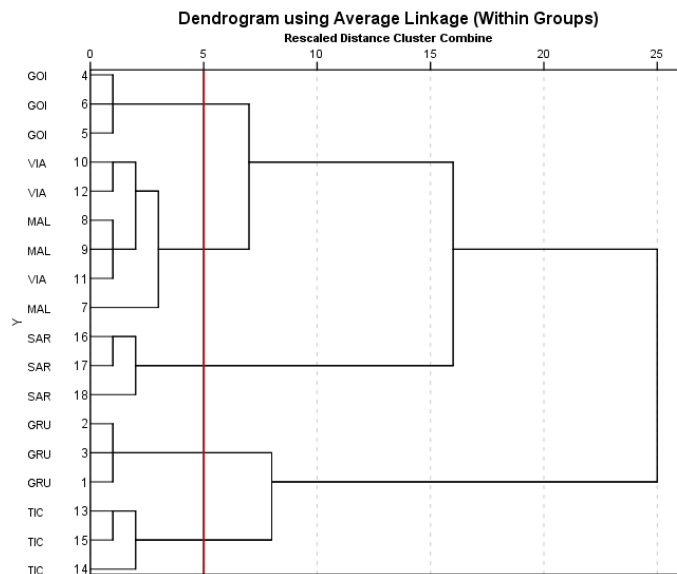


Figure S4. Cluster analysis of salted caviar samples from six investigated fish farms (GOI, VIA, MAL, SAR, GRU, TIC) using mathematically determined  $n(^{87}\text{Sr})/n(^{86}\text{Sr})$  isotope ratios of water in salted caviar and experimentally assessed elemental mass fractions of Cu and Mo of salted caviar using Within-groups linkage analysis on standardized values

**III. Analysis of  $n(^{87}\text{Sr})/n(^{86}\text{Sr})$ ,  $\delta^{88}\text{Sr}/^{86}\text{Sr}_{\text{SRM987}}$  and elemental pattern to characterise groundwater and recharge of saline ponds in a clastic aquifer in East Austria**

*Anastassiya Tchaikovsky, Hermann Häusler, Martin Kralik, Andreas Zitek, Johanna Irrgeher and Thomas Prohaska*

*Isotopes in Environmental and Health Studies, 2019 (published)*

<https://doi.org/10.1080/10256016.2019.1577832>





# Analysis of $n(^{87}\text{Sr})/n(^{86}\text{Sr})$ , $\delta^{88}\text{Sr}/^{86}\text{Sr}_{\text{SRM987}}$ and elemental pattern to characterise groundwater and recharge of saline ponds in a clastic aquifer in East Austria

Anastasiya Tchaikovsky<sup>a</sup>, Hermann Häusler<sup>b</sup>, Martin Kralik<sup>b</sup>, Andreas Zitek<sup>a</sup>, Johanna Irrgeher<sup>c,d</sup> and Thomas Prohaska<sup>a,d</sup>

<sup>a</sup>VIRIS Laboratory, Department of Chemistry, University of Natural Resources and Life Sciences Vienna, Tulln, Austria; <sup>b</sup>Department of Environmental Geosciences, University of Vienna, Vienna, Austria; <sup>c</sup>Department for Marine Bioanalytical Chemistry, Helmholtz Centre for Materials and Coastal Research, Institute for Coastal Research, Geesthacht, Germany; <sup>d</sup>Chair of General and Analytical Chemistry, Montanuniversität Leoben, Leoben, Austria

## ABSTRACT

Elemental and isotopic pattern of  $n(^{87}\text{Sr})/n(^{86}\text{Sr})$  and  $\delta^{88}\text{Sr}/^{86}\text{Sr}_{\text{SRM987}}$  were used to characterise groundwater and recharge of saline ponds in a clastic aquifer in East Austria. Therefore, shallow, artesian and thermal groundwaters of the investigated aquifer along with rainfall and rivers were analysed using (MC) ICP-MS. The  $n(^{87}\text{Sr})/n(^{86}\text{Sr})$  ratio and elemental pattern changed with aquifer depth as a result of progressing bedrock leaching and dissolution with increasing groundwater residence time. The  $n(^{87}\text{Sr})/n(^{86}\text{Sr})$  ratio of shallow groundwater below saline ponds of  $0.71019 \pm 0.00044$  was significantly different from thermal groundwater of  $0.71205 \pm 0.00035$  ( $U, k=2$ ). In contrast to previous theories, this result suggested no recharge of saline ponds by upwelling paleo-seawater. Isotope pattern deconvolution revealed that rainfall accounted to about 60% of the  $n(^{87}\text{Sr})/n(^{86}\text{Sr})$  ratio of shallow groundwater below saline ponds. The  $\delta^{88}\text{Sr}/^{86}\text{Sr}_{\text{SRM987}}$  values of groundwater decreased from about 0.25 ‰ in most shallow, to predominantly negative values of about -0.24 ‰ in artesian groundwater. This result indicated leaching and dissolution of weathered minerals. In turn, the  $\delta^{88}\text{Sr}/^{86}\text{Sr}_{\text{SRM987}}$  of deep thermal groundwater showed positive values of about 0.12 ‰, which suggested removal of  $^{86}\text{Sr}$  from solution by carbonate precipitation. These results highlight the potential of  $\delta^{88}\text{Sr}/^{86}\text{Sr}_{\text{SRM987}}$  signature as an additional geochemical tracer.

## ARTICLE HISTORY

Received 3 August 2018  
Accepted 4 January 2019


## KEYWORDS

Chemometrics; isotope fractionation; isotope geochemistry; non-traditional stable isotopes; Lake Neusiedl-Seewinkel Basin; strontium

## 1. Introduction

Strontium isotopes are well-established environmental tracers in hydrologic studies [1–4]. Strontium is a natural non-toxic element consisting of four stable isotopes  $^{84}\text{Sr}$ ,  $^{86}\text{Sr}$ ,  $^{87}\text{Sr}$  and  $^{88}\text{Sr}$ . The isotope displaying the highest variability in nature is  $^{87}\text{Sr}$  due to the radioactive  $\beta^-$ -decay of  $^{87}\text{Rb}$  to  $^{87}\text{Sr}$ . In general, the  $^{87}\text{Sr}$  isotope abundance is expressed as

**CONTACT** Thomas Prohaska  thomas.prohaska@unileoben.ac.at

 Supplemental data for this article can be accessed at <https://doi.org/10.1080/10256016.2019.1577832>.

© 2019 Informa UK Limited, trading as Taylor & Francis Group

the isotope amount ratio  $n(^{87}\text{Sr})/n(^{86}\text{Sr})$ . (This isotope notation –  $n(^i\text{Sr})/n(^j\text{Sr})$  – is recommended by the Commission on Isotopic Abundances and Atomic Weights of the International Union of Pure and Applied Chemistry (IUPAC) and will be used throughout the publication [5,6]. If the ratio is stated as general ratio,  $^j\text{Sr}/^i\text{Sr}$  is used.) Its relative amount in nature is a function of the Rb/Sr elemental ratio and the age of the geological bedrock with reported  $n(^{87}\text{Sr})/n(^{86}\text{Sr})$  isotope amount ratios between 0.70 and 0.78 [7,8]. Chemical weathering releases strontium from bedrocks to surface water allowing to infer on the lithology of drainage basins [9], to quantify silicate vs. carbonate weathering [10] or to determine strontium inputs to the oceans over geologic history [11].

In groundwater the  $n(^{87}\text{Sr})/n(^{86}\text{Sr})$  isotopic composition is determined by the dissolution of the most leachable mineral phases of the bedrock [2,9,12,13]. Montgomery et al. [14] observed a general correlation of the  $n(^{87}\text{Sr})/n(^{86}\text{Sr})$  isotope ratio of mineral water and aquifer host rock composition. They reported that water from older rock aquifers had a more radiogenic signature than those from younger rock aquifers. Shand et al. [2] used the  $n(^{87}\text{Sr})/n(^{86}\text{Sr})$  isotope ratio to determine sources and mixing relationships of groundwater. Woods et al. [15] attributed differences in the  $n(^{87}\text{Sr})/n(^{86}\text{Sr})$  isotope ratio of young and old groundwater to different degrees of water–rock interaction. Therefore, the radiogenic strontium isotope ratio represents a geogenic tracer useful in hydrologic studies e.g. for the inference on the lithologic type and age of the aquifer bedrock, groundwater mixing along flow paths and residence time.

In recent years, advances in mass spectrometry facilitated the determination of the variation of the  $n(^{88}\text{Sr})/n(^{86}\text{Sr})$  isotope amount ratio, which had previously been considered constant in nature [16,17]. This isotope ratio is conventionally expressed in the  $\delta$ -notation relative to the certified reference material NIST SRM 987. (In the ‘Guidelines and recommended terms for expressing stable-isotope-ratio and gas-ratio measurement results’ the IUPAC recommended a notation of the isotope ratio as  $\delta^{88}\text{Sr}/^{86}\text{Sr}_{\text{SRM987}}$  [5]. It has been reported as important to indicate the reference standard, which is in this case NIST SRM 987.) The reported variation of the  $\delta^{88}\text{Sr}/^{86}\text{Sr}_{\text{SRM987}}$  in nature ranges from about  $-1.1$  to  $+1.4$  ‰ as a result of mass-dependent isotope fractionation [18]. For example, Böhm et al. [19] demonstrated  $^{88}\text{Sr}/^{86}\text{Sr}$  isotope fractionation during inorganic calcite precipitation. DeSouza et al. [20] found preferential uptake of  $^{86}\text{Sr}$  by plants such that their  $\delta^{88}\text{Sr}/^{86}\text{Sr}_{\text{SRM987}}$  value was significantly lower than those of soils in which they grew in. Halicz et al. [21] reported strontium isotope fractionation in soils which they attributed to different degrees of chemical weathering. These observations suggested that the  $\delta^{88}\text{Sr}/^{86}\text{Sr}_{\text{SRM987}}$  has a high potential for the investigation of eco-geochemical processes as well.

The  $^{88}\text{Sr}/^{86}\text{Sr}$  ratio of groundwater bears therefore a high potential to give additional insights on the genesis of minerals which form the aquifer host rock as well as geochemical reactions such as precipitation.

In this work, the applicability of  $n(^{87}\text{Sr})/n(^{86}\text{Sr})$ ,  $\delta^{88}\text{Sr}/^{86}\text{Sr}_{\text{SRM987}}$  and elemental pattern for groundwater characterisation was investigated in the clastic aquifer of the Neogene Lake Neusiedl-Seewinkel Basin, East Austria. It consists of about 1000 m thick brackish to fluvial deposits forming the bedrock of shallow, deeper artesian and deep thermal aquifers. A peculiarity of the study area is the occurrence of larger saline lakes and smaller saline ponds. Tauber [22] postulated that their saline water resulted from upwelling of deep marine connate water of Badenian to Sarmatian age along faults. This hypothesis

was termed ‘ascending theory’ and was supported by ice-free ponds during winter, which were interpreted as a result of ascending thermal water. However, recent research demonstrated that these ice-free ponds resulted from emanating methane, which prevented ice formation [23,24]. These findings challenged the hypothesis of upwelling thermal groundwater, calling out for further investigations of groundwater of the clastic aquifer.

The two major aims of this work were 1) to evaluate the potential of combining the  $n(^{87}\text{Sr})/n(^{86}\text{Sr})$ ,  $\delta^{88}\text{Sr}/^{86}\text{Sr}_{\text{SRM987}}$  and elemental pattern for groundwater characterisation along the vertical profile of the clastic aquifer, and 2) to use the isotopic and elemental information to investigate potential recharge sources to shallow groundwater below saline ponds of the Lake Neusiedl-Seewinkel Basin.

## 2. Material and methods

### 2.1. Study area

The Lake Neusiedl-Seewinkel Basin is located 40 km southeast of Vienna in East Austria, Central Europe (Figure 1). It encompasses an area of approximately 1100 km<sup>2</sup> and represents a lowland region characterised by warm climate and low amounts of wet precipitation [25,26]. A large part of the study area is covered by the second largest endorheic lake in Europe, Lake Neusiedl and the Lake District Seewinkel. The surroundings of these open water systems represent an important habitat for migrating birds and are protected by the Ramsar Convention on Wetlands [27,28].

The study area represents a subsided basin filled with marine sediments of Badenian to Sarmatian age (11.5–16 Ma) and brackish to lacustrine sediments of Pannonian age (5.5–11.5 Ma) deposited by the Paratethys, the Neogene remnant of the former Tethys ocean. This resulted in the formation of a 1000 m thick clastic aquifer comprised of a mixture and intercalation of gravel, sand, silt and clay [24]. In the Quaternary (ca. 1.8 Ma), within fluvial deposits a saline soil layer came into existence in the Seewinkel underlying saline lakes and saline ponds [31].

The Leitha Mountains to the north and the Rosalia Mountains and the Rust Range to the west represent the potential recharge area of the clastic aquifer [25]. The altitude of these elevations is 250–700 m above the sea level. The Leitha and Rosalia Mountains consist of crystalline basement predominantly made up of metamorphic Paleozoic and Mesozoic schists, with Triassic dolomites and quartzites as well as Neogene limestone deposits at the flanks ([24]; Figure 1).

The investigated clastic aquifer comprised of three floors: shallow groundwater, artesian groundwater and deep thermal groundwater. The latter displays temperatures of more than 35 °C and is used in spas [32], while some artesian springs are used as potable and mineral water [24]. Studies showed no connection between the groundwater of these three clastic aquifer-types and the Lake Neusiedl [23,33].

### 2.2. Sample collection

Figure 1 shows the twenty-six investigated sampling sites. Water samples were collected from three rivers draining the Leitha and Rosalia Mountains (ID 1–3) as well as five shallow

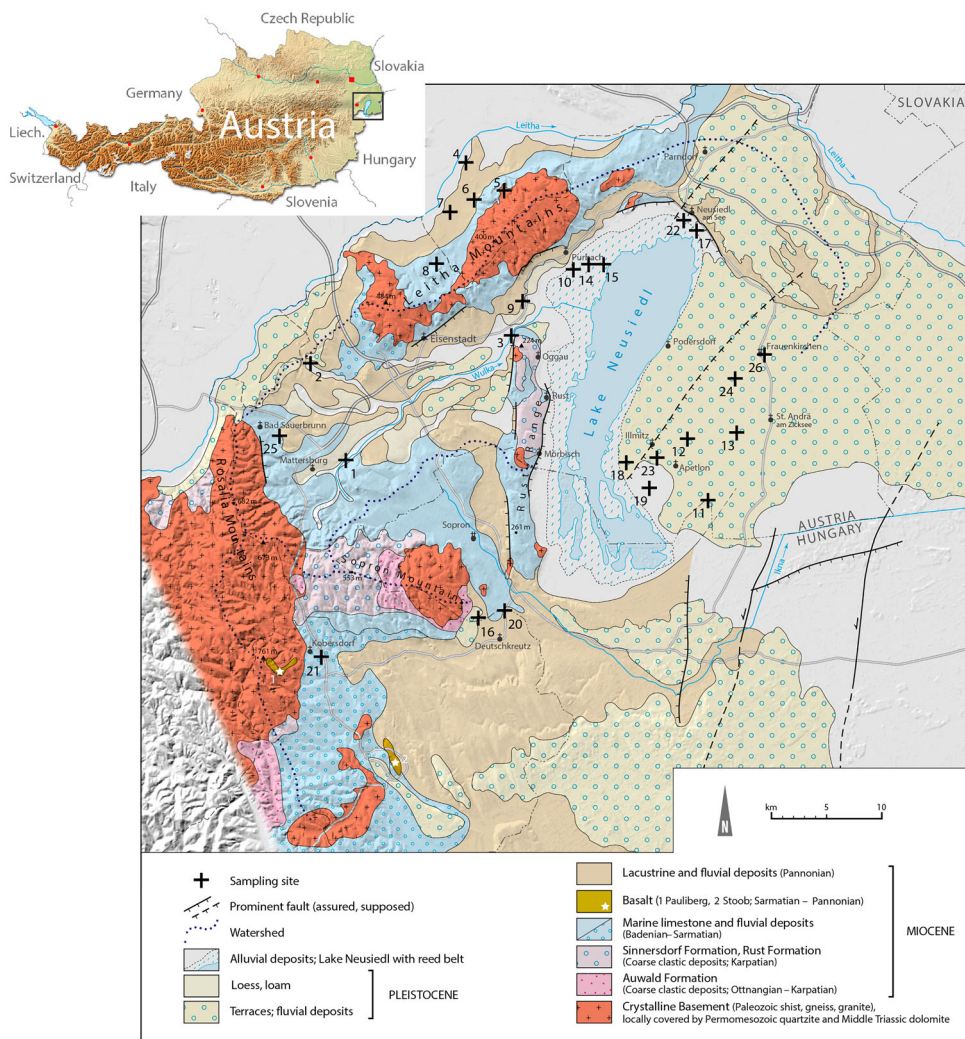


**Figure 1.** Sampling sites and geological map of the study area, Burgenland, East Austria modified after Herrmann et al. and Brix et al. [29,30].

(ID 11–15), eight artesian (ID 16–23) and two thermal (ID 24, 25) clastic aquifers. All samples were collected in pre-cleaned polyethylene bottles following the procedure by Mook et al. [34]. Surface and spring water was collected below surface. Groundwater was sampled from wells to depths that ranged from 5 to 1050 m below ground surface (bgs). The electrical conductivity (EC) was determined in-field using a portable conductivity meter (Cond 3110, WTW, Weilheim i. OB, Germany). Local wet precipitation was sampled in Frauenkirchen in the Seewinkel (ID 26) in pre-cleaned polyethylene bottles. In addition, the VIRIS laboratory provided the  $n(^{87}\text{Sr})/n(^{86}\text{Sr})$  strontium isotope amount ratio data of seven additional surface water samples from the assumed recharge area of the Leitha Mountains (ID 4–10) collected within the course of another project. River water was sampled using pre-cleaned polyethylene bottles and analysed for their strontium

**Table 1.** Hydrological and chemical parameters of investigated water samples; n.a. denotes not analysed; LOQ of K = 2.06  $\mu\text{g g}^{-1}$  and Ca = 6.71  $\mu\text{g g}^{-1}$ ; uncertainties of the electrical conductivity (EC), elemental amount fractions,  $n(^{87}\text{Sr})/n(^{86}\text{Sr})$  ratios and  $\delta^{88}\text{Sr}/^{86}\text{Sr}_{\text{SRM987}}$  values correspond to 0.05%, 10%, 0.00025 and 0.10 ‰ ( $U, k = 2$ ), respectively; significant numbers of digits are given according to EURACHEM guidelines.

ID	Location	Water Source	Lat	Long	Date	Type	Lithology	Depth m bgs	EC $\mu\text{S cm}^{-1}$	Na $\mu\text{g g}^{-1}$	Mg $\mu\text{g g}^{-1}$	K $\mu\text{g g}^{-1}$	Ca $\mu\text{g g}^{-1}$	Sr $\mu\text{g g}^{-1}$	$n(^{87}\text{Sr})/n(^{86}\text{Sr})$	$\delta^{88}\text{Sr}/^{86}\text{Sr}_{\text{SRM987}}$ ‰
1	Wulka catchment	Marz brook	47.738908	16.418761	Jul 2013	Surface	ALLUV	0	812	22.8	32	4.2	109	0.283	0.71048	-0.14
2	Wulka catchment	Zillingtal brook	47.828228	16.389267	Jul 2013	Surface	ALLUV	0	1094	13.2	112	<LOQ	178	0.33	0.71137	0.14
3	Wulka catchment	River Wulka	47.850964	16.630158	Jul 2013	Surface	ALLUV	0	1053	48	47	13.9	111	0.42	0.71019	0.21
4	Leitha Mountains	Ar brook (down hill)	47.980540	16.563880	Jul 2011	Surface	ALLUV	0	n.a.	n.a.	n.a.	n.a.	n.a.	n.a.	0.71064	n.a.
5	Leitha Mountains	Ar brook (up hill)	47.957800	16.586430	Jul 2011	Surface	ALLUV	0	n.a.	n.a.	n.a.	n.a.	n.a.	n.a.	0.71267	n.a.
6	Leitha Mountains	Au brook	47.948810	16.559170	Jul 2011	Surface	ALLUV	0	n.a.	n.a.	n.a.	n.a.	n.a.	n.a.	0.71074	n.a.
7	Leitha Mountains	Hofer-Grenz brook	47.944370	16.541040	Jul 2011	Surface	ALLUV	0	n.a.	n.a.	n.a.	n.a.	n.a.	n.a.	0.70985	n.a.
8	Leitha Mountains	Erl brook	47.918990	16.541710	Jul 2011	Surface	ALLUV	0	n.a.	n.a.	n.a.	n.a.	n.a.	n.a.	0.70907	n.a.
9	Leitha Mountains	Wolfsbrunn brook	47.881060	16.647480	Jul 2011	Surface	ALLUV	0	n.a.	n.a.	n.a.	n.a.	n.a.	n.a.	0.71106	n.a.
10	Leitha Mountains	Anger brook	47.907450	16.705790	Jul 2011	Surface	ALLUV	0	n.a.	n.a.	n.a.	n.a.	n.a.	n.a.	0.70993	n.a.
11	Seewinkel	Borehole Arbesthau Lacke	47.906889	16.699869	Oct 2013	Shallow	SAL	2	2500	320	118	23.8	130	1.62	0.71067	0.28
12	Seewinkel	Borehole Xix-See	47.907181	16.700314	Oct 2013	Shallow	SAL	2	3390	742	110	27.5	249	0.91	0.71003	0.23
13	Seewinkel	Borehole Lange Lacke	47.719472	16.845906	Oct 2013	Shallow	SAL	2	1722	266	229	36	681	1.39	0.70987	-0.05
14	Purbach	Fischergasse	47.759294	16.842006	Oct 2013	Shallow	CLAST	5	947	41	39	16.2	49	0.50	0.71029	0.25
15	Purbach	Purgina	47.759394	16.885000	Oct 2013	Shallow	CLAST	5	8321	1229	588	39	322	3.7	0.70901	0.23
16	Deutschkreutz	Rudolfsquelle	47.945225	16.847833	Aug 2013	Artesian	CLAST	17	2970	409	67	23.1	228	2.07	0.71212	0.25
17	Neusiedl	Klosterschule	47.951683	16.835519	Jul 2013	Artesian	CLAST	56	714	22.7	33	2.09	91	0.187	0.70993	-0.45
18	Seewinkel	Sandeck	47.700036	16.809928	Jul 2013	Artesian	CLAST	68	903	74	45	2.20	74	0.71	0.71086	-0.18
19	Seewinkel	Neudegg	47.733781	16.766411	Jul 2013	Artesian	CLAST	85	530	27.4	34	1.83	52	0.67	0.71094	-0.12
20	Deutschkreutz	Juvena	47.761728	16.799894	Aug 2013	Artesian	CLAST	100	2520	281	58	18.1	249	1.92	0.71183	-0.09
21	Kobersdorf	Gemeindequelle	47.619442	16.619722	Sep 2013	Artesian	CLAST	125	2640	190	69	18.4	340	2.54	0.71378	-0.38
22	Neusiedl	District commisson	47.618917	16.620022	Jul 2013	Artesian	CLAST	138	4290	490	237	41	399	13.8	0.70952	-0.23
23	Illmitz	Bartholomäusquelle	47.595683	16.394278	Jul 2013	Artesian	CLAST	190	4030	958	35	11.5	53	0.75	0.71137	-0.23
24	Frauenkirchen	Spa	47.808778	16.915939	Aug 2013	Thermal	CLAST	865	1426	329	4.2	4.2	<LOQ	0.46	0.71182	0.03
25	Bad Sauerbrunn	Spa	47.780453	16.339136	Aug 2013	Thermal	CLAST	1050	2370	785	62	28.8	59	5.2	0.71228	0.20
26	Frauenkirchen	Bahnstraße	47.839736	16.917775	Sep 2018	Precipitation	-	-	n.a.	0.15	0.28	0.22	3.9	0.0053	0.70887	0.20

isotope ratios following standard protocols [35,36]. Details on the geographical location and sampling time are given in Table 1.

### 2.3. Elemental and strontium isotopic analysis

Water and wet precipitation samples (ID 1–3 and 11–26) were analysed for their elemental and strontium isotopic composition at the University of Natural Resources and Life Sciences Vienna, Department of Chemistry. Preparatory laboratory work was performed in an ISO class 8 clean room according to ISO 14644-1. Laboratory water type I (18 MΩ cm, F + L GmbH, Vienna, Austria) was further purified using a sub-boiling distillation system (Milestone-MLS GmbH, Leutkirch, Germany). Nitric acid (p.a., 65% w/w; Merck-Millipore, Darmstadt, Germany) was double sub-boiled in a DST-1000 sub-boiling distillation system (AHF Analysentechnik, Tübingen, Germany) previous to use in the laboratory. All laboratory consumables (polyethylene bottles, tubes, pipette tips) were double acid washed (10% and 1% HNO<sub>3</sub> w/w) before use.

Water samples were acidified to 2% HNO<sub>3</sub> (v/v) and filtered using a 0.45 μm pore size filter (Sartorius, Göttingen, Germany). The elemental composition of Na, Mg, K, Ca and Sr in water was measured using an inductively coupled plasma quadrupole mass spectrometer (ICP-QMS, NexION 300 D or Elan DRC-e, PerkinElmer, Waltham, USA) in standard mode using a PFA (perfluoroalkoxy) nebuliser (Microflow ST Nebulizer, Elemental Scientific Inc., Nebraska, USA) in combination with a cyclonic spray chamber (PerkinElmer). Samples were diluted as required for the working range of the calibration. Elemental amount fractions were determined following blank correction, normalisation to indium as internal normalisation standard (single element ICP-MS standard, CertiPur, Merck, Darmstadt, Germany) and external calibration applying a 5-point calibration (multi elemental ICP-MS standard VI, CertiPur, Merck). The limit of quantification (LOQ) was calculated as equivalent to ten times the standard deviation of the instrument blank taking into account the dilution factor. Results were validated using in-house quality control standards and certified reference materials SLRS-5 river water (National Research Council Canada, Ottawa, Canada) and IAPSO seawater standard (Batch num. P143, OSIL Ltd, Havant, UK) processed in the same way as the samples. The measured values of these elements in the reference materials and the in-house quality-control standard were in agreement to their certified or target values (Table S1 Supplementary material; [37,38]).

Prior to the strontium isotope ratio measurements water samples underwent Sr/matrix separation using a strontium specific extraction resin (Triskem, Bruz, France) following a protocol of Tchaikovsky et al. [39]. Subsequently, the  $n(^{87}\text{Sr})/n(^{86}\text{Sr})$ ,  $n(^{88}\text{Sr})/n(^{86}\text{Sr})$  and  $n(^{84}\text{Sr})/n(^{86}\text{Sr})$  ratios of the investigated water samples were assessed using a multi-collector inductively coupled plasma mass spectrometer (MC ICP-MS, Nu Plasma HR, Nu Instruments Ltd., Wrexham, UK) equipped with a self-aspirating PFA nebuliser (Microflow ST Nebulizer, Elemental Scientific Inc.) connected to a desolvation unit (either DSN-100, Nu Instruments or Aridus II, Cetac Technologies, Omaha, Nebraska). Strontium isotope ratios were corrected for blank, residual <sup>87</sup>Rb and instrumental isotope fractionation according to the procedure described by Horsky et al. [36].

The instrumental isotope fractionation of the  $n(^{87}\text{Sr})/n(^{86}\text{Sr})$ ,  $n(^{88}\text{Sr})/n(^{86}\text{Sr})$  and  $n(^{84}\text{Sr})/n(^{86}\text{Sr})$  ratios were corrected by a combination of internal inter-elemental correction using

zirconium as an internal isotope standard (single element ICP-MS standard, Inorganic Ventures, Christiansburg, USA) and standard-sample-bracketing using the isotope certified reference material NIST SRM 987 (National Institute of Standards and Technology, Gaithersburg, USA) [40]. This calibration approach corrects for mass-dependent and mass-independent instrumental isotope mass fractionation [41]. The final ratio corresponds to the absolute isotope ratio, reflecting both the radiogenic contribution and mass-dependent fractionation for  $n(^{87}\text{Sr})/n(^{86}\text{Sr})$  and variation of  $n(^{88}\text{Sr})/n(^{86}\text{Sr})$  and  $n(^{88}\text{Sr})/n(^{84}\text{Sr})$  as a consequence of mass-dependent natural fractionation. The  $n(^{88}\text{Sr})/n(^{86}\text{Sr})$  ratio is reported as  $\delta^{88}\text{Sr}/^{86}\text{Sr}_{\text{SRM987}}$  value. This value is calculated as relative difference (in ‰) to the certified  $n(^{88}\text{Sr})/n(^{86}\text{Sr})$  amount ratio of NIST SRM 987. The repeatability (i.e. measurement precision [42]) of the  $n(^{87}\text{Sr})/n(^{86}\text{Sr})$  ratio and the  $\delta^{88}\text{Sr}/^{86}\text{Sr}_{\text{SRM987}}$  value accounted to 0.000032 and 0.03 ‰, respectively and was determined using the NIST SRM 987 bracketing standard under the same measurement conditions by the same operator on the same measuring system.

The reference material IAPSO was subjected to the same preparation procedure as the samples. Furthermore, the NIST SRM 987 was separated to monitor potential on-column fractionation. The determined  $n(^{87}\text{Sr})/n(^{86}\text{Sr})$  ratios of the NIST SRM 987 and IAPSO accounted to  $0.71015 \pm 0.00044$  ( $n = 8$ ;  $U, k = 2$ ) and  $0.70931 \pm 0.00029$  ( $n = 2$ ;  $U, k = 2$ ), respectively and were in agreement with the reference values of  $0.71034 \pm 0.00026$  ( $U, k = 2$ ) and  $0.70931 \pm 0.00009$  ( $n = 10$ ; 2 SE; [43]). The measured  $n(^{88}\text{Sr})/n(^{86}\text{Sr})$  ratios of the NIST SRM 987 and the IAPSO corresponded to  $8.3793 \pm 0.0049$  ( $n = 8$ ;  $U, k = 2$ ; reference value  $8.3786 \pm 0.0033$ ) and  $8.3817 \pm 0.0039$  ( $n = 2$ ;  $U, k = 2$ ; reference value  $8.38183 \pm 0.00004$ ,  $n = 10$ ; 2 SE; [43]), respectively. This corresponds to  $\delta^{88}\text{Sr}/^{86}\text{Sr}_{\text{SRM987}}$  values of the NIST SRM 987 of  $0.09 \text{ ‰} \pm 0.48 \text{ ‰}$  ( $n = 8$ ;  $U, k = 2$ ) and the IAPSO of  $0.37 \text{ ‰} \pm 0.22 \text{ ‰}$  ( $n = 2$ ;  $U, k = 2$ ), respectively which overlapped with the target values within limits of uncertainty (Table S1 Supplementary material; uncertainties in this study correspond to the expanded combined uncertainty, see below; sample heterogeneity was the biggest source to the uncertainty of the NIST SRM 987 and IAPSO).

#### 2.4. Measurement uncertainty

The measurement uncertainty indicates the quality of the analytical result and represents the combination of all uncertainty contributions (e.g. measurement precision, blank, heterogeneity of the samples, etc.) to the measurement result [44]. Uncertainties were calculated in a step-by-step procedure following the Kragten approach [45]. If not stated elsewhere, all uncertainties in this study correspond to the expanded uncertainty ( $U, k = 2$ ) ( $k = 2$  corresponds to a confidence level of 95%).

Following to the procedure by Horsky et al. the uncertainties of the strontium isotope ratios were determined taking into account the uncertainties of the blank, measurement precision, instrumental isotopic fractionation correction, heterogeneity of the samples and  $^{87}\text{Rb}$ -correction [36]. The uncertainty of the  $n(^{87}\text{Sr})/n(^{86}\text{Sr})$  and the  $\delta^{88}\text{Sr}/^{86}\text{Sr}_{\text{SRM987}}$  value accounted to 0.00025 and 0.10 ‰, respectively. Average elemental and strontium isotopic results included additionally the contribution of the heterogeneity of the samples (i.e. their standard deviation) to the uncertainty. The uncertainty of molar fractions obtained by isotope pattern deconvolution was determined according to Tchaikovsky et al. [39]. The uncertainty of the elemental mass fractions of Na, Mg, K, Ca and Sr accounted to 10%

including the uncertainty contribution of the blank, measurement precision and slope of the calibration curve.

## 2.5. Isotope pattern deconvolution

Isotope pattern deconvolution (IPD) was used to calculate the contribution of strontium from wet precipitation and leached bedrock to the  $n(^{87}\text{Sr})/n(^{86}\text{Sr})$  ratio of shallow groundwater below saline ponds. This chemometrical method is used in multiple-spike isotope dilution mass spectrometry (IDMS) [46], but can also be applied for the calculation of the contribution of natural sources to the strontium isotopic composition of environmental samples [39]. Therefore, the  $n(^{87}\text{Sr})/n(^{86}\text{Sr})$ ,  $n(^{88}\text{Sr})/n(^{86}\text{Sr})$  and  $n(^{84}\text{Sr})/n(^{86}\text{Sr})$  ratios of the individual components and the mixture have to be assessed. The determined isotope ratios can then be converted into isotope abundances and used as input variables in a set of simple linear equations. Equation 1 shows an example of the linear equation system for a sample comprised of two components, written in the matrix notation. It is composed of the isotope abundances of the isotope  $i$  of strontium  $A^i$ , the respective molar fractions of the sources  $x_{\text{source},n}$  and an error vector  $e$ . The molar fractions of the sources  $x_{\text{source},n}$  can be determined by multiple-linear regression modelling using the isotope abundances of the individual sources and the sample as input variables in the LINEST-function in Microsoft Excel®.

$$\begin{bmatrix} A_{\text{sample}}^{84} \\ A_{\text{sample}}^{86} \\ A_{\text{sample}}^{87} \\ A_{\text{sample}}^{88} \end{bmatrix} = \begin{bmatrix} A_{\text{source}_1}^{84} & A_{\text{source}_2}^{84} \\ A_{\text{source}_1}^{86} & A_{\text{source}_2}^{86} \\ A_{\text{source}_1}^{87} & A_{\text{source}_2}^{87} \\ A_{\text{source}_1}^{88} & A_{\text{source}_2}^{88} \end{bmatrix} \cdot \begin{bmatrix} x_{\text{source}_1} \\ x_{\text{source}_2} \end{bmatrix} + \begin{bmatrix} e^{84} \\ e^{86} \\ e^{87} \\ e^{88} \end{bmatrix} \quad (1)$$

As strontium has four stable isotopes, it is possible to construct up to four equations with four unknowns. Thus, IPD allows for determining the contribution of up to four individual sources to the  $n(^{87}\text{Sr})/n(^{86}\text{Sr})$  amount ratio of a sample. This represents a specific feature of IPD in comparison to classical mixing model calculations, which allow for the determination of the contribution of two sources to the strontium isotopic composition of a sample only [9]. Furthermore, similar to IDMS calculations, IPD does not require the strontium elemental content of the end members for the calculation. This has the advantage that variables used in IPD are independent of geochemical processes such as evaporation, which can increase the strontium content in the solution, but do not affect the strontium isotopic composition of water [47].

An example on the calculation of the contribution of wet precipitation and the most leachable minerals of the clastic bedrock, represented by thermal water, to the  $n(^{87}\text{Sr})/n(^{86}\text{Sr})$  ratio of shallow groundwater below saline ponds by isotope pattern deconvolution and mixing model calculations using Microsoft Excel® is given in the Supplementary Material 2. The uncertainties were calculated using the Kragten approach [45].

## 2.6. Statistical data evaluation

Statistical data evaluation was performed using SPSS® (IBM SPSS Statistics 24, Armonk, USA). A one sided  $t$ -test allowed comparison of the  $n(^{87}\text{Sr})/n(^{86}\text{Sr})$  ratios of 1) thermal



groundwater to seawater of Badenian to Pannonian age [11], and 2) wet precipitation to shallow, artesian and thermal groundwater of the clastic aquifer, respectively. Furthermore, a two-sided *t*-test for independent samples was used to investigate potential differences of the  $n(^{87}\text{Sr})/n(^{86}\text{Sr})$  ratio of 1) thermal groundwater and shallow groundwater below saline ponds, and 2) shallow groundwater below saline ponds and shallow groundwater extracted from wells of the clastic aquifer. In addition, a two-sided *t*-test for independent samples was used to determine potential differences in the elemental content of calcium between artesian and thermal groundwater. The statistical significance level corresponded to  $\alpha = 0.05$ . Furthermore, according to the EURACHEM guidelines values which overlap within limits of uncertainty have to be considered equal [44].

### 3. Results and discussion

Table 1 summarises the determined electrical conductivity (EC),  $n(^{87}\text{Sr})/n(^{86}\text{Sr})$  ratios,  $\delta^{88}\text{Sr}/^{86}\text{Sr}_{\text{SRM987}}$  values and Na, Mg, K, Ca and Sr elemental composition of surface water, shallow, artesian and thermal groundwater of the clastic aquifer and local precipitation. The lithology comprised of alluvial deposits (ALLUV), saline soils mixed with clastic deposits (SAL) and clastic deposits (CLAST).

#### 3.1. Electrical conductivity of rivers and groundwater

The electrical conductivity of the investigated river water and groundwater of the shallow, artesian and thermal aquifers ranged between  $530 \mu\text{S cm}^{-1}$  (ID 19, Neudegg) and  $8321 \mu\text{S cm}^{-1}$  (ID 15, Purgina). The obtained EC of river and groundwater samples in the Lake Neusiedl-Seewinkel area were comparable to measured values by Boroviczény et al. [33] and Cuculic et al. [48]. The different mineralisation of the investigated groundwater was determined by the occurrence of different water types within close vicinity as well as variation in the discharge rates [49]. For example, the artesian spring District commission in Neusiedl (ID 22) was a carbonated spring water of magnesium-sodium-calcium-hydrogen-type [49]. In contrast, shallow groundwater of well Purgina in Purbach (ID 15), which showed the highest EC values, was a magnesium-sodium-sulfate-chloride-type mineral water with a pH of 7.8 [49,50]. It exhibited a discharge rate of estimated less than  $1 \text{ mL s}^{-1}$ , which resulted in the enrichment of this groundwater with leached bedrock minerals. Zötl and Goldbrunner [49] interpreted the high chloride content of about  $2500 \text{ mg L}^{-1}$  of this groundwater (of a sample analysed in 1963) as a result of upwelling paleo-marine porewater from lower groundwater floors. However, low bromide and iodide content of less than  $0.8 \text{ mg L}^{-1}$  argued against recharge of this groundwater by paleo-seawater. Furthermore, recent analysis of groundwater from well Purgina in Purbach showed a lower chloride content of  $125 \text{ mg L}^{-1}$  only [50].

#### 3.2. Elemental composition of precipitation, rivers and groundwater

Figure 2 shows the relative composition of Ca, Mg and Na + K of wet precipitation, rivers and groundwater of the Lake Neusiedl-Seewinkel area. Rainfall showed a Ca-HCO<sub>3</sub>-type water composition, which indicated dissolution of calcareous dust in rainwater. Surface water had a Ca,Mg-HCO<sub>3</sub>-type water composition reflecting carbonates which form

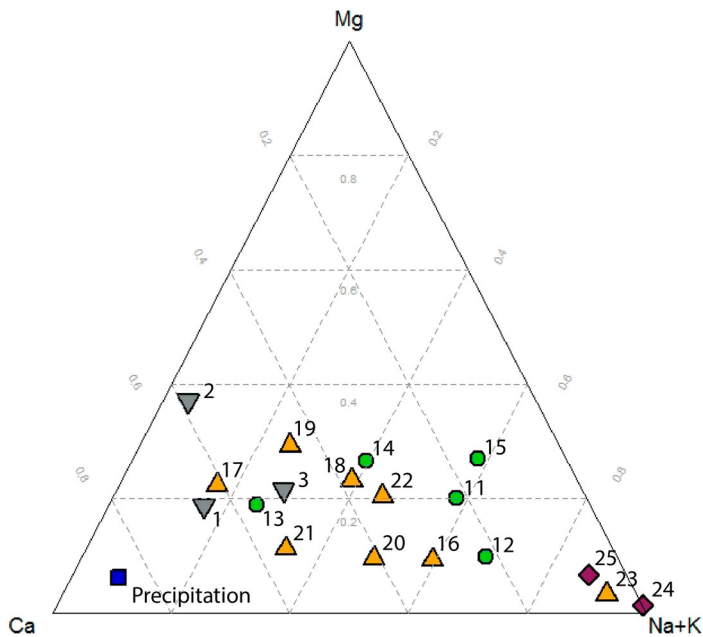


**Figure 2.** Ternary diagram of major cations in wet precipitation (square), rivers (down-pointing triangles) and groundwater of shallow (circles), artesian (up-pointing triangles) and thermal (diamonds) clastic aquifers.

parts of the drainage basin and dissolve quickly upon contact with water [51]. Groundwater of the clastic aquifer showed a trend from Ca,Mg-HCO<sub>3</sub>-type shallow and artesian water towards Na + K-HCO<sub>3</sub>-type thermal groundwater. These results were in accordance to findings by Wurm [50].

High sodium and potassium content of thermal groundwater would support the hypothesis of the existence of paleo-seawater in deep aquifers of the Lake Neusiedl-See-winkel Basin proposed by Tauber [22]. However, the sodium content of 330–780  $\mu\text{g g}^{-1}$  in thermal water of the clastic aquifer was more than one order of magnitude lower than of sea water (Na elemental mass fraction of 10,350  $\mu\text{g g}^{-1}$ ; [52]). In addition, the investigated thermal groundwater showed a lower sodium content than known mixtures of meteoric and paleo-seawater of Bad Pirawarth located about 50 km north of the study site (Na elemental mass fraction of 8,000  $\mu\text{g g}^{-1}$ ; [32, 49]). Furthermore, Elster et al. [32] and Bor-oviczény et al. [33] reported  $\delta^{18}\text{O}$  values of thermal groundwater of the clastic aquifer of the Lake Neusiedl-Seewinkel area ranging between  $-11.57$  and  $-12.25$  ‰, which were in accordance with published  $\delta^{18}\text{O}$  values of old meteoric water in Central Europe [53]. These values were significantly different to  $\delta^{18}\text{O}$  of sea water of 0 ‰ [54]. Therefore, the elemental pattern in groundwater of the clastic aquifer rather reflected different degrees of leaching and dissolution of the siliciclastic host rock than mixing of fresh and marine connate water. This hypothesis was further supported by observations in other areas that mineral water extracted from aquifers formed by silicate hard rocks

such as schist, quartzite, granite and sandstone was enriched in Na and K with respect to other cations [51].

### 3.3. The $n(^{87}\text{Sr})/n(^{86}\text{Sr})$ ratio of groundwater and potential recharge sources

Figure 3 shows the  $n(^{87}\text{Sr})/n(^{86}\text{Sr})$  ratios of local precipitation, rivers draining the assumed recharge area of the Leitha and Rosalia mountains, groundwater of the clastic aquifer and a paleo-seawater reference value of Badenian to Pannonian age of 5.5–16 Ma according to Veizer et al. [11]. Precipitation sampled at Frauenkirchen showed a  $n(^{87}\text{Sr})/n(^{86}\text{Sr})$  ratio of  $0.70889 \pm 0.00025$  ( $U, k = 2$ ), which was in accordance with strontium isotope values of 0.70875–0.70908 determined in diagenetically modified limestone of the adjacent Leitha Mountains (Figure 1; Personal communication 2017 M. Wagreich, University of Vienna, Department of Geodynamics and Sedimentology). This result fostered the observations that rainwater reflected geochemical signatures of local carbonate dust.

The investigated rivers showed a  $n(^{87}\text{Sr})/n(^{86}\text{Sr})$  ratio of  $0.71060 \pm 0.00099$  ( $n = 10$ ;  $U, k = 2$ ) reflecting the lithology of the Leitha and Rosalia Mountains, which are predominantly comprised of metamorphic Paleozoic formations such as schists, gneisses and granites as well as limestone (Figure 1, [24]). The strontium isotopic composition of rivers can serve as a proxy for rainfall infiltrating the ground and forming subsurface runoff

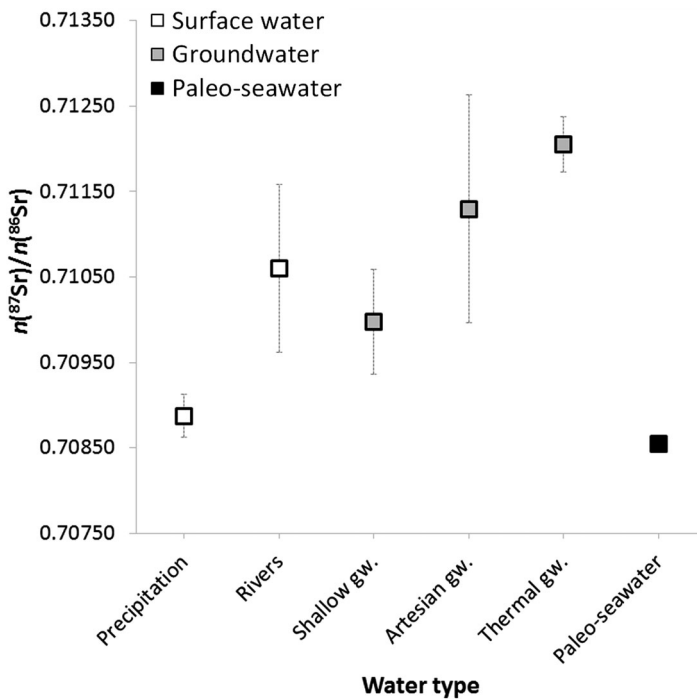


**Figure 3.** Comparison of the  $n(^{87}\text{Sr})/n(^{86}\text{Sr})$  ratios of wet precipitation ( $n = 1$ ), surface water ( $n = 10$ ), shallow ( $n = 5$ ), artesian ( $n = 8$ ) and thermal ( $n = 2$ ) groundwater of the clastic aquifer as well as a paleo-seawater reference value of Badenian to Pannonian age 5.5–16 Ma according to Veizer et al. [11]; error bars correspond to the expanded combined uncertainty ( $U, k = 2$ ).

[1,12,15,55]. Gattinger [25,56] assumed that rivers represented a potential recharge sources to the investigated artesian clastic aquifers.

Shallow groundwater of the clastic aquifer showed an average  $n(^{87}\text{Sr})/n(^{86}\text{Sr})$  ratio of  $0.70997 \pm 0.00063$  ( $n = 5$ ;  $U$ ,  $k = 2$ ). A comparison of the  $n(^{87}\text{Sr})/n(^{86}\text{Sr})$  ratio of three shallow groundwater samples obtained below saline ponds (ID 11–13) and two shallow groundwater samples extracted from wells (ID 14 and 15) of the clastic aquifer of the Lake Neusiedl-Seewinkel area revealed no statistical differences (two-sided  $t$ -test;  $p > 0.05$ ). The investigated shallow aquifers were not connected to the main first (unconfined) groundwater horizon [24]. Thus, shallow groundwater replenishment from surrounding mountains can be excluded. Boroviczény et al. [33] reported that rainfall represented the main recharge source to shallow aquifers of the Lake Neusiedl-Seewinkel Basin. However, the strontium isotopic composition of groundwater of the clastic aquifer was significantly different from local wet precipitation (one-sample  $t$ -test;  $p < 0.05$ , Figure 3), which indicated strontium inputs from more radiogenic strontium sources.

Very few studies investigated the mineral composition of sediments in the Lake Neusiedl-Seewinkel area. Studies of saline Lake Zicksee in the Seewinkel by Stojanovic et al. [57] showed that silicates determined 37% ( $w/w$ ), carbonates 58% ( $w/w$ ) and organic matter 5% ( $w/w$ ) of the suspended particulate matter. Analysis of turbid lake water at the same site revealed that quartz and plagioclase composed more than half of suspended fine-grained material [48]. These studies investigated the uppermost layer of Seewinkel sediments. Deeper sediments of Pannonian age comprising the bedrock of the clastic aquifer of the Lake Neusiedl-Seewinkel area were not mineralogically investigated yet. They are most likely comprised of mineral and rock particles derived from weathering and erosion of rocks of the adjacent Leitha and Rosalia mountains as well as of the Rust range. These minerals might be predominantly quartz, mica and feldspar, which exhibit higher  $n(^{87}\text{Sr})/n(^{86}\text{Sr})$  ratios [2,58] mixed with minerals of Mesozoic carbonates and Neogene Leitha limestone.

Figure 3 shows that the average  $n(^{87}\text{Sr})/n(^{86}\text{Sr})$  ratio of groundwater increased from shallow ( $0.70997 \pm 0.00063$ ,  $n = 5$ ;  $U$ ,  $k = 2$ ) to deeper artesian ( $0.7113 \pm 0.0013$ ;  $n = 8$ ;  $U$ ,  $k = 2$ ) and deep thermal ( $0.71205 \pm 0.00035$ ;  $n = 2$ ;  $U$ ,  $k = 2$ ) groundwater. Shallow groundwater has a mean groundwater residence time of several tens of years, while thermal groundwater has a mean groundwater residence time of more than 35,000 years [33]. Thus, the increase of the  $n(^{87}\text{Sr})/n(^{86}\text{Sr})$  ratios of groundwater with depth could be associated with increased bedrock leaching and dissolution due to longer water–rock interaction. The large variation of the strontium isotope ratio of artesian water indicated different degrees of aquifer host rock leaching and dissolution, which could be influenced by variation in temperature,  $\text{CO}_2$  concentration and residence time [33].

The average strontium isotope ratio of thermal groundwater of  $0.71205 \pm 0.00035$  ( $n = 2$ ;  $U$ ,  $k = 2$ ) was significantly different from published values of seawater at time of aquifer formation (0.70855; Badenium to Pannonium of 5.5–16 Ma; one-sample  $t$ -test;  $p < 0.05$ ; [11]; Figure 3) as well as shallow groundwater below saline ponds ( $0.71019 \pm 0.00044$ ;  $n = 3$ ;  $U$ ,  $k = 2$ ; two-sided  $t$ -test;  $p < 0.05$ ). These results further supported the observation that deep groundwater of the clastic aquifer was not of marine origin. Furthermore, these findings challenged the ‘ascending theory’ indicating no discharge of upwelling thermal water to shallow groundwater below saline ponds. Consequently, shallow groundwater

most likely derived its strontium isotope pattern from rainfall along with leaching and dissolution of the aquifer bedrock.

### 3.4. The $n(^{87}\text{Sr})/n(^{86}\text{Sr})$ ratio of groundwater below saline ponds

The  $n(^{87}\text{Sr})/n(^{86}\text{Sr})$  ratio of shallow groundwater below saline ponds was assumed to be determined by strontium inputs from wet precipitation and host rock leaching and dissolution. Rainwater was considered to reflect the  $n(^{87}\text{Sr})/n(^{86}\text{Sr})$  ratios of locally derived dust from the subaerially exposed soil, sediments and bedrock as well as anthropogenic sources [1]. The rock-derived strontium isotope pattern was assumed to represent the most leachable minerals of the siliciclastic aquifer bedrock. This process included dissolution of the most leachable minerals, ion-exchange, leaching of surface sites and release of fluid inclusions [59]. Such considerations were crucial as Shand et al. [2] pointed out that the reaction kinetics of mineral dissolution varies over orders of magnitude. Therefore, the strontium isotope ratio of solutes will be dominated by the most easily leachable minerals of the bedrock [2,9,12,13]. For example, Kralik et al. [60] demonstrated that the  $n(^{87}\text{Sr})/n(^{86}\text{Sr})$  ratio of 0.716 of bulk granite at Wolfsthal, North of Lake Neusiedl, was significantly different from the  $n(^{87}\text{Sr})/n(^{86}\text{Sr})$  ratio of 0.709 of pore water of the same rock. Thus, the enclosed pore water did not reflect the strontium isotopic composition of the granitic host rock. Therefore, we considered the strontium isotopic signature of the most leachable minerals as an end-member instead of the  $n(^{87}\text{Sr})/n(^{86}\text{Sr})$  ratio of the whole rock (i.e. the sum of all mineral phases). Such  $n(^{87}\text{Sr})/n(^{86}\text{Sr})$  pattern is reflected by deep and geochemically mature groundwater. For example, Frape et al. [3] reported that deep saline waters and brines of the Canadian Shield almost totally lost their primary isotopic and chemical composition due to extensive, low-temperature water-rock interaction. This observation was supported by investigations of oilfield brines in the USA, which reflected the  $n(^{87}\text{Sr})/n(^{86}\text{Sr})$  ratio of the bedrock instead of seawater at the time of deposition of the host rock [61,62].

Thermal water of the investigated area has a mean groundwater residence time of more than 35,000 years and temperatures of more than 35°C. Long groundwater residence times lead to greater water-rock interaction [2]. Furthermore, increased temperatures enhance solubility of siliceous materials [63], which form the bedrock of the clastic aquifer. This assumption was supported by increasing  $n(^{87}\text{Sr})/n(^{86}\text{Sr})$  ratio along the vertical profile of the clastic aquifer and high mineralisation of the investigated thermal groundwater. Moreover, studies by Elster et al. [32] showed that the investigated thermal water had  $\delta^{18}\text{O}$  and  $\delta^2\text{H}$  values of  $-11.57$  to  $-12.25$  ‰ and  $-81.0$  to  $-93.8$  ‰, which suggested meteoric origin. Rainfall has generally low strontium content [1] and, upon contact with rocks, absorbs the strontium isotopic and elemental composition of the most leachable bedrock minerals ([12] and this study). Therefore, we assumed that the primary chemical signal of ancient rainfall in thermal groundwater of the clastic aquifer can be neglected. Consequently, thermal groundwater could be considered as a proxy for the most leachable mineral phases of the host rock of the clastic aquifer of the Lake Neusiedl-Seewinkel Basin.

Table 2 shows the input variables used for the calculation of the contribution of wet precipitation and the most leachable mineral phases of the clastic bedrock, represented by thermal water, to shallow groundwater below saline ponds. The  $n(^{87}\text{Sr})/n(^{86}\text{Sr})$ ,

**Table 2.** Average strontium isotope ratios and elemental amount fractions of wet precipitation (ID 26), thermal water (ID 24 and 25) and shallow groundwater obtained from boreholes below saline ponds (ID 11, 12 and 13) used as input variables in isotope pattern deconvolution [39] and mixing model calculations according to Faure and Mensing [9]; uncertainties correspond to the expanded combined uncertainty ( $U, k = 2$ ); significant numbers of digits are given according to EURACHEM guidelines.

Water type	Sr $\mu\text{g g}^{-1}$	$U, k = 2$	$n(^{87}\text{Sr})/n(^{86}\text{Sr})$	$U, k = 2$	$n(^{88}\text{Sr})/n(^{86}\text{Sr})$	$U, k = 2$	$n(^{84}\text{Sr})/n(^{86}\text{Sr})$	$U, k = 2$
Precipitation	0.0053	0.0005	0.70887	0.00025	8.3803	0.0037	0.05654	0.00008
Thermal groundwater	2.8	3.4	0.71205	0.00070	8.3796	0.0042	0.05614	0.00008
Shallow groundwater	1.31	0.39	0.71019	0.00049	8.3799	0.0040	0.05641	0.00030

$n(^{88}\text{Sr})/n(^{86}\text{Sr})$  and  $n(^{84}\text{Sr})/n(^{86}\text{Sr})$  ratios of the individual components and the mixture were converted to the respective strontium isotope abundances of  $^{84}\text{Sr}$ ,  $^{86}\text{Sr}$ ,  $^{87}\text{Sr}$  and  $^{88}\text{Sr}$  and used in Equation 1. Isotope pattern deconvolution revealed that rainfall accounted to  $58\% \pm 7\%$  ( $U, k = 2$ ) and bedrock leaching and dissolution to  $42\% \pm 7\%$  ( $U, k = 2$ ) of the  $n(^{87}\text{Sr})/n(^{86}\text{Sr})$  ratio of shallow groundwater below saline ponds. These results were confirmed by classical mixing model calculations showing  $53\% \pm 29\%$  ( $U, k = 2$ ) contribution from wet precipitation and  $47\% \pm 29\%$  ( $U, k = 2$ ) from bedrock leaching and dissolution to the strontium isotope pattern of shallow groundwater below saline ponds. While both calculations yielded comparable results, the uncertainty of the molar fractions obtained by isotope pattern deconvolution was about 4-times lower than that of mixing model calculations. The higher uncertainty of the molar fractions determined by the mixing model approach was a result of the high uncertainty of the average elemental amount fraction of thermal water (Sr elemental mass fraction of  $2.8 \mu\text{g g}^{-1} \pm 3.4 \mu\text{g g}^{-1}$ ;  $U, k = 2$ ; average of sample ID 24 and ID 25). The uncertainty of this variable contributed to 92% of the total uncertainty of the determined molar fractions. (Note: IPD does not require the elemental amount of strontium in the endmembers, see before.) In contrast, although the  $n(^{84}\text{Sr})/n(^{86}\text{Sr})$  ratio is often difficult to measure due to the low isotopic abundance of  $^{84}\text{Sr}$  of  $0.56\% \pm 0.02\%$  [64], its uncertainty had little influence on the overall uncertainty of the molar fractions obtained by IPD (see uncertainty calculation in the Supplementary Material 2, worksheet IPD\_Kragten\_Summary). The  $n(^{84}\text{Sr})/n(^{86}\text{Sr})$  ratios showed the lowest variation, thus had no significant impact on the results obtained by multiple linear regression modelling.

Consequently, rainfall represented the major strontium source to the  $n(^{87}\text{Sr})/n(^{86}\text{Sr})$  isotopic composition of shallow groundwater below saline ponds of the clastic aquifer, while bedrock leaching was less dominant due to short mean groundwater residence time.

### 3.5. Fractionation of the $\delta^{88}\text{Sr}/^{86}\text{Sr}_{\text{SRM987}}$ in groundwater with depth

Figure 4 shows a  $n(^{87}\text{Sr})/n(^{86}\text{Sr})$  vs.  $\delta^{88}\text{Sr}/^{86}\text{Sr}_{\text{SRM987}}$  plot of local precipitation, groundwater of shallow, artesian and thermal aquifers and a reference value of modern seawater according to Scher et al. [65]. The  $\delta^{88}\text{Sr}/^{86}\text{Sr}_{\text{SRM987}}$  values of about 0.25 ‰ in most shallow groundwater changed to predominantly negative values of about  $-0.24$  ‰ in artesian groundwater and back to positive values of about 0.12 ‰ in thermal groundwater.

Previous investigations in other regions showed that water reflected the  $\delta^{88}\text{Sr}/^{86}\text{Sr}_{\text{SRM987}}$  value of the bedrock material [20,43,66–68]. Indeed,  $\delta^{88}\text{Sr}/^{86}\text{Sr}_{\text{SRM987}}$  ratio of shallow groundwater were in accordance to wet precipitation potentially reflecting

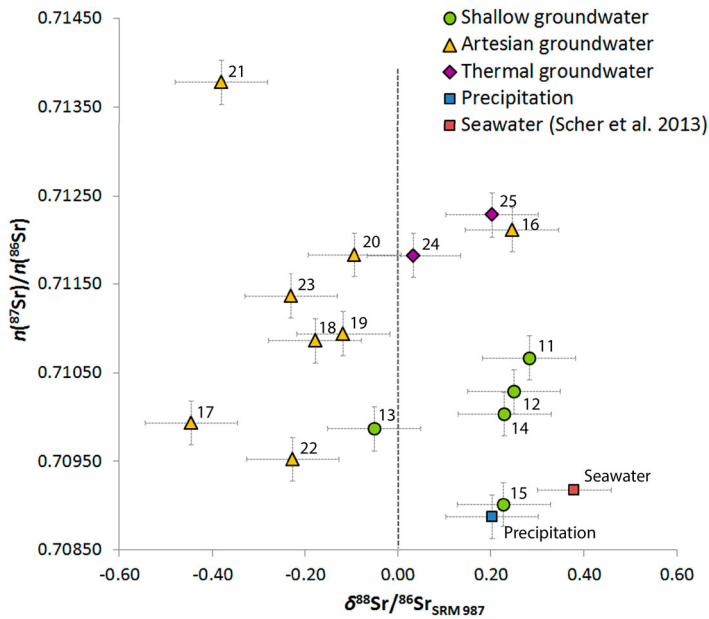


**Figure 4.**  $n(^{87}\text{Sr})/n(^{86}\text{Sr})$  vs.  $\delta^{88}\text{Sr}/^{86}\text{Sr}_{\text{SRM987}}$  plot of local wet precipitation (square), shallow (circles), artesian (triangles) and thermal (diamonds) groundwater of the clastic aquifers as well as a seawater reference value (square) according to Scher et al. [65]; line denotes 0 ‰ according to the NIST SRM 987; error bars of this study correspond to the expanded combined uncertainty ( $U$ ,  $k=2$ ) and Scher et al. to 2  $SD$ .

strontium isotopic composition of local carbonate dust (Figure 4). The shift to negative  $\delta^{88}\text{Sr}/^{86}\text{Sr}_{\text{SRM987}}$  values of artesian groundwater indicated leaching and dissolution of aquifer host rock minerals due to longer residence time. Halicz et al. [21] reported  $\delta^{88}\text{Sr}/^{86}\text{Sr}_{\text{SRM987}}$  of about  $-0.17$  ‰ in soils which comprised of secondary minerals, mostly clays and quartz grains. Chao et al. [69] observed in laboratory-based leaching experiments that  $\delta^{88}\text{Sr}/^{86}\text{Sr}_{\text{SRM987}}$  of residues of Peiliao Shales in Taiwan, composed of quartz, feldspar, illite and chlorite, showed lower  $\delta^{88}\text{Sr}/^{86}\text{Sr}_{\text{SRM987}}$  values than the leachates. They attributed these differences to preferential leaching and dissolution of minerals with higher  $\delta^{88}\text{Sr}/^{86}\text{Sr}_{\text{SRM987}}$  values. These findings suggested that negative  $\delta^{88}\text{Sr}/^{86}\text{Sr}_{\text{SRM987}}$  values of artesian groundwater could potentially reflect leaching and dissolution of bedrock minerals with low  $\delta^{88}\text{Sr}/^{86}\text{Sr}_{\text{SRM987}}$ , which were formed by weathering processes prior to sedimentation in the aquifer.

The return to positive  $\delta^{88}\text{Sr}/^{86}\text{Sr}_{\text{SRM987}}$  values of thermal groundwater in the investigated area could be a result of precipitation of carbonates (and other secondary phases), which preferentially incorporate  $^{86}\text{Sr}$  leaving the residual solution enriched in  $^{88}\text{Sr}$  [19]. Carbonate precipitation could have been a result of changes in the saturation state of thermal groundwater of the clastic aquifer driven by long water–rock interaction of more than 35,000 years [33], increased temperatures of more than  $35^\circ\text{C}$  [32] and pH of about 7–8 [70]. This hypothesis was supported by statistical analysis revealing significantly lower elemental content of calcium in thermal groundwater than in artesian water (two-sided  $t$ -test,  $p < 0.05$ ; Figure 5).

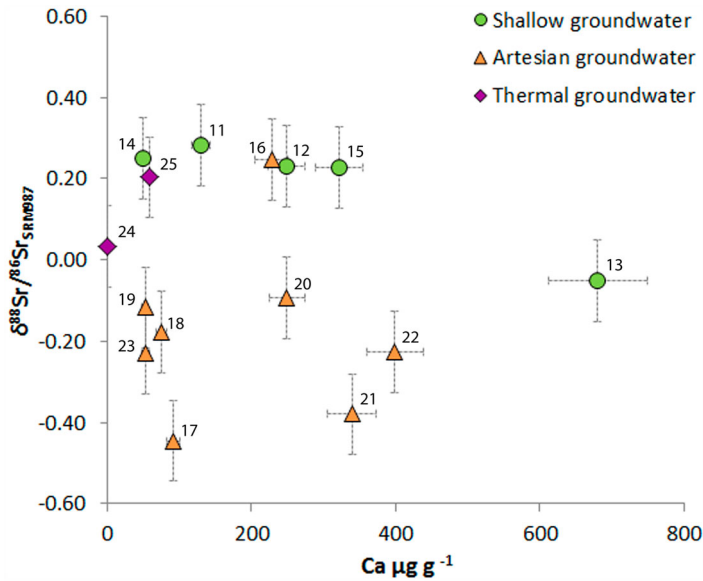


**Figure 5.**  $\delta^{88}\text{Sr}/^{86}\text{Sr}_{\text{SRM987}}$  vs. Ca elemental mass fraction plot of shallow (circles), artesian (triangles) and thermal (diamonds) groundwater of the clastic aquifers; error bars correspond to the expanded combined uncertainty ( $U, k = 2$ ).

Preferential incorporation of the lighter  $^{86}\text{Sr}$  isotopes into carbonate precipitates might also be responsible for positive  $\delta^{88}\text{Sr}/^{86}\text{Sr}_{\text{SRM987}}$  values of one artesian groundwater sample showing sinter deposits at the well ( $\delta^{88}\text{Sr}/^{86}\text{Sr}_{\text{SRM987}}$  of  $0.25 \pm 0.10$  ‰;  $U, k = 2$ ; ID 16; [71]). In contrast, the slightly negative  $\delta^{88}\text{Sr}/^{86}\text{Sr}_{\text{SRM987}}$  values of one shallow groundwater below saline lakes of the Seewinkel might indicate higher degrees of aquifer host rock dissolution or influences of other water sources ( $-0.05 \pm 0.10$  ‰;  $U, k = 2$ ; ID 13).

#### 4. Conclusion

This study showed that the  $n(^{87}\text{Sr})/n(^{86}\text{Sr})$  isotopic and elemental pattern of groundwater of the investigated clastic aquifer changed with depth as a result of progressive aquifer bedrock leaching and dissolution. This process was accompanied by increasing mean groundwater residence time suggesting a continuous groundwater flow path from shallow over artesian to thermal aquifers. The latter showed  $n(^{87}\text{Sr})/n(^{86}\text{Sr})$  isotopic and elemental pattern typical for groundwater in host rock aquifers comprised of siliceous minerals, which was in contrast to previous theories suggesting occurrence of marine connate water in deep clastic aquifers of the Lake Neusiedl-Seewinkel region.

The  $n(^{87}\text{Sr})/n(^{86}\text{Sr})$  ratio of shallow groundwater below saline ponds was significantly different from thermal groundwater suggesting no upwelling of deep groundwater to the surface. This was further supported by isotope pattern deconvolution revealing that recent rainfall accounted to  $58\% \pm 7\%$  ( $U, k = 2$ ) and bedrock leaching to  $42\% \pm 7\%$  ( $U, k = 2$ ) of the  $n(^{87}\text{Sr})/n(^{86}\text{Sr})$  ratio of shallow groundwater below saline ponds.

The  $\delta^{88}\text{Sr}/^{86}\text{Sr}_{\text{SRM987}}$  of groundwater changed from positive  $\delta^{88}\text{Sr}/^{86}\text{Sr}_{\text{SRM987}}$  values of shallow groundwater to negative values of artesian groundwater, potentially reflecting



leaching and dissolution of bedrock subjected to intense weathering processes before sedimentation. The transition from negative artesian to positive  $\delta^{88}\text{Sr}/^{86}\text{Sr}_{\text{SRM987}}$  values of deep thermal groundwater indicated removal of  $^{86}\text{Sr}$  from solution, which occurred most likely as a result of carbonate precipitation. These results underline the potential of the  $\delta^{88}\text{Sr}/^{86}\text{Sr}_{\text{SRM987}}$  signature as a tracer for the investigation of geochemical processes in aquatic and terrestrial environments.

Further research should focus on the combination of the  $n(^{87}\text{Sr})/n(^{86}\text{Sr})$   $\delta^{88}\text{Sr}/^{86}\text{Sr}_{\text{SRM987}}$  and elemental pattern with  $\delta^{18}\text{O}$  for delineating an enhanced hydrological model of the investigated clastic aquifer. In addition, a series of leaching experiments of cores of the siliciclastic bedrock have the potential to better understand the geochemical processes occurring in the clastic aquifer of the Lake Neusiedl-Seewinkel Basin along with geochemical modelling techniques.

## Acknowledgments

The authors would like to acknowledge Christine Opper and Jennifer Sarne for help with sample preparation as well as two anonymous referees for their highly constructive and valuable comments.

## Disclosure Statement

No potential conflict of interest was reported by the authors.

## References

- [1] Capo RC, Stewart BW, Chadwick OA. Strontium isotopes as tracers of ecosystem processes: theory and methods. *Geoderma*. 1998;82(1–3):197–225.
- [2] Shand P, Darbyshire DPF, Love AJ, et al. Sr isotopes in natural waters: applications to source characterisation and water–rock interaction in contrasting landscapes. *Appl Geochem*. 2009;24(4):574–586.
- [3] Frape SK, Fritz P, McNutt RH. Water–rock interaction and chemistry of groundwaters from the Canadian shield. *Geochim Cosmochim Acta*. 1984;48(8):1617–1627.
- [4] Palmer MR, Edmond JM. Controls over the strontium isotope composition of river water. *Geochim Cosmochim Acta*. 1992;56(5):2099–2111.
- [5] Coplen TB. Guidelines and recommended terms for expression of stable-isotope-ratio and gas-ratio measurement results. *Rapid Commun Mass Spectrom*. 2011;25(17):2538–2560.
- [6] Wieser M, Holden N, Coplen T, et al. Atomic weights of the elements 2011 (IUPAC technical report). *Pure Appl Chem*. 2013;85(5):1047–1078.
- [7] Bentley RA. Strontium isotopes from the earth to the archaeological skeleton: a review. *J Archaeol Method Theory*. 2006;13(3):135–187.
- [8] Voerkelius S, Lorenz GD, Rummel S, et al. Strontium isotopic signatures of natural mineral waters, the reference to a simple geological map and its potential for authentication of food. *Food Chem*. 2010;118(4):933–940.
- [9] Faure G, Mensing T. *Isotopes: principles and applications*. 3rd ed. Hoboken (NJ): John Wiley & Sons; 2005.
- [10] Blum J, Erel Y. Radiogenic isotopes in weathering and hydrology. In: Drever JI, editor. *Surface and ground water, weathering, and soils*. Amsterdam: Elsevier; 2003. p. 365–392.
- [11] Veizer J, Ala D, Azmy K, et al.  $^{87}\text{Sr}/^{86}\text{Sr}$ ,  $\delta^{13}\text{C}$  and  $\delta^{18}\text{O}$  evolution of Phanerozoic seawater. *Chem Geol*. 1999;161(1–3):59–88.

- [12] Graustein WC.  $^{87}\text{Sr}/^{86}\text{Sr}$  ratios measure the sources and flow of strontium in terrestrial ecosystems. In: Rundel PW, Ehleringer JR, Nagy KA, editor. *Stable isotopes in ecological research*. New York, NY: Springer; 1989. p. 491–512.
- [13] Aberg G. The use of natural strontium isotopes as tracers in environmental studies. *Water Air Soil Pollut.* 1995;79(1–4):309–322.
- [14] Montgomery J, Evans JA, Wildman G.  $^{87}\text{Sr}/^{86}\text{Sr}$  isotope composition of bottled British mineral waters for environmental and forensic purposes. *Appl Geochem.* 2006;21(10):1626–1634.
- [15] Woods T, Fullagar P, Spruill R, et al. Strontium isotopes and major elements as tracers of ground water evolution: example from the upper Castle Hayne aquifer of North Carolina. *Groundwater.* 2000;38(5):762–771.
- [16] Ohno T, Hirata T. Simultaneous determination of mass-dependent isotopic fractionation and radiogenic isotope variation of strontium in geochemical samples by multiple collector-ICP-mass spectrometry. *Anal Sci.* 2007;23(11):1275–1280.
- [17] Fietzke J, Eisenhauer A. Determination of temperature-dependent stable strontium isotope ( $^{88}\text{Sr}/^{86}\text{Sr}$ ) fractionation via bracketing standard MC-ICP-MS. *Geochem Geophys Geosyst.* 2006;7(8):Q08009.
- [18] Neymark LA, Premo WR, Mel’Nikov NN, et al. Precise determination of  $\delta^{88}\text{Sr}$  in rocks, minerals, and waters by double-spike TIMS: a powerful tool in the study of geological, hydrological and biological processes. *J Anal At Spectrom.* 2014;29(1):65–75.
- [19] Böhm F, Eisenhauer A, Tang J, et al. Strontium isotope fractionation of planktic foraminifera and inorganic calcite. *Geochim Cosmochim Acta.* 2012;93:300–314.
- [20] Souza GFD, Reynolds BC, Kiczka M, et al. Evidence for mass-dependent isotopic fractionation of strontium in a glaciated granitic watershed. *Geochim Cosmochim Acta.* 2010;74(9):2596–2614.
- [21] Halicz L, Segal I, Fruchter N, et al. Strontium stable isotopes fractionate in the soil environments? *Earth Planet Sci Lett.* 2008;272(1–2):406–411.
- [22] Tauber A. Neusiedlersee – Mineralwasser und Mineralwasserlagerstätte. In: *Allgemeine Landestopographie des Burgenlandes. Band 2. Der Verwaltungsbezirk Eisenstadt und die Freistädte Eisenstadt und Rust*. Eisenstadt: Amt der Burgenländischen Landesregierung; 1963. p. 786–809. German.
- [23] Rank D, Papesch W, Rajner V. Verweilzeiten der jungen Grundwässer im Seewinkel. Illmitz: Biologisches Forschungsinstitut für Burgenland; 1986; German.
- [24] Häusler H. Geologische Karte der Republik Österreich 1:50.000, Erläuterungen zur Geologischen Karte 78 Rust. Vienna: Geological Survey of Austria; 2010.
- [25] Gattinger T. Das hydrogeologische Einzugsgebiet des Neusiedlersees. Vienna: Geological Survey of Austria; 1975; German.
- [26] Auer I, Böhm R, Jurkovic A, et al. HISTALP—historical instrumental climatological surface time series of the greater Alpine region. *Int J Climatol.* 2007;27(1):17–46.
- [27] Winkler H, Berthold P, Leisler B. Monitoring of bird population in the Lake Neusiedl area; [cited 2018 Jul 21]. Available from: [http://www.zobodat.at/pdf/STAPFIA\\_0031\\_0029-0036.pdf](http://www.zobodat.at/pdf/STAPFIA_0031_0029-0036.pdf).
- [28] Ramsar Convention. [cited 2018 Jul 21]. Available from: <https://www.ramsar.org/wetland/austria>.
- [29] Herrmann P, Pascher G, Pistotnik J. Geologische Karte der Republik Österreich 1:50.000, 78 Rust. Vienna: Geological Survey of Austria; 1993; German.
- [30] Brix F, Pascher G. Geologische Karte der Republik Österreich 1:50.000, 77 Eisenstadt. Vienna: Geologic Survey of Austria; 1994; German.
- [31] Nestroy O. *Den Boden verstehen*. Graz: Leopold Stocker Verlag; 2015; German.
- [32] Elster D, Goldbrunner J, Wessely G, et al. Erläuterungen zur geologischen Themenkarte Thermalwässer in Österreich 1:500 000. Vienna: Geological Survey of Austria; 2016; p. 296. German.
- [33] Boroviczény F, Deák J, Liebe P, et al. *Wasserhaushaltsstudie für den Neusiedlersee mit Hilfe der Geophysik und Geochemie 1980–1990.*: Institute of Hydraulic Engineering and Water Resources Management, Vienna University of Technology; 1992. German.
- [34] Mook WG, Rozanski K, Stichler W, et al. *Environmental isotopes in the hydrological cycle – principles and applications*. Vol. 1. Paris/Vienna: IAEA-UNESCO; 2000.

- [35] Swoboda S, Brunner M, Boulyga SF, et al. Identification of marchfeld asparagus using Sr isotope ratio measurements by MC-ICP-MS. *Anal Bioanal Chem.* 2008;390(2):487–494.
- [36] Horsky M, Irrgeher J, Prohaska T. Evaluation strategies and uncertainty calculation of isotope amount ratios measured by MC ICP-MS on the example of Sr. *Anal Bioanal Chem.* 2016;408(2):351–367.
- [37] Burton J. The ocean: a global geochemical system. In: Summerhayes C, Thorpe S, editor. *Oceanography: An illustrated guide.* London: Manson; 1996. p. 165–181.
- [38] Yeghicheyan D, Bossy C, Bouhnik Le Coz M, et al. A compilation of silicon, rare earth element and twenty-one other trace element concentrations in the natural river water reference material SLRS-5 (NRC-CNRC). *Geostand Geoanal Res.* 2013;37(4):449–467.
- [39] Tchaikovsky A, Irrgeher J, Zitek A, et al. Isotope pattern deconvolution of different sources of stable strontium isotopes in natural systems. *J Anal At Spectrom.* 2017;32:2300–2307.
- [40] Irrgeher J, Vogel J, Santner J, et al. In: Prohaska T, Irrgeher J, Zitek A, et al., editor. *Sector field mass spectrometry for elemental and isotopic analysis.* Cambridge: Royal Society of Chemistry; 2015. p. 126–149.
- [41] Irrgeher J, Prohaska T, Sturgeon RE, et al. Determination of strontium isotope amount ratios in biological tissues using MC-ICPMS. *Anal Methods.* 2013;5(7):1687–1694.
- [42] ISO. Evaluation of measurement data – Guide to the expression of uncertainty in measurement. Joint Committee for Guides in Metrology. Standard No.: JCGM. 2008;100:1–134.
- [43] Krabbenhöft A, Fietzke J, Eisenhauer A, et al. Determination of radiogenic and stable strontium isotope ratios ( $^{87}\text{Sr}/^{86}\text{Sr}$ ;  $\delta^{88}/^{86}\text{Sr}$ ) by thermal ionization mass spectrometry applying an  $^{87}\text{Sr}/^{84}\text{Sr}$  double spike. *J Anal At Spectrom.* 2009;24(9):1267–1271.
- [44] Ellison SLR, Williams A, editors. *EURACHEM/CITAC guide: quantifying uncertainty in analytical measurement*; 2012. Available from [www.eurachem.org](http://www.eurachem.org).
- [45] Kragten J. Tutorial review. Calculating standard deviations and confidence intervals with a universally applicable spreadsheet technique. *Analyst.* 1994;119(10):2161–2165.
- [46] Garcia Alonso JI, Rodriguez-Gonzalez P. *Isotope dilution mass spectrometry.* Cambridge: Royal Society of Chemistry; 2013.
- [47] Faure G. *Principles of isotope geology.* 2nd ed. Hoboken (NJ): John Wiley & Sons; 1986.
- [48] Cuculić V, Frančišković-Bilinski S, Bilinski H, et al. Multi-methodological approach to evaluate trace elements and major components in wetland system with subsaline and freshwater characteristics. *Environ Earth Sci.* 2016;75(20):1351.
- [49] Zötl J, Goldbrunner J. *Die Mineral- und Heilwässer Österreichs: geologische Grundlagen und Spurenelemente.* Vienna: Springer; 1993; German.
- [50] Wurm M. *Hydrogeochemische Methodik zur Klärung von Interaktionsprozessen von Formations-, Mineral-, Tiefengrund- und oberflächennahen Grundwässern im Einzugsgebiet des Neusiedlersees.* Leoben: Montanuniversität Leoben; 2000; German.
- [51] Appelo CAJ, Postma D. *Minerals and water. geochemistry, groundwater and pollution.* 2nd ed. Leiden: A.A. Balkema Publishers; 2010.
- [52] Besson P, Degboe J, Berge B, et al. Calcium, Na, K and Mg concentrations in seawater by inductively coupled plasma-atomic emission spectrometry: applications to IAPSO seawater reference material, hydrothermal fluids and synthetic seawater solutions. *Geostand Geoanal Res.* 2013; 38(3):355–362.
- [53] Rozanski K. Deuterium and oxygen-18 in European groundwaters — Links to atmospheric circulation in the past. *Chem Geol Isot Geosci Sect.* 1985;52(3):349–363.
- [54] Harzhauser M, Latal C, Piller WE. The stable isotope archive of Lake Pannon as a mirror of Late Miocene climate change. *Palaeogeogr Palaeoclimatol Palaeoecol.* 2007;249(3):335–350.
- [55] Jones LM, Faure G. A study of strontium isotopes in lakes and surficial deposits of the ice-free valleys, southern Victoria Land, Antarctica. *Chem Geol.* 1978;22:107–120.
- [56] Gattinger T. *The hydrology of Neusiedlersee and its catchment area. Neusiedlersee: the limnology of a shallow lake in Central Europe.* The Hague: Dr. W. Junk bv Publishers; 1979.
- [57] Stojanovic A, Kogelnig D, Mitteregger B, et al. Major and trace element geochemistry of superficial sediments and suspended particulate matter of shallow saline lakes in Eastern Austria. *Chem Erde–Geochem.* 2009;69(3):223–234.

- [58] Faure G, Powell JL. Strontium isotope geology. Berlin: Springer Verlag; 1972.
- [59] McNutt R. – In: Saline water and gases in crystalline rocks. Vol. 33. St. John's, Nfld., Canada: Geological Association of Canada; 1987. p. 81–88. (Geological Association of Canada – Special Paper; 33).
- [60] Kralik M, Maringer F, Papesch W, et al., editors. Long-term water percolation around waste disposal sites revealed using natural isotope tracers ( $^3\text{H}$ ,  $^{18}\text{O}$ ,  $^{87}\text{Sr}$ ,  $^{226}\text{Ra}/^{238}\text{U}$ ). In: Tracers and modelling in hydrogeology. TraM'2000 2000. Liege (Belgium): IAHS. p. 371–375. (IAHS Publ.; 262).
- [61] Chaudhuri S. Strontium isotopic composition of several oilfield brines from Kansas and Colorado. *Geochim Cosmochim Acta*. 1978;42(3):329–331.
- [62] Sunwall MT, Pushkar P. The isotopic composition of strontium in brines from petroleum fields of southeastern Ohio. *Chem Geol*. 1979;24(3):189–197.
- [63] Langmuir D. Aqueous environmental geochemistry. Upper Saddle River, NJ: Prentice-Hall, Inc.; 1997.
- [64] Meija J, Coplen TB, Berglund M, et al. Isotopic compositions of the elements 2013 (IUPAC technical report). *Pure Appl. Chem*. 2016;88(3):293–306.
- [65] Scher HD, Griffith EM, Buckley WP. Accuracy and precision of  $^{88}\text{Sr}/^{86}\text{Sr}$  and  $^{87}\text{Sr}/^{86}\text{Sr}$  measurements by MC-ICPMS compromised by high barium concentrations. *Geochem Geophys Geosyst*. 2014;15(2):499–508.
- [66] Pearce CR, Parkinson IJ, Gaillardet J, et al. Reassessing the stable ( $\delta^{88}/^{86}\text{Sr}$ ) and radiogenic ( $^{87}\text{Sr}/^{86}\text{Sr}$ ) strontium isotopic composition of marine inputs. *Geochim Cosmochim Acta*. 2015;157:125–146.
- [67] Wei G, Ma J, Liu Y, et al. Seasonal changes in the radiogenic and stable strontium isotopic composition of Xijiang river water: implications for chemical weathering. *Chem Geol*. 2013;343:67–75.
- [68] Krabbenhöft A, Eisenhauer A, Böhm F, et al. Constraining the marine strontium budget with natural strontium isotope fractionations ( $^{87}\text{Sr}/^{86}\text{Sr}$ \*,  $\delta^{88}/^{86}\text{Sr}$ ) of carbonates, hydrothermal solutions and river waters. *Geochim Cosmochim Acta*. 2010;74(14):4097–4109.
- [69] Chao HC, You CF, Liu HC, et al. Evidence for stable Sr isotope fractionation by silicate weathering in a small sedimentary watershed in southwestern Taiwan. *Geochim Cosmochim Acta*. 2015;165:324–341.
- [70] Webpage. St. Martins Spa Lodge; [cited 2018 Sep 19]. Available from: <https://www.stmartins.at/en/water-pools.html>.
- [71] Kümel F. Geologische Karte der Republik Österreich 1:50.000 Mattersburg – Deutschkreutz. Vienna: Geologic Survey of Austria; 1957; German.

**Analysis of  $n(^{87}\text{Sr})/n(^{86}\text{Sr})$ ,  $\delta^{88}\text{Sr}/^{86}\text{Sr}_{\text{SRM987}}$  and elemental pattern to characterise groundwater and recharge of saline ponds in a clastic aquifer in East Austria**

A. Tchaikovsky, H. Häusler, M. Kralik, A. Zitek, J. Irrgeher and T. Prohaska

**Supplementary material 1**

Sample ID	LOQ	measured value	reference value
<b>SRM 987</b>			
$n(^{87}\text{Sr})/n(^{86}\text{Sr})$		0.71015 (44)	0.71034 (26)
$n(^{88}\text{Sr})/n(^{86}\text{Sr})$		8.3793 (49)	8.3786 (33)
$n(^{84}\text{Sr})/n(^{86}\text{Sr})$		0.05657 (12)	0.05655 (14)
$\delta^{88}\text{Sr}/^{86}\text{Sr}_{\text{SRM987}}$ ‰		0.09 (48)	0.00
<b>IAPSO</b>			
$n(^{87}\text{Sr})/n(^{86}\text{Sr})$		0.70931 (29)	0.70931 (9)
$n(^{88}\text{Sr})/n(^{86}\text{Sr})$		8.3817 (39)	8.38183 (4)
$n(^{84}\text{Sr})/n(^{86}\text{Sr})$		0.05653 (10)	-
$\delta^{88}\text{Sr}/^{86}\text{Sr}_{\text{SRM987}}$ ‰		0.37 (22)	0.386 (5)
Mg	mg g <sup>-1</sup>	2.18E-05	1.45 (28)
K	mg g <sup>-1</sup>	2.33E-04	0.41 (10)
Ca	mg g <sup>-1</sup>	2.04E-04	0.40 (7)
Sr	µg g <sup>-1</sup>	9.72E-04	7.6 (7)
<b>SLRS-5</b>			
Na	µg g <sup>-1</sup>	2.64E-01	5.3 (5)
Mg	µg g <sup>-1</sup>	9.76E-01	2.55 (26)
K	µg g <sup>-1</sup>	2.06E+00	<LOQ
Ca	µg g <sup>-1</sup>	6.71E+00	10 (1)
Sr	ng g <sup>-1</sup>	1.02E+01	48 (5)
<b>VIRIS QC Standard</b>			
Mg	µg g <sup>-1</sup>	6.44E-03	0.112 (11)
K	µg g <sup>-1</sup>	6.18E-03	0.117 (12)
Ca	µg g <sup>-1</sup>	3.74E-02	0.93 (9)
Na	ng g <sup>-1</sup>	3.26E-01	44 (4)
Sr	ng g <sup>-1</sup>	6.71E-02	22 (2)

Table S1. Comparison of measured values to reference values of the strontium isotope ratios of the reference materials NIST SRM 987 ( $n=8$ ) and IAPSO ( $n=2$ ) as well as the elemental amount fraction of the reference materials IAPSO, SLRS-5 and in-house quality control standard VIRIS QC Standard; uncertainties of determined values correspond to the expanded combined uncertainty ( $U$ ,  $k=2$ ) including measurement uncertainty and sample heterogeneity; sample heterogeneity was the biggest source to the uncertainty of the strontium isotope ratios of NIST SRM 987 and IAPSO; uncertainties of the reference strontium isotope ratios of the IAPSO correspond to  $2 SE$  [41]; significant numbers of digits are given according to EURACHEM guidelines

#### **IV. The $^{87}\text{Sr}/^{86}\text{Sr}$ river water isoscape of the Danube catchment**

*Andreas Zitek, Anastassiya Tchaikovsky, Johanna Irrgeher, Herwig Waidbacher and Thomas Prohaska*

*Joint Danube Survey 3, 2014 (published)*

*ISBN: 978-3-200-03795-3*



---

## 33 The $^{87}\text{Sr}/^{86}\text{Sr}$ river water isoscape of the Danube catchment

---



Andreas Zitek, Anastassiya Tchaikovsky, Johanna Irrgeher, Herwig Waidbacher, Thomas Prohaska

### 33.1 Introduction

Isoscapes are spatial maps of the distribution of isotopes on Earth. As a basis for ecological studies such as long distance migrations of animals, the study of environmental fluxes or for determining the origin and provenance of e.g. plants, food or other goods these tools have been developed on a global and local level. Isoscape models of different quality are available for the stable H, C, N and O isotopes on a global and local range. Especially the  $\delta^2\text{H}$  and  $\delta^{18}\text{O}$  values vary significantly due to physical fractionation on a continental scale what makes them efficient large scale environmental tracers, while  $\delta^{13}\text{C}$  values primarily reflect effects related to the transformation of carbon from organic material (Bowen 2010). The spatial variation of N isotopes in terrestrial and aquatic ecosystems can be related to climatic controls on N cycle fluxes (global-scale) (Bowen 2010) or to anthropogenic influences (local to catchment scale) (Lake *et al.* 2001, Borderelle *et al.* 2009, Karube *et al.* 2010), and has been used successfully for ecological (Harrington *et al.* 1998) and traceability (Fox & Papanicolaou 2008) studies. On a catchment level  $\delta^2\text{H}$  and  $\delta^{18}\text{O}$  show significant time variation on seasonal and interannual scales (Gibson *et al.* 2002, Rank *et al.* 2009) which limit their applicability to specific ecological studies like migration and dispersal on this spatial level.

Due to its relative local and temporal stability over time, the  $^{87}\text{Sr}/^{86}\text{Sr}$  isotope ratio is increasingly recognized as important eco-geochemical tracer in many fields of science like ecology (Capo *et al.* 1998), anthropology (Price *et al.* 2002, Prohaska *et al.* 2002), food science (Kelly *et al.* 2005, Swoboda *et al.* 2008, Voerkelius *et al.* 2010) and forensics (Beard & Johnson 2000, Muynck & Winne 2012).

The  $^{87}\text{Sr}/^{86}\text{Sr}$  isotope ratio varies naturally in the environment as a result of the underlying geology (Faure & Mensing 2005). The reason for its local variation is the constant radioactive  $\beta$ -decay of  $^{87}\text{Rb}$  into  $^{87}\text{Sr}$  over geological time scales (half-life =  $48.8 \times 10^9$  years, Holden (1990)) while the absolute amount of  $^{86}\text{Sr}$  remains stable over time, which leads to higher  $^{87}\text{Sr}/^{86}\text{Sr}$  isotope ratios in older rocks or rocks with higher Rb/Sr ratio (Faure & Mensing 2005) (Figure 167). By weathering, Sr is released from the rocks influencing the local  $^{87}\text{Sr}$  concentration in soils and water and is incorporated into living organisms according to its availability without any further fractionation (Graustein 1989, Capo *et al.* 1998, Blum *et al.* 2000) via the food chain.

As far as variations in the isotopic distribution in a studied area exist, the isotopic composition bears the potential to be used as natural tracer e.g. for ecological questions concerning e.g. provenance and migration, but also to study physical processes like erosion, and the determination of material sources and sinks. Therefore, as central basis for ecosystem studies, isoscapes reflecting the spatial distribution of the  $^{87}\text{Sr}/^{86}\text{Sr}$  isotope ratio are being increasingly developed for terrestrial (Evans *et al.* 2010, Bataille & Bowen 2012, Willmes *et al.* 2014) but also for aquatic (Muhlfeld *et al.* 2012) systems. For large river systems, because of their specific features, the  $^{87}\text{Sr}/^{86}\text{Sr}$  isotope ratio has been recognized as important research and management tool (Gibson *et al.* 2002, Zitek *et al.* 2011). For example, as the local  $^{87}\text{Sr}/^{86}\text{Sr}$  isotope ratio is incorporated in fish hard parts like otoliths, it offers the unique potential to trace fish migrations between zones of different isotopic composition (Kennedy *et al.* 2000).

Within the JDS3, the  $^{87}\text{Sr}/^{86}\text{Sr}$  isotope ratio pattern within the Danube catchment from the source to the Delta was mapped for the first time.

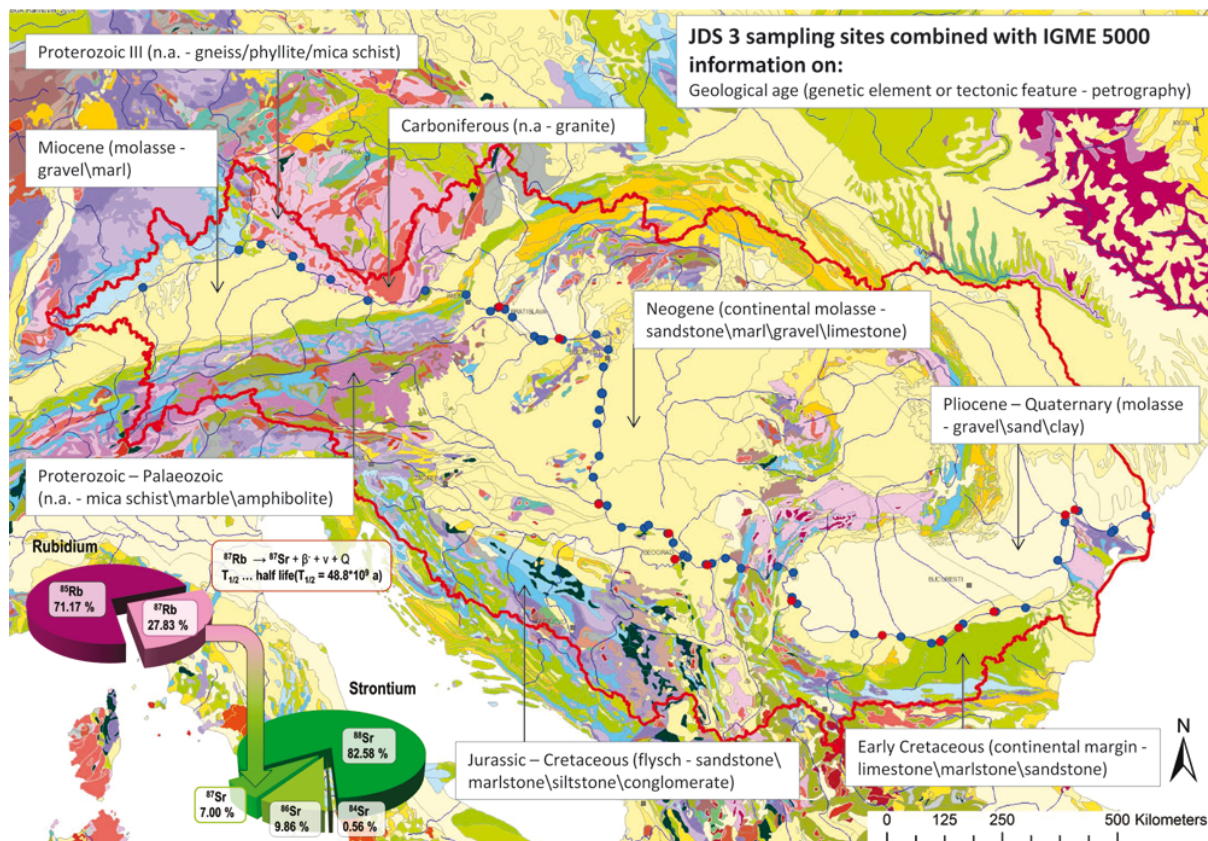


Figure 167: JDS3 sampling sites (Danube river sampling sites - blue circles; tributary sampling sites - red circles), selected information on geological formations (age, genetic element/tectonic feature and petrography) and the Rb/Sr isotope systems (Berglund & Wieser 2011) with the radioactive  $^{87}\text{Rb}$  to  $^{87}\text{Sr}$   $\beta$ -decay (Holden 1990) (Copyrights: Danube catchment by WISE River Basin Districts version 1.3, European Environment Agency (EEA); Data source of geological information and rivers: IGME5000, copyright by BGR Hannover, 2007)

### 33.2 Methods

During the JDS3, water samples from 68 sampling sites in the Danube and in the major tributaries were collected (Figure 167). Triplicate water samples were taken at each site along the Danube at about 10 cm below the water surface in pre-cleaned and pre-labelled PE-bottles (3\*100 ml) individually sealed in LDPE-bags. (Cleaning was accomplished by acid-washing (in 10% (m/m)  $\text{HNO}_3$  followed by a bath in 1% (m/m)  $\text{HNO}_3$  for 24 hours and rinsing by purified water (18 M $\Omega$  cm) (TKA Wasseraufbereitungssysteme GmbH 'Part of Thermo Fischer Scientific', Niederelbert, Germany). Bottles were filled up to  $\frac{3}{4}$ , and kept frozen at  $-20^\circ\text{C}$  until further processing in the laboratory.

Water samples were defrosted, acidified to 2% (v/v)  $\text{HNO}_3$  (double subboiled from p.A. grade acid, Merck, Darmstadt, Germany) and filtered using a cellulose acetate filter membrane (Minisart 0.45  $\mu\text{m}$  syringe filter units, Minisart, Sartorius, Göttingen, Germany) prior to analysis.

In a first step, quantification of the Sr mass fraction in water was performed using an inductively coupled plasma quadrupole mass spectrometer (ICP-QMS) (NexION 300D, Perkin Elmer, Waltham, MA, USA). External calibration using the ICP Multi-Element Standard Solution VI (CertiPur, suprapure, Merck KGaA, Darmstadt, Germany) and internal normalisation using the Indium ICP Standard, 1000 mg l $^{-1}$  (CertiPur, suprapure, Merck KGaA, Darmstadt, Germany) at a mass fraction of 1 ng g $^{-1}$  were performed.



After this step, samples were further processed for isotopic analysis by accomplishing Rb/Sr separation performed using a Sr-specific resin (EiChroM Industries, Inc., Darien, IL, USA) based on established protocols according to Swoboda *et al.* (2008).

The Sr isotope ratios of the water samples were measured with a double-focusing sector field multiple collector inductively coupled plasma mass spectrometer (MC ICP-MS) (Nu Plasma HR, Nu Instruments, Wrexham, UK) equipped with a desolvating membrane nebuliser (DSN 100, Nu Instruments, Wrexham, UK). Calibration was performed following an external intra-elemental strategy (*aka* sample-standard bracketing) using the NIST SRM 987 (NIST, Gaithersburg, MD, USA), which is a certified reference material for the natural Sr isotopic composition.

Blank correction was done on-peak by aspirating a 2%  $\text{HNO}_3$  blank solution. After blank correction data was mathematically corrected for interferences (remaining Rb). Instrumental isotopic fractionation was corrected for using the above mentioned calibration. Finally, combined standard uncertainties were calculated following EURACHEM/GUM guidelines.

### 33.3 Results

The  $^{87}\text{Sr}/^{86}\text{Sr}$  isotope ratio along the course of the Danube showed only slight variations.  $^{87}\text{Sr}/^{86}\text{Sr}$  isotope ratios varied around 0.709, with some significant lower values between 0.7084-0.7086 at some upstream sites (sampling sites JDS1, JDS2, JDS5) (Figure 168).

Significant differences of  $^{87}\text{Sr}/^{86}\text{Sr}$  isotope ratio were mainly found between the Danube and most of the tributaries.  $^{87}\text{Sr}/^{86}\text{Sr}$  isotope ratios in Morava, Drava, Tisa, Timok, Iskar, Jantra, Russenski Lom, Arges and Prut differed significantly from the adjacent Danube sections.

Morava showed the highest  $^{87}\text{Sr}/^{86}\text{Sr}$  isotope ratio (0.7111) and Timok the lowest (0.7068). The mean value along the Danube was 0.7091 ( $\pm 0.0002$  SD).

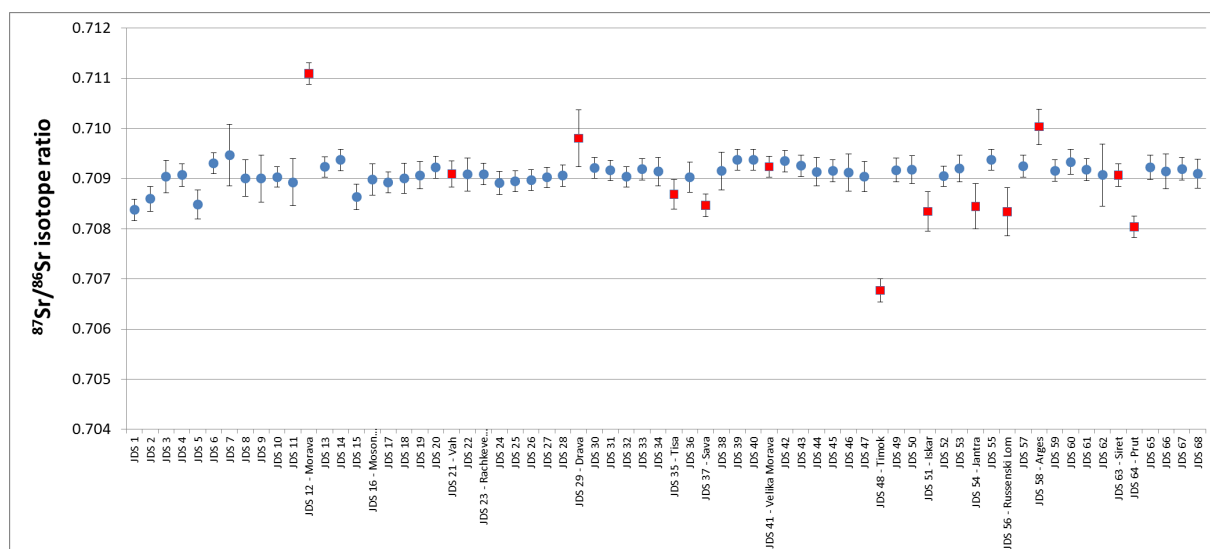


**Figure 168:**  $^{87}\text{Sr}/^{86}\text{Sr}$  isotope ratios along the course of the river Danube with blue circles representing Danube river sampling sites, and red squares tributary sampling sites; mean values of all sampling sites are based on triplicate samples, except for JDS5, JDS10, JDS11, JDS43, JDS60, JDS62 which are based on two samples; error bars represent combined standard uncertainties ( $u_c$ ,  $k=2$ )

### 33.4 Discussion

Analyses of mid water samples along the course of the Danube yielded relative small variations in the  $^{87}\text{Sr}/^{86}\text{Sr}$  isotope ratios along the main course of the Danube itself. Except for some upstream sampling sites,  $^{87}\text{Sr}/^{86}\text{Sr}$  isotope ratios in the Danube itself varied around 0.709, with a mean value along its full

course of 0.7091 ( $\pm 0.0002$  SD). This is in accordance with a  $^{87}\text{Sr}/^{86}\text{Sr}$  isotope ratio reported by Palmer and Edmond (1989) for the Danube of 0.7089 (with no information on the location of the sampling site). Pawellek *et al.* (2002) reported lower  $^{87}\text{Sr}/^{86}\text{Sr}$  isotope ratio for the first 400 km of the Danube downstream of the source as well, with values around 0.709 for the following river section from km 400 to km 1100 downstream to Kamenice.

Within JDS3, most sampled tributaries showed a significant difference of the  $^{87}\text{Sr}/^{86}\text{Sr}$  isotope ratio from the Danube itself. These local variations between the tributaries and the Danube itself indicate the influence of varying geological compositions in these subcatchments. Pawellek *et al.* (2002) reported significantly higher  $^{87}\text{Sr}/^{86}\text{Sr}$  isotope ratio values for the silicate-dominated subcatchments in the upper Danube, and the percentage of igneous rocks in subcatchments was found to be positively correlated with the  $^{87}\text{Sr}/^{86}\text{Sr}$  ratio for the Austrian section of the Danube and its tributaries (Zitek *et al.* 2011) (see also Figure 167 with regard to the distribution of different geological formations according to their composition and age).

Especially the documented differences in the  $^{87}\text{Sr}/^{86}\text{Sr}$  isotope ratios between the tributaries and the Danube itself bear the potential to be applied as tool to study natural migration phenomena of fish in the Danube catchment. As Pawellek *et al.* (2002) and Zitek *et al.* (2011) showed for the upper Danube catchment, significant small scale differences in  $^{87}\text{Sr}/^{86}\text{Sr}$  isotope ratios between the Danube and its tributaries exist, allowing the application of  $^{87}\text{Sr}/^{86}\text{Sr}$  isotope ratios to fish ecological questions even at relatively small spatial scales. In addition to the  $^{87}\text{Sr}/^{86}\text{Sr}$  isotope ratio, the Sr/Ca ratio is able to serve as an important additional tracer to discriminate fish from different sites in the Danube catchment (Zitek *et al.* 2010).

Future efforts will focus on combining the data of the JDS3 with existing data on  $^{87}\text{Sr}/^{86}\text{Sr}$  isotope ratios along the Austrian part of the Danube catchment, modelling the  $^{87}\text{Sr}/^{86}\text{Sr}$  isotope ratio in river water in relation to the geology (Hegg *et al.* 2013), and finally linking the information to fish ecological questions in the Danube catchment.

### 33.5 Conclusion

The documented differences of the  $^{87}\text{Sr}/^{86}\text{Sr}$  isotope ratios between the Danube and most of its tributaries bear the potential to be applied as tool for studying fish migrations and fish dispersal especially in Danube-tributary systems. The combination with other relevant natural chemical tracers like the Sr/Ca ratio will further enhance the possibilities for reconstructing migrations fish based on otolith chemistry in the Danube catchment.

### 33.6 Outlook

The spatially distinct data on  $^{87}\text{Sr}/^{86}\text{Sr}$  isotope ratios along the course of the Danube collected during the JDS3 in combination with existing data mainly from the upper section of the Danube will be used to develop the aquatic  $^{87}\text{Sr}/^{86}\text{Sr}$  isoscape of the Danube catchment. In combination with other chemical tracers, e.g. like the Sr/Ca ratio, the Danube catchment isoscape will serve as an important input for studying e.g. migrations of aquatic animals like fish and weathering and erosion processes in the Danube catchment.

### 33.7 References

- BATAILLE, C.P. & BOWEN, G.J. (2012) Mapping  $^{87}\text{Sr}/^{86}\text{Sr}$  variations in bedrock and water for large scale provenance studies. *Chemical Geology*, **304–305**, 39-52.
- BEARD, B.L. & JOHNSON, C.M. (2000) Strontium isotope composition of skeletal material can determine the birth place and geographic mobility of humans and animals. *Journal of Forensic Sciences*, **45**, 1049-1061.
- BERGLUND, M. & WIESER, M.E. (2011) Isotopic compositions of the elements 2009 (IUPAC Technical Report). *Pure and Applied Chemistry*, **83**, 397-410.
- BLUM, J., TALIAFERRO, E.H., WEISSE, M. & HOLMES, R. (2000) Changes in Sr/Ca, Ba/Ca and  $^{87}\text{Sr}/^{86}\text{Sr}$  ratios between trophic levels in two forest ecosystems in the northeastern U.S.A. *Biogeochemistry*, **49**, 87-101.
- BORDERELLE, A.-L., GERDEAUX, D., GIRAUDOUX, P. & VERNEAUX, V. (2009) Influence of watershed's anthropogenic activities on fish nitrogen and carbon stable isotope ratios in nine French lakes. *Knowl. Managt. Aquatic Ecosyst.*, 01.

- BOWEN, G.J. (2010) Isoscapes: Spatial Pattern in Isotopic Biogeochemistry. *Annual Review of Earth and Planetary Sciences*, **38**, 161-187.
- CAPO, R.C., STEWART, B.W. & CHADWICK, O.A. (1998) Strontium isotopes as tracers of ecosystem processes: theory and methods. *Geoderma*, **82**, 197-225.
- EVANS, J., MONTGOMERY, J., WILDMAN, G. & BOULTON, N. (2010) Spatial variations in biosphere  $^{87}\text{Sr}/^{86}\text{Sr}$  in Britain. *Journal of the Geological Society*, **167**, 1-4.
- FAURE, G. & MENSING, T. (2005) *Isotopes: Principles and Applications*. 3 ed. Hoboken, NJ, USA: Wiley.
- FOX, J.F. & PAPANICOLAOU, A.N. (2008) Application of the spatial distribution of nitrogen stable isotopes for sediment tracing at the watershed scale. *Journal of Hydrology*, **358**, 46-55.
- GIBSON, J.J., AGGARWAL, P., HOGAN, J., KENDALL, C., MARTINELLI, L.A., STICHLER, W., RANK, D., GONI, I., CHOUDHRY, M. & GAT, J. (2002) Isotope studies in large river basins: a new global research focus. *Eos, Transactions American Geophysical Union*, **83**, 613-617.
- GRAUSTEIN, W.C. (1989)  $^{87}\text{Sr}/^{86}\text{Sr}$  Ratios Measure the Sources and Flow of Strontium in Terrestrial Ecosystems. In: P.W. Rundel, J.R. Ehleringer & K.A. Nagy (eds.) *Stable Isotopes in Ecological Research*. Springer New York.
- HARRINGTON, R.R., KENNEDY, B.P., CHAMBERLAIN, C.P., BLUM, J.D. & FOLT, C.L. (1998)  $^{15}\text{N}$  enrichment in agricultural catchments: field patterns and applications to tracking Atlantic salmon (*Salmo salar*). *Chemical Geology*, **147**, 281-294.
- HEGG, J.C., KENNEDY, B.P. & FREMIER, A.K. (2013) Predicting strontium isotope variation and fish location with bedrock geology: Understanding the effects of geologic heterogeneity. *Chemical Geology*, **360-361**, 89-98.
- HOLDEN, N.E. (1990) Total half-lives for selected nuclides. *Pure and Applied Chemistry*, **62**, 941-958.
- KARUBE, Z.I., SAKAI, Y., TAKEYAMA, T., OKUDA, N., KOHZU, A., YOSHIMIZU, C., NAGATA, T. & TAYASU, I. (2010) Carbon and nitrogen stable isotope ratios of macroinvertebrates in the littoral zone of Lake Biwa as indicators of anthropogenic activities in the watershed. *Ecological Research*, **25**, 847-855.
- KELLY, S., HEATON, K. & HOOGEWERFF, J. (2005) Tracing the geographical origin of food: The application of multi-element and multi-isotope analysis. *Trends in Food Science & Technology*, **16**, 555-567.
- KENNEDY, B.P., BLUM, J.D., FOLT, C.L. & NISLOW, K.H. (2000) Using natural strontium isotopic signatures as fish markers: methodology and application. *Canadian Journal of Fisheries and Aquatic Sciences*, **57**, 2280-2292.
- LAKE, J.L., MCKINNEY, R.A., OSTERMAN, F.A., PRUELL, R.J., KIDDON, J., RYBA, S.A. & LIBBY, A.D. (2001) Stable nitrogen isotopes as indicators of anthropogenic activities in small freshwater systems. *Canadian Journal of Fisheries and Aquatic Sciences*, **58**, 870-878.
- MUHLFELD, C.C., THORROLD, S.R., MCMAHON, T.E. & MAROTZ, B. (2012) Estimating westslope cutthroat trout (*Oncorhynchus clarkii lewisi*) movements in a river network using strontium isoscapes. *Canadian Journal of Fisheries and Aquatic Sciences*, **69**, 906-915.
- MUYNCK, D. & WINNE, J. (2012) Strontium isotopic analysis as an experimental auxiliary technique in forensic identification of human remains. *Analytical Methods*, **4**, 2674-2679.
- PALMER, M.R. & EDMOND, J.M. (1989) The strontium isotope budget of the modern ocean. *Earth and Planetary Science Letters*, **92**, 11-26.
- PAWELLEK, F., FRAUENSTEIN, F. & VEIZER, J. (2002) Hydrochemistry and isotope geochemistry of the upper Danube River. *Geochimica et Cosmochimica Acta*, **66**, 3839-3854.
- PRICE, T.D., BURTON, J.H. & BENTLEY, R.A. (2002) The characterization of biologically available strontium isotope ratios for the study of prehistoric migration. *Archaeometry*, **44**, 117-135.
- PROHASKA, T., LATKOCZY, C., SCHULTHEIS, G., TESCHLER-NICOLA, M. & STINGEDER, G. (2002) Investigation of Sr isotope ratios in prehistoric human bones and teeth using laser ablation ICP-MS and ICP-MS after Rb/Sr separation. *Journal of Analytical Atomic Spectrometry*, **17**, 887-891.
- RANK, D., PAPESCH, W., HEISS, G. & TESCH, R. (2009) Isotopic composition of river water in the Danube Basin-results from the Joint Danube Survey 2 (2007). *Austrian J Earth Sci*, **102**, 170-180.
- SWOBODA, S., BRUNNER, M., BOULYGA, S., GALLER, P., HORACEK, M., STINGEDER, G. & PROHASKA, T. (2008) Identification of the geographic origin of asparagus using Sr isotope ratio measurements by MC-ICP-MS. *Analytical and Bioanalytical Chemistry*, **390**, 487-494.
- VOERKELIUS, S., LORENZ, G.D., RUMMEL, S., QUÉTEL, C.R., HEISS, G., BAXTER, M., BRACH-PAPA, C., DETERS-ITZELSBERGER, P., HOELZL, S. & HOOGEWERFF, J. (2010) Strontium isotopic signatures of natural mineral waters, the reference to a simple geological map and its potential for authentication of food. *Food Chemistry*, **118**, 933-940.

WILLMES, M., MCMORROW, L., KINSLEY, L., ARMSTRONG, R., AUBERT, M., EGGINS, S., FALGUÈRES, C., MAUREILLE, B., MOFFAT, I. & GRÜN, R. (2014) The IRHUM (Isotopic Reconstruction of Human Migration) database &ndash; bioavailable strontium isotope ratios for geochemical fingerprinting in France. *Earth Syst. Sci. Data*, **6**, 117-122.

ZITEK, A., IRRGEHER, J., SAILER, K., TRAUTWEIN, C., KRALIK, M., WAIDBACHER, H., HEIN, T. & PROHASKA, T. (2011) Isoscapes - a powerful tool for the management of large river systems. In: H. Habersack, B. Schober & D. Walling (eds.) *Conference Abstract Book of the International Conference on the Status and Future of the World's Large Rivers*. Vienna, Austria.

ZITEK, A., STURM, M., WAIDBACHER, H. & PROHASKA, T. (2010) Discrimination of wild and hatchery trout by natural chronological patterns of elements and isotopes in otoliths using LA-ICP-MS. *Fisheries Management and Ecology*, **17**, 435-445.

**V. The potential of  $^{87}\text{Sr}/^{86}\text{Sr}$  and Sr elemental mass fractions in fish otoliths as a fisheries management tool in a European pre-alpine river catchment**

*Andreas Zitek, Johannes Oehm, Johanna Irrgeher, Michael Schober, Anastassiya Tchaikovsky, Anika Retzmann, Barbara Thalinger, Michael Traugott and Thomas Prohaska (in preparation)*

# The potential of $^{87}\text{Sr}/^{86}\text{Sr}$ and Sr elemental mass fractions in fish otoliths as a fisheries management tool in a European pre-alpine river catchment

Andreas Zitek<sup>1\*</sup>, Johannes Oehm<sup>2</sup>, Johanna Irrgeher<sup>3</sup>, Michael Schober<sup>1</sup>, Anastassiya Tchaikovsky<sup>1</sup>, Anika Retzmann<sup>1</sup>, Bettina Thalinger<sup>2</sup>, Michael Traugott<sup>2</sup>, Thomas Prohaska<sup>1</sup>

<sup>1</sup>University of Natural Resources and Life Sciences, Vienna, BOKU-UFT, Department of Chemistry, Division of Analytical Chemistry – VIRIS Laboratory for Analytical Ecogeochemistry, Konrad-Lorenz-Straße 24, A-3430, Tulln, Austria.

<sup>2</sup>University of Innsbruck, Institute of Ecology, Technikerstraße 25, 6020 Innsbruck, Austria

<sup>3</sup>Helmholtz-Centre for Materials and Coastal Research, Institute for Coastal Research, Dept. for Marine Bioanalytical Chemistry, Max-Planck Strasse 1, 21502 Geesthacht, Germany

\*Corresponding author: [andreas.zitek@boku.ac.at](mailto:andreas.zitek@boku.ac.at)

## Abstract

The focus of this study was the development of a systematic approach to discriminate fish otoliths of different European freshwater fish species according to their habitat of origin by  $^{87}\text{Sr}/^{86}\text{Sr}$  isotope and Sr elemental mass fractions as a potential tool for fisheries management in a pre-alpine catchment region around lake Chiemsee, Germany, an important region for recreational and economic fisheries.  $^{87}\text{Sr}/^{86}\text{Sr}$  isotope and Sr/Ca ratios in water samples from 26 sites and the  $^{87}\text{Sr}/^{86}\text{Sr}$  isotope ratios together with the Sr elemental mass fractions in otoliths of associated fish from 17 species were determined using (laser ablation) inductively coupled plasma-mass spectrometry ((LA-)ICP-MS). The habitats could be discriminated into three distinct strontium isotope regions (SIGs) and 7 clusters with characteristic  $^{87}\text{Sr}/^{86}\text{Sr}$  isotope and Sr/Ca ratios. The direct comparison of  $^{87}\text{Sr}/^{86}\text{Sr}$  isotope ratios in water and otolith samples considering the measurement uncertainties allowed to identify fish that might have been a) migrated, b) transferred from other water bodies or c) stocked. Sr/Ca ratios in water and the Sr elemental mass fraction in otoliths were highly correlated, although significant differences between species with regard to the Sr uptake from the environment were found. The Sr mass fractions in otoliths of *Perca fluviatilis* were about 60 % of those in otoliths of roach *Rutilus rutilus* and *Coregonus spp* from the same habitats. Discrimination of fish by habitat clusters defined by  $^{87}\text{Sr}/^{86}\text{Sr}$  isotope and Sr/Ca ratios was possible with success rates ranging from 90 % to 100 % for cyprinids, European perch *Perca fluviatilis*, whitefish *Coregonus spp.* and European grayling, *Thymallus thymallus*. The presented data and methodology provide an important contribution for the application of otolith chemistry to the management of typical European freshwater fish species in pre-alpine catchment regions.

## Summary and Conclusion

This PhD thesis focused on 1) the investigation of geographical differences in the strontium isotopic and elemental composition of water and their relation to the underlying geology; 2) using strontium isotopic and elemental fingerprints for source determination of groundwater and fish; and 3) the development of chemometric tools for improved origin determination of salted fish products.

Surface water samples were collected from a small watershed in East Austria; a larger catchment in the Alpine foreland of Bavaria, Germany; along the course of the second largest river in Europe, the Danube River; and from fish farm pool water from Europe and Iran. Water from rivers and brooks draining the Leitha and Rosalia Mountains in East Austria showed an average  $n(^{87}\text{Sr})/n(^{86}\text{Sr})$  isotopic composition of  $0.71060 \pm 0.00099$  ( $n=10$ ;  $U$ ,  $k=2$ ) reflecting schist, gneisses, granites and limestone comprising the underlying bedrock. The strontium isotopic composition of water from rivers, lakes and ponds in the Lake Chiemsee region in Germany ranged between 0.70781 and 0.70988. This variation was a result of the diverse geology of this area consisting of a mosaic of calcareous rocks, flysch, Helveticum, and sediments thereof. The combination of the  $n(^{87}\text{Sr})/n(^{86}\text{Sr})$  isotope and Sr/Ca elemental amount ratio of the investigated surface water allowed differentiation of water samples into seven groups. Water collected along the course of the Danube River showed a mean  $n(^{87}\text{Sr})/n(^{86}\text{Sr})$  isotope amount ratio of  $0.70910 \pm 0.00020$  (55 sampling sites; 1  $SD$ ). Water of the tributaries Morava, Drava, Tisa, Timok, Iskar, Jantra, Russenski Lom, Ages and Prut had a significantly different  $n(^{87}\text{Sr})/n(^{86}\text{Sr})$  isotopic composition in comparison to the adjacent Danube section, reflecting the lithology of their sub-catchments. The  $n(^{87}\text{Sr})/n(^{86}\text{Sr})$  isotope amount ratio of surface water samples collected at one fish farm in Austria, four fish farms in Italy and one fish farm in Iran ranged between 0.70843 and 0.70945. Variance analysis revealed significant differences of the  $n(^{87}\text{Sr})/n(^{86}\text{Sr})$  isotope ratio; the Ca, Na, Mg, K, Fe, Sr, Mn, Co, Cu, As, Rb and Mo elemental and the element/Ca composition of water from the investigated fish farms.

Investigations of groundwater of the clastic aquifer in the Lake Neusiedl-Seewinkel area in East Austria revealed changes of the strontium isotopic and elemental composition of groundwater with depth. The  $n(^{87}\text{Sr})/n(^{86}\text{Sr})$  isotope amount ratio increased from  $0.70997 \pm 0.00063$  ( $n=5$ ;  $U$ ,  $k=2$ ) of shallow to  $0.71205 \pm 0.00035$  ( $n=2$ ;  $U$ ,  $k=2$ ) of deep thermal groundwater. The elemental composition changed from Ca,Mg-HCO<sub>3</sub>-type shallow to Na+K-HCO<sub>3</sub>-type thermal groundwater. The change of the strontium isotopic and elemental composition along the vertical profile of the clastic aquifer was associated with progressive leaching and dissolution of the siliciclastic bedrock due to increasing groundwater residence time. This observation suggested a continuous groundwater flow path from shallow over



artesian to deep thermal groundwater. In contrast to previous theories, these results indicated no recharge of groundwater below saline ponds by upwelling thermal groundwater. Furthermore, the  $\delta(^{88/86}\text{Sr})_{\text{SRM987}}$  isotopic composition of groundwater gave additional insights on aquifer bedrock formation and potential carbonate precipitation at depth of 1000 m.

In summary, investigated water reflected the  $n(^{87}\text{Sr})/n(^{86}\text{Sr})$  isotope amount ratios and elemental mass fractions of minerals that formed the local geology. Dissolution and leaching of the aquifer bedrock and mean groundwater residence time determined the strontium isotopic and elemental composition of groundwater. Investigation of these geochemical fingerprints allowed inference on groundwater flow. These findings represent important information for groundwater management. Furthermore, surface water samples from different geographic areas could be differentiated according to their strontium isotopic and elemental pattern. The obtained environmental reference samples form the basis for geographic origin determination of fish and fish products.

Fish from the investigated rivers, lakes and ponds in the Lake Chiemsee region absorbed the  $n(^{87}\text{Sr})/n(^{86}\text{Sr})$  isotope amount ratio of their water body of origin into their otoliths. This process was independent of the investigated fish family (e.g. Salmonidae, Cyprinidae, etc.). In contrast, the strontium elemental mass fraction taken up by fish from water into otoliths varied between fish families. This result suggested that each fish family has to be investigated separately. Statistical analysis revealed a significant positive correlation of the strontium elemental mass fraction of otoliths from the same fish family and the Sr/Ca elemental amount ratio of their habitat. Therefore, the  $n(^{87}\text{Sr})/n(^{86}\text{Sr})$  isotopic and the Sr/Ca elemental amount ratio could be used to attribute fish to their water body of origin with high accuracy. The presented data and procedure provide a systematic tool for freshwater fish management.

Multiple linear regression showed that sturgeons from aquaculture production in Europe and Iran absorbed the  $n(^{87}\text{Sr})/n(^{86}\text{Sr})$  isotope amount ratio; the Na, Mn, Cu, and Mo elemental content and the Fe/Ca elemental amount ratio from fish farm water into raw (*i.e.* unsalted) caviar. These variables reflected local geology, thus represented site-specific markers. All investigated fish belonged to the Acipenseridae family. Salting significantly changed the composition of four markers in salted caviar ( $n(^{87}\text{Sr})/n(^{86}\text{Sr})$ , Na, Mn and Fe/Ca). The alteration of the chemical composition of salted sturgeon caviar was mainly influenced by the high elemental mass fractions of Na, Mn, Fe and Sr in salt. Washing of salted caviar did not fully remove the influence of salt on the strontium and elemental composition of salted sturgeon caviar.

The  $n(^{87}\text{Sr})/n(^{86}\text{Sr})$  isotope amount ratio represents a key tracer for origin determination of water and fish products. In order to quantify the contribution of individual sources to the strontium isotopic composition of natural samples three chemometric methods based on 1)

isotope pattern deconvolution (IPD); 2) linear-algebra calculations; and 3) mixing model calculations were investigated. Best results were achieved using isotope pattern deconvolution, which facilitated the determination of the contribution of individual natural sources to a two- and three component system with lowest uncertainties.

Isotope pattern deconvolution was applied in two studies focusing on origin determination of groundwater and fish. Analysing groundwater, IPD showed that recent rainfall accounted for  $58 \% \pm 7 \% (U, k=2)$  and bedrock leaching for  $42 \% \pm 7 \% (U, k=2)$  of the  $n(^{87}\text{Sr})/n(^{86}\text{Sr})$  isotopic composition of shallow groundwater below saline ponds of the clastic aquifer in East Austria. This result supported previous observations that precipitation represented the main source of water to shallow groundwater in the investigated area. Investigating fish products, IPD revealed that strontium isotopic composition of raw caviar and otoliths was made up of 80 % water and 20 % fish feed. In the case of salted sturgeon caviar, salt determined up to 78 % of the  $n(^{87}\text{Sr})/n(^{86}\text{Sr})$  isotope amount ratio of samples treated with salt containing high amount of strontium.

IPD provided the basis for the development of reverse-mixing models. This significantly novel mathematical method was capable of determining the theoretical  $n(^{87}\text{Sr})/n(^{86}\text{Sr})$  isotope amount ratio absorbed from ambient water into salted sturgeon caviar. The assessed strontium isotope amount ratio was a proxy for the environmental tag and independent of the production process (feeding, salting). The presented methodology forms the basis for origin determination of sturgeon caviar using geochemical fingerprints transferred from water into fish. This paves the way towards the use of analytical methods in the fight against illegal caviar trade.

Future work should focus on the combination of the  $n(^{87}\text{Sr})/n(^{86}\text{Sr})$  isotope amount ratio and elemental fingerprints with additional isotopic markers. This complimentary information could further improve origin determination of water and fish products. Furthermore, the developed statistical and mathematical methods could give insights on other natural mixing processes, which determine the chemical composition of environmental samples. Finally, dedicated software scripts developed e.g. in R or Python could be used for a systematic and comparable data processing, uncertainty calculations and statistical evaluation of a large number of samples and variables. This chemometric approach has the potential to reveal even more information on ecosystem processes, thus broadening the spectrum of analytical ecogeochemistry.

# Appendices

## List of Abbreviations

AAS	Atomic absorption spectrometry
bgs	Below ground surface
CITES	Convention on international trade in endangered species of wild fauna and flora
EC	Electrical conductivity
HPLC	High pressure liquid chromatography
ICP-MS	Inductively coupled plasma mass spectrometry
ICP-QMS	Inductively coupled plasma quadrupole mass spectrometry
ICP-SFMS	Inductively coupled plasma sector field mass spectrometry
ICP-TOFMS	Inductively coupled plasma time-of-flight mass spectrometry
IDMS	Isotope dilution mass spectrometry
IIF	Instrumental isotopic fractionation
IPD	Isotope pattern deconvolution
ISO	International organization for standardization
IUPAC	International union of pure and applied chemistry
<i>k</i>	Coverage factor
LA-ICP-MS	Laser ablation inductively coupled plasma mass spectrometry
LIBS	Laser induced breakdown spectroscopy
LOQ	Limit of quantification
MC ICP-MS	Multi-collector inductively coupled plasma mass spectrometry
<i>m/z</i>	Mass to charge ratio
<i>n</i>	Number of samples
OES	Optical emission spectrometry
<i>P</i>	Probability value
PFA	Perfluoroalkoxy
<i>SD</i>	Standard deviation
SI	International system of units
TIMS	Thermal ionisation mass spectrometry
<i>U</i>	Expanded combined uncertainty
XRF	X-ray fluorescence

## Curriculum Vitae

### DI ANASTASSIYA TCHAIKOVSKY

Email: [anastassiya.tchaikovsky@univie.ac.at](mailto:anastassiya.tchaikovsky@univie.ac.at)

Address: Währingerstr. 38 1090 Wien

Phone: +43 1 4277 9805011

Date of birth: 15<sup>th</sup> Oct 1985



## Education

---

- 2013— UNIVERSITY OF NATURAL RESOURCES AND LIFE SCIENCES VIENNA  
*PhD candidate, Doctoral program*
- Thesis title: *Strontium isotopic and elemental fingerprints as tools for source determination in aquatic ecosystems*  
Supervisors Prof. Thomas Prohaska and Dr. Andreas Zitek
- 2004—2013 VIENNA UNIVERSITY OF TECHNOLOGY  
*Diploma Program, Technical Chemistry (passed with distinction)*
- Thesis title: *Development of a novel separation method for uranium and thorium by surface functionalized nanoparticles for uranium age determination*  
Supervisors Prof. Andreas Limbeck and Dr. Sergei Bulyha; conducted in cooperation between the Vienna University of Technology and the International Atomic Energy Agency
- 1996—2004 BUNDESREALGYMNASIUM GRG 23 ALT ERLAA  
*Matura (passed with distinction)*

## Professional career

---

- 10.2018— **Research associate**; University of Vienna; Department of Analytical Chemistry; Research Group for Environmental Chemistry; Vienna; Austria
- 01—10.2018 **Research associate – PhD**; Competence center for Feed and Food Quality, Safety and Innovation; Blue Area: Authenticity and Origin; Tulln; Austria
- 2013—2017 **Research associate – PhD**; University of Natural Resources and Life Sciences, Vienna; Department of Chemistry; VIRIS Laboratory for Analytical Ecogeochemistry; Tulln; Austria
- 2007—2012 **Research associate – Diploma student**; International Atomic Energy Agency; Safeguards Analytical Laboratories; ICP-MS Laboratory; Seibersdorf; Austria
- 2006—2007 **Laboratory technician**; International Atomic Energy Agency; Safeguards Analytical Laboratories; Uranium Laboratory; Seibersdorf; Austria
- 07—08.2006 **Trainee**; Novartis Research Institutes; Vienna; Austria

## Key skills

---

### ANALYTICAL CHEMISTRY

- Trace and ultra-trace elemental and isotopic analysis under cleanroom conditions using (MC) ICP-MS
- Direct analysis of solid samples using Laser Ablation ICP-MS
- Isotope dilution mass spectrometry, size-exclusion chromatography, solid phase extraction
- Data evaluation using Microsoft Excel and multi variate statistics using SPSS and R (learning)
- Method validation according to metrological criteria (EURACHEM)
- Sample preparation (matrix separation, microwave-assisted acid digestion, etc.)

## TEACHING

- Co-supervision of visiting scientists: Carmella Zannella (2016, University of Naples Federico II, Italy), Alba Gallo (2017, Ca'Foscari University of Venice, Italy), Agnese Aguzzoni (2017, Free University of Bolzano, Italy), Václav Štursa (2018, Brno University of Technology, Czech Republic)
- Co-supervision of bachelor theses: Rudolf Scheiber (2016), Sabrina van den Oever (2016)
- Co-supervision of trainees: Ann Salvatierra, Sebrina Obaro, Sara Knezevic, Susanne Schwendinger, Elena Mandl, Valentina Laure, Ivanna Mykhaylyuk and Helene Mühlehner
- Teaching and preparation of materials for high school students on the fundamentals of elements, isotopes and mass spectrometry in the framework of the CSI: TRACE your FOOD!<sup>1</sup> project
- Teaching Assistant in the lecture on *Holistic Sciences* and *Isotopic tools for the investigation of the ecosystem* at the University of Natural Resources and Life Sciences, Vienna
- Tutor in the *Quantitative Analytical Chemistry* and *Instrumental Analysis and Bio analytics* lab-courses at the Vienna University of Technology

## ORGANISATION

- Organisation of a module at the 'Lange Nacht der Forschung' 2016/2018; 'Wiener Forschungsfest' 2018
- Organisation of conferences and meetings:
  - o European Winter Conference on Plasma Spectrochemistry 2017 (Organising committee)
  - o Young Scientist Career Event at the European Winter Conference on Plasma Spectrochemistry 2017 (Co-Chair)
  - o STEM workshop for girls, 2016 (Chair)
  - o PhD Conference DocDay, 2015 (Chair)
  - o Hyperspectral-imaging Workshop 2015 (Organising committee)
  - o Science Film Festival 2015 (Organising committee)
  - o ASAC Junganalytikerforum 2014 (Organising committee)
  - o ASAC Junganalytikerforum 2013 (Organising committee)

## COMPUTER SKILLS AND LANGUAGES

- MS Office, SPSS, GUM Workbench, EndNote, Illustrator, Photoshop, Origin, R (learning)
- German (native), Russian (native), English (fluent), French (intermediate)

## Grants and Awards

---

- 2016 IsoPROTECT, Austrian Science Fund, role: co-investigator, PI: Prof. Thomas Prohaska  
2016 CEEPUS mobility grant  
2014 Award: best talk at the 2<sup>nd</sup> DocDay, Tulln, Austria  
2013 Merit scholarship, Vienna University of Technology  
2013 ESF scholarship, European Commission  
2012 Award: best student lecture, 23<sup>rd</sup> ICPMS User Meeting Tulln, Austria  
2012 Research scholarship, Vienna University of Technology

## Schools and Trainings

---

- 2018 Statistics using R, Vienna, Austria  
2017 Automation of environmental assays in risk assessment studies, Vienna, Austria  
2017 Mycotoxin Summer Academy, Tulln, Austria  
2016 Winter School on Biotechnology and Food Sciences, Nitra, Slovak Republic  
2015 Training on Metrology in Chemistry, Vienna, Austria  
2015 Hyperspectral-imaging Workshop, Tulln, Austria  
2013 Workshop on Fish passages in regulated rivers, Moscow-Kasnodar, Russia

<sup>1</sup> [http://csi-traceyourfood.boku.ac.at/crbst\\_1.html](http://csi-traceyourfood.boku.ac.at/crbst_1.html)

## Publications and Reports

---

**Tchaikovsky, A;** Häusler, H; Kralik, M; Zitek, A; Irrgeher, J; Prohaska, T (2019). *Analysis of  $n(^{87}\text{Sr})/n(^{86}\text{Sr})$ ,  $\delta^{88}\text{Sr}/^{86}\text{Sr}_{\text{SRM987}}$  and elemental pattern to characterise groundwater and recharge of saline ponds in a clastic aquifer in East Austria*. *Isotopes in Environmental and Health Studies*, p. 1-20, DOI: 10.1080/10256016.2019.1577832

**Tchaikovsky, A;** Zitek, A; Irrgeher, J; Opper, C; Scheiber, R; Moder, K; Congiu, L; Prohaska, T (2019). *Chemometric tools for determining site-specific elemental and strontium isotopic fingerprints in sturgeon caviar*. submitted to *European Food Research and Technology*

**Tchaikovsky, A;** Irrgeher, J; Zitek, A; Prohaska, T (2017). *Isotope pattern deconvolution of different sources of stable strontium isotopes in natural systems*. *Journal of Analytical Atomic Spectrometry*, 32, 11, p. 2300-2307, DOI: 10.1039/C7JA00251C

Zitek, A; **Tchaikovsky, A;** Irrgeher, J; Waidbacher, H; Prohaska, T (2015). *The  $^{87}\text{Sr}/^{86}\text{Sr}$  river water isoscape of the Danube catchment*. ICPDR, Joint Danube Survey 3: A Comprehensive Analysis of Danube Water Quality, Chapter 33, p. 349-354, ISBN: 978-3-200-03795-3

## Publications in preparation

---

Zitek, A; Oehm, J; Irrgeher, J; Schober, M; **Tchaikovsky, A;** Retzmann, A; Thalinger, B; Traugott, M; Prohaska T. *The potential of  $^{87}\text{Sr}/^{86}\text{Sr}$  and Sr elemental mass fractions in fish otoliths as a fisheries management tool in a European pre-alpine river catchment*. in preparation

Bakhshalizadeh, S; Zitek A; **Tchaikovsky, A;** Bani, A; Prohaska, T. *Determining the origin of juvenile age-0 Persian sturgeon from hatcheries in the east and west of the Caspian Sea using the natural tag of fin spine microchemistry*. in preparation

## Selected presentations at conferences

---

**Tchaikovsky, A;** Emin, S; Schoeberl, A; Galvez, L; Koellensperger, G (2019). *Uncertainty evaluation of Fe and S quantification in ferritin enriched by centrifugal ultrafiltration*. [Poster] European Winter Conference on Plasma Spectrochemistry, Pau, France

**Tchaikovsky, A;** Zitek, A; Boner, M; Prohaska, T (2018). *Authenticity and origin of sturgeon caviar - towards a European database for caviar traceability*. [Poster] 2<sup>nd</sup> International MoniQA Symposium on Food Fraud Prevention and Effective Food Allergen Management, Vösendorf, Austria

**Tchaikovsky, A;** Zitek, A; Irrgeher, J; Opper, C; Scheiber, R; Prohaska, T (2017). *Analytical challenges of origin determination of processed authentic food on the example of sturgeon caviar and aquacultured fish*. 8<sup>th</sup> International Symposium on Recent Advances in Food Analysis, Prague, Czech Republic

**Tchaikovsky, A;** Zitek, A; Irrgeher, J; Opper, C; Sarne, J; Scheiber, R; Prohaska, T (2015).  *$^{87}\text{Sr}/^{86}\text{Sr}$  isotope pattern as a tool for provenancing of sturgeon caviar*. 7<sup>th</sup> International Symposium on Recent Advances in Food Analysis, Prague, Czech Republic

**Tchaikovsky, A;** Zitek, A; Irrgeher, J; Prohaska, T (2014). *Danube catchment water chemistry monitoring - elemental pattern determination from source to mouth using ICP-MS*. [Poster] European Geosciences Union General Assembly, Vienna, Austria

**Tchaikovsky, A;** Limbeck, A (2013). *Introduction of a novel separation method for uranium and thorium by surface functionalized nanoparticles for uranium age determination*. [Poster] European Winter Conference on Plasma Spectrochemistry, Krakow, Poland

## Eidesstattliche Erklärung

Ich erkläre ehrenwörtlich, dass ich die vorliegende Arbeit selbständig und ohne fremde Hilfe verfasst habe, andere als die angegebenen Quellen nicht verwendet habe und die den benutzten Quellen wörtlich oder inhaltlich entnommenen Stellen als solche kenntlich gemacht habe.

---

Anastassiya Tchaikovsky

Wien, am 09.04.2019